

RHODES UNIVERSITY
Where leaders learn

The *de novo* biosynthesis of biotin is required for the optimal growth of *Salmonella enterica* serovar Typhimurium in the intracellular environment

A thesis submitted in fulfilment of the requirement for the degree of

**MASTER OF SCIENCE
Microbiology**

at

**RHODES UNIVERSITY
Grahamstown**

By

CLAIRE McLAUGHLIN

March 2021

Abstract

Salmonella enterica serovar Typhimurium (*S. Typhimurium*) is a foodborne pathogen infecting humans and animals, contributing to significant morbidity and mortality worldwide each year. The increase in antibiotic-resistant *S. Typhimurium* infections in recent years has highlighted the need for new antibacterial drugs and drug targets. *S. Typhimurium* can acquire biotin through *de novo* biosynthesis or via transport from its extracellular environment. The importance of the vitamin for bacterial survival, coupled with the absence of the biotin biosynthetic pathway in humans, makes the biotin biosynthetic enzymes attractive targets for drug discovery. The study's primary aim was to determine the relative importance of the biotin biosynthesis and transport pathways for the *in vitro* and *ex vivo* growth and survival of *S. Typhimurium*, with the goal of validating the pathways as valid targets for antimicrobial drug development. In order to achieve this aim, we generated *S. Typhimurium* mutant strains harbouring deletions in either the biotin biosynthetic gene, *bioB*, or putative high-affinity biotin transporter, *yigM* ($\Delta bioB$ and $\Delta yigM$, respectively), as well as a double mutant in which the two mutations were combined ($\Delta bioB \Delta yigM$). Since the simultaneous disruption of biotin biosynthesis and transport in the double mutant may form a synthetic lethal combination, preventing further analysis of the strain, we also constructed a conditional mutant in which the promoter of the *yigM* gene was replaced by the arabinose-regulatable, P_{BAD} promoter in the $\Delta bioB$ background ($\Delta bioB$ P_{BAD}::*yigM*). Since the expression of the YigM in this strain is arabinose-regulatable, its role as a biotin transporter can be evaluated by altering the arabinose concentration in the growth media.

Once the mutant strains were isolated and verified genetically, their growth and that of their genetically complemented counterparts were analysed in liquid and/or solid M9 minimal medium in the absence of biotin. Consistent with previous observations, the $\Delta bioB$ auxotrophic mutant's growth was severely compromised in minimal media in the absence of biotin. The growth of the strain could, however, be restored by supplementation with exogenous biotin or expression of the wild type *bioB* gene from an episomal plasmid. The ability of biotin to reverse the growth defect of the $\Delta bioB$ mutant strain was, however, dependent on the presence of a functional YigM, since biotin supplementation did not affect the growth of the $\Delta bioB \Delta yigM$ double mutant strain. The introduction of a second copy of the *yigM* gene in the $\Delta bioB \Delta yigM$ background, however, restored the growth of the strain in the presence, but not absence, of biotin. The dependence of the double

mutant on both YigM and biotin for growth supports the idea that the protein functions as the sole or primary biotin transporter in *S. Typhimurium*, as it has recently been shown for *E. coli* (Ringsletter, 2010; Finkenwirth *et al.*, 2013). The essentiality of YigM for biotin transport was subsequently verified by two independent means. Firstly, the growth of the $\Delta bioB$ $P_{BAD}::yigM$ promoter-replacement mutant was strictly dependent on the inclusion of arabinose in biotin-supplemented M9 minimal media supplemented, indicating that the expression of YigM from the P_{BAD} promoter is essential for biotin transport. Secondly, following treatment with a known small-molecule inhibitor of the biotin biosynthesis, MAC-13772, exogenous biotin was capable of restoring the growth defect of the YigM⁺ wild type *S. Typhimurium* strain, but not the YigM⁻ $\Delta yigM$ mutant. Taken together, these findings confirm that YigM serves as the biotin transporter for *S. Typhimurium* and that the corresponding $\Delta yigM$ mutant is, as a result, defective for biotin transport.

Having confirmed the genotypes and phenotypes of the $\Delta bioB$, $\Delta yigM$, and $\Delta bioB \Delta yigM$ mutants, we next analysed the importance of the biotin biosynthesis and transport pathways for the growth and survival of *S. Typhimurium* within the intracellular environment. To this end, we determined the proliferation of each of the mutant strains following infection of HeLa epithelial and RAW264.7 macrophage-like cell lines. Our results revealed that the *de novo* biosynthesis of biotin is required for the optimal growth of *S. Typhimurium* following infection of both epithelial and macrophage-like cell lines. Disruption of biotin transport, by contrast, had no significant effect on the intracellular proliferation of *S. Typhimurium* when a functional pathway for the biosynthesis of biotin was present. The simultaneous disruption of biotin biosynthesis and transport, however, resulted in significant attenuation of *S. Typhimurium* in epithelial cells, while bacterial survival in macrophages decreased to below the limit of detection. Overall, our results suggest the *S. Typhimurium* relies primarily on biotin produced by the *de novo* biosynthesis pathway to support its growth in the intracellular environment. While YigM-mediated biotin transport is essential for sustaining the viability of intracellular *S. Typhimurium* in the absence of *de novo* biosynthesis, it appears to play a relatively minor role in the acquisition of biotin during growth in the nutrient-limited *Salmonella* containing vacuole. Our findings suggest that inhibiting biotin biosynthesis may be a viable strategy for combating systemic infections caused by *Salmonella*, as has been recently proposed for other medically important bacterial pathogens (Carfrae *et al.*, 2020).

Table of Contents

Abstract	ii
Table of Contents	iv
List of Figures	vii
List of Tables	ix
List of Abbreviations	x
Acknowledgements	xii
Chapter 1: Literature Review	1
1.1 Introduction.....	1
1.2 Classification and nomenclature of <i>Salmonella</i>	1
1.3 <i>Salmonella</i> Pathogenesis.....	2
1.3.1 Overview	2
1.3.2 The Typhoidal <i>Salmonella</i> serovars and Enteric fever	3
1.3.3 The Non-typhoidal <i>Salmonella</i> serovars.....	4
1.4 Treatment and Prevention of <i>Salmonella</i> infections.....	6
1.5 <i>Salmonella</i> Infection and the host environment.....	7
1.6 <i>Salmonella</i> metabolism in the host	11
1.6.1 The nutritional environment in the intestinal lumen.....	12
1.6.2 The nutritional environment in the SCV	13
1.7 Biotin Metabolism	14
1.7.1 Biological roles of biotin	15
1.7.2 Biotin Metabolism	16
1.8 Rationale	22
1.9 Aims and objectives.....	22
Chapter 2: Materials and Methods	24
2.1 Bacterial strains.....	24
2.2 Bacterial media, growth and storage conditions	24
2.3 Growth assays	25
2.3.1 Growth assays in liquid medium.....	25
2.3.2 Growth assays on solid medium	25
2.3.3 Bacterial viability assays.....	26
2.3.4 Broth microdilution assays	26
2.4 Chemicals and reagents.....	27
2.5 DNA isolation and purification.....	27
2.6 DNA quantification.....	27
2.7 General recombinant DNA procedures.....	28

2.7.1 Restriction Enzyme Digestion	28
2.7.2 Dephosphorylation reactions	28
2.7.3 Ligation reactions.....	28
2.7.4 Polymerase Chain Reaction (PCR).....	29
2.8 Agarose gel electrophoresis	31
2.9 DNA sequencing.....	33
2.10 Bioinformatic tools and software.....	33
2.11 Bacterial transformation.....	33
2.11.1 Preparation of chemically competent cells	33
2.11.2 Transformation of chemically competent cells.....	34
2.11.3 Preparation of electrocompetent cells.....	34
2.11.4 Transformation of electrocompetent cells	34
2.12 Generation of mutant strains.....	35
2.12.1 Generation of <i>S. Tm</i> $\Delta bioB$ and $\Delta yigM$ deletion mutant strains.....	35
2.12.2 Generation of <i>S. Tm</i> <i>yigM</i> promoter-replacement mutant ($P_{BADyigM}$)	36
2.12.3 Phage P22 mediated transduction of mutant alleles	36
2.12.4 Generation of unmarked mutant strains.....	37
2.12.5 Generation of <i>S. Tm</i> $\Delta bioB$ $\Delta yigM$ double mutant	38
2.12.6 Generation of <i>S. Tm</i> $\Delta bioB::P_{BAD}::yigM$ mutant	38
2.13 Generation of plasmids for genetic complementation of <i>bioB</i> and <i>yigM</i>	38
2.14 Growth and maintenance of mammalian cells.....	39
2.14.1 Intracellular survival assay using HeLa cells.....	39
2.14.2 Intracellular survival assay using RAW264.7 cells	39
2.14.3 Chemical inhibition of biotin biosynthesis in mammalian cells.....	40
Chapter 3: Results.....	42
3.1 Introduction.....	42
3.2. Generation and genotypic confirmation of <i>S. Tm</i> single mutant strains.....	43
3.2.1 Generation and confirmation of the <i>S. Tm</i> $\Delta yigM$ mutant.....	44
3.2.2 Generation and confirmation of an <i>S. Tm</i> $\Delta bioB$ mutant	49
3.2.3 Construction and confirmation of an <i>S. Tm</i> $\Delta bioB::Km^R$ $\Delta yigM$ double mutant	53
3.2.4 Generation of complementation vectors pBioB and pYigM	54
3.2.5 Growth analysis of <i>S. Tm</i> mutants in liquid minimal medium.....	54
3.2.6 Growth kinetics of the <i>S. Tm</i> mutants on solid minimal medium	55
3.2.7 <i>De novo</i> biotin biosynthesis is essential for <i>S. Tm</i> viability in M9 minimal media	57
3.2.8 Generation of a $\Delta bioB::Km^R P_{BAD}::yigM$ conditional mutant.....	58
3.2.9 Growth analysis of the $\Delta bioB::Km^R P_{BAD}::yigM$ promoter replacement mutant	61

3.3 Chemical genetic studies to confirm the role of YigM in biotin transport	62
3.4. Assessment of the role of biotin biosynthesis and transport in the intracellular growth and survival of <i>S. Tm</i>	64
3.4.1. Intracellular replication of <i>S. Tm</i> in human HeLa epithelial cells.....	65
3.4.2 Intracellular replication of <i>S. Tm</i> in murine RAW264.7 macrophages	66
3.5 Chemical inhibition of biotin biosynthesis reduces <i>S. Tm</i> proliferation in mammalian cells	68
Chapter 4: Discussion	70
4.1 Summary	75
5. Reference List.....	77
Appendix A: Chemicals and Reagents.....	94
Appendix B: Molecular Weight Markers	97
Appendix C: Plasmid Construction	98
C1: Construction of BioB complement construct pBioB	98
C2: Construction of YigM complement construct: pYigM	101

List of Figures

Figure 1.1: The infection scheme of pathogenic <i>Salmonella</i> species.....	8
Figure 1.2: Chemical structure of biotin.....	15
Figure 1.3: Schematic diagram of the late-stage biotin biosynthesis pathway and putative biotin transporter YigM.....	18
Figure 1.4: Schematic diagram of the bi-directional <i>bio</i> operon.....	19
Figure 3.1: Expression of selected genes involved in biotin metabolism in <i>S. Tm</i>	43
Figure 3.2: Schematic representation of the targeted deletion of the <i>bioB</i> and <i>yigM</i> genes of <i>S. Tm</i> and subsequent removal of the Km ^R cassette.....	45
Figure 3.3: PCR amplification of the <i>yigM</i> -specific Km ^R cassette from pKD4.....	46
Figure 3.4: PCR confirmation of the genotype of the putative <i>yigM</i> ::Km ^R mutant clones.....	47
Figure 3.5: PCR confirmation of the successful transduction of the <i>yigM</i> ::Km ^R allele into a clean WT <i>S. Tm</i> background.....	48
Figure 3.6: PCR Confirmation of the removal of the Km ^R marker from the <i>S. Tm</i> $\Delta yigM$::Km ^R strain.....	49
Figure 3.7: PCR amplification of the <i>bioB</i> -specific Km ^R cassette from pKD13.....	50
Figure 3.8: Schematic representation of the <i>bioB</i> gene of <i>S. Tm</i>	51
Figure 3.9: PCR confirmation of the genotype of the putative $\Delta bioB$::Km ^R mutant clones.....	51
Figure 3.10: Confirmation of the genotype of the putative $\Delta bioB$::Km ^R mutant clones by PCR..	52
Figure 3.11: Genotypic analysis of the <i>yigM</i> and <i>bioB</i> alleles present in putative <i>S. Tm</i> $\Delta bioB$::Km ^R $\Delta yigM$ double mutant strains.....	53
Figure 3.12: <i>S. Tm</i> mutants deficient in both the <i>de novo</i> biosynthesis and transport of biotin are defective for growth in M9 minimal media broth.....	55
Figure 3.13: <i>S. Tm</i> mutants deficient in both the <i>de novo</i> biosynthesis and transport of biotin are defective for growth on solid M9 minimal media.....	56
Figure 3.14: <i>S. Tm</i> mutants lacking BioB are dependent on YigM-mediated biotin transport for growth.....	58
Figure 3.15: Schematic representation of the <i>yigM</i> locus of <i>S. Tm</i> and expected sizes of the marked and unmarked <i>yigM</i> and P _{BAD} :: <i>yigM</i> alleles	59

Figure 3.16: Generation of the <i>yigM</i> promoter-specific Km ^R cassette by PCR amplification	59
Figure 3.17: PCR confirmation of the genotypes of the <i>yigM</i> and <i>bioB</i> alleles present in the <i>S. Tm</i> WT and mutant strains.....	60
Figure 3.18: The growth of the <i>S. Tm</i> $\Delta bioB::Km^R P_{BAD}::yigM$ promoter replacement mutant is dependent on the arabinose induced expression of YigM.....	61
Figure 3.19: MAC-13772 inhibits biotin biosynthesis in both <i>E. coli</i> and <i>S. Tm</i>	62
Figure 3.20: Chemical inhibition of <i>de novo</i> biotin biosynthesis in the $\Delta yigM$ mutant results in a synthetic lethal phenotype.....	64
Figure 3.21: <i>S. Tm</i> biotin <i>de novo</i> biosynthesis mutants are attenuated in HeLa cells.....	66
Figure 3.22: <i>S. Tm</i> biotin <i>de novo</i> biosynthesis mutants are attenuated in RAW264.7 cells.....	67
Figure 3.23: Inhibitory effect of MAC-13772 on <i>S. Tm</i> WT and mutant strains in RAW264.7 cells.....	69
Figure B1: Molecular Weight Markers used in this study.....	95
Figure C1.1: Generation of a construct for genetic complementation of the <i>bioB</i> gene.....	97
Figure C1.2: Restriction endonuclease digests of recombinant pBioB plasmids.....	97
Figure C1.3: Complement construct pBioB map.....	98
Figure C2.1: Generation of a construct for genetic complementation of the <i>yigM</i> gene.....	99
Figure C2.2: Restriction endonuclease digests of recombinant pYigM plasmids.....	100
Figure C2.3: Complement construct pYigM map.....	101

List of Tables

Table 2.1: Bacterial strains and plasmids used and generated in this study.....	25
Table 2.2: List of oligonucleotide primers used in this study.....	30
Table 2.3: Expected PCR product sizes when amplifying WT and mutant strains with the indicated primer pairs.....	32
Table A1: List of chemicals and reagents used in this study.....	93-94

List of Abbreviations

ABC	ATP binding cassette
AGE	Agarose gel electrophoresis
Amp	Ampicillin
Amp ^R	Ampicillin resistant
Amp ^S	Ampicillin sensitive
AP	Alkaline phosphatase
Ara	Arabinose
ATP	Adenosine triphosphate
ATR	Acid tolerance response
bp	Base pairs
CFU	Colony forming unit
DAPA	7,8-diaminopelargonic acid
dH ₂ O	Distilled water
DMEM	Dulbecco's modified eagle medium
DS	Downstream
EBU	Evans blue uranine
ECF	Energy coupling factor
EGTA	Ethylene glycol-bis(β-aminoethyl ether)-N,N,N',N'-tetraacetic acid
FBS	Fetal bovine serum
FRT	Flippase recognition sites
Glu	Glucose
Gly	Glycerol
HF	High-fidelity
HIV	Human immunodeficiency virus
ITPG	Isopropyl β-D-1-thiogalactopyranoside
KAPA	7-keto-8-aminopelargonic acid
kb	Kilobases
Km	Kanamycin
Km ^R	Kanamycin resistant
Km ^S	Kanamycin sensitive
Gm	Gentamycin
LA	Luria agar
LB	Luria broth

MCS	Multiple cloning site
MCT	Mammalian monocarboxylate transporter
MM	Minimal media
MIC	Minimal inhibitory concentration
MOI	Multiplicity of infection
nt	Nucleotides
OD	Optical density
Orf	Open reading frame
P _{BAD}	araBAD promoter
PBS	Phosphate buffered saline
PCR	Polymerase chain reaction
pfu	Plaque-forming unit
p.i.	Post infection
RBS	Ribosomal binding site
RE	Restriction enzyme
RPMI	Roswell Park Memorial Institute
SCV	<i>Salmonella</i> containing vacuole
SI	Supplementary information
SMVT	Sodium-dependent multivitamin transporter
SPI	<i>Salmonella</i> pathogenicity island
<i>S. Tm</i>	<i>Salmonella</i> Typhimurium
TTSS	Type three secretion system
US	Upstream
UV	Ultra-violet
WT	Wild type
X-Gal	5-bromo-4-chloro-3-indolyl- β -D-galactopyranoside

Acknowledgements

A special thanks to my wonderful supervisor Dr Garth Abrahams for his patience, help, and guidance throughout my post-graduate career. Without your banter and dark sense of humor, I would not have made it through this project. To my lab mates past and present thank you for the help, encouragement, and distraction along the way. To the NRF for the partial financial support of this project.

Chapter 1: Literature Review

1.1 Introduction

Salmonella enterica is a Gram-negative, food-borne pathogen that causes human diseases ranging from relatively mild gastroenteritis to potentially life-threatening systemic infections (Crump and Wain, 2017; Farrar *et al.*, 2013). More than 2,600 *S. enterica* serovars have been identified to date (Grimont and Weill, 2007). These include the host-restricted Typhoidal serovars such as Typhi and Paratyphi that cause enteric fever in humans, as well as the broad-host-range, non-Typhoidal *Salmonella* (NTS) serovars, which cause localised, gastrointestinal infections. Infections caused by *S. enterica* serovars are a significant cause of morbidity and mortality worldwide (Dougan and Baker, 2014; Fabrega and Vila, 2013). According to the most recent estimates, the *S. enterica* serovars were collectively responsible for more than 100 million illnesses and 250,000 deaths worldwide in 2017 alone (Stanaway *et al.*, 2019a; Stanaway *et al.*, 2019b). Effective antibiotic therapies are required to decrease the burden associated with *Salmonella* infections. The recent emergence and spread of multi-drug resistant (MDR) *Salmonella* strains have, however, led to decreased treatment success with corresponding increases in morbidity and mortality. These observations highlight the need to identify new drugs for the treatment of infections caused by this group of medically important bacteria (Carfrae *et al.*, 2020; Ellis *et al.*, 2019).

1.2 Classification and nomenclature of *Salmonella*

The genus *Salmonella* is a member of the *Enterobacteriaceae*, which are non-spore-forming, oxidase negative, catalase-positive, Gram-negative bacilli (Garrity, 2007; Popoff and Le Minor, 2015). *Salmonella* are facultative anaerobes and the majority of serovars display motility by peritrichous flagella. From an evolutionary perspective, they are thought to have diverged from a common ancestor with *Escherichia coli* approximately 100-150 million years ago. Based on differences in their 16s rRNA sequences, the genus is comprised of two species, *Salmonella enterica* and *Salmonella bongori*, (Fookes *et al.*, 2011; Grimont and Weill, 2007; Reeves *et al.*, 1989). *S. enterica* is the type species of the genus and is comprised of six subspecies (subsp. I, II, IIIa, IIIb, IV, and VI) based on differences in their biochemical and genomic properties (Boyd *et al.*, 1996; Reeves *et al.*, 1989). The six subspecies include the following: *S. enterica* subsp. *enterica* (subsp. I), *S. enterica* subsp. *salamae* (subsp. II), *S. enterica* subsp. *arizonae* (subsp. IIIa), *S. enterica* subsp. *diarizonae* (subsp. IIIb), *S. enterica* subsp. *houtenae* (subsp. IV), and *S. enterica* subsp. *indica* (subsp. VI). Of the six subspecies *S. enterica* subsp. *enterica* (subsp. I) is the most

widely distributed and is typically found in association with mammals. It is also responsible for the vast majority (> 99 %) of infections caused by *Salmonella* spp. in both humans, as well as other warm-blooded animals. *Salmonella bongori*, which was previously classified as *S. enterica* subsp. V before its elevation to the species level, together with the five remaining *S. enterica* subspecies are primarily associated with environmental reservoirs or cold-blooded animals. These *Salmonella* strains are not typically associated with disease in humans, although they may occasionally act as opportunistic pathogens in immunocompromised hosts (Farrar *et al.*, 2013; Lathrop *et al.*, 2015; Lê-Bury *et al.*, 2020).

In addition to the nomenclatural system described above, the genus can also be classified into serological variants (or serovars) according to the White-Kauffmann-Le Minor scheme. This system classifies *Salmonella* strains based on differences in specific surface antigens, which include the somatic (lipopolysaccharide O-antigen), flagellar (H-antigen), and Vi capsular (K-antigen, when present) antigens (Farrar *et al.*, 2013; Garrity, 2007; Grimont and Weill, 2007; Popoff and Le Minor, 2015). At present, 2,659 *Salmonella* serovars have been identified, with 1048 of these being classified as either *S. bongori* (22 serovars) or *S. enterica* subsp. II – VI (1026 serovars) (Grimont and Weill, 2007; Issenhuth-Jeanjean *et al.*, 2014). The remaining 1586 serovars belong to *S. enterica* subsp. *enterica* (subsp. I), which includes most of the pathogenic *Salmonella* serovars. To simplify the naming of the serovars, which employs species, subspecies, and serovar designations, the subspecies name is often omitted (Brenner *et al.*, 2000; Tindall *et al.*, 2005). According to this naming convention, the name of the genus is followed by that of the serovar, with the first letter of the serovar name capitalised and lacking italicization. *Salmonella enterica* subsp. *enterica* serovar Typhimurium can therefore be abbreviated as *Salmonella* Typhimurium or *S.* Typhimurium (*S.* Tm), which will be the naming convention used in the remainder of this document.

1.3 *Salmonella* Pathogenesis

1.3.1 Overview

S. enterica serovars can invade, replicate, and survive in a variety of mammalian cells. As such, they possess the potential to cause disease in a variety of susceptible human and animal species (Crump and Wain, 2017). The nature, course and severity of the disease are, however, dependent on several factors that include the identity of the infecting serovar, the host species infected, and the immune status of the host (Gal-Mor *et al.*, 2014). *S. enterica* serovars have traditionally been

categorised into two classes based on their host-range and the manifestation of disease following human infections (Eng *et al.*, 2015; Gal-Mor *et al.*, 2014). The Typhoidal *Salmonella* serovars, *S. enterica* subsp. *enterica* ser. Typhi (*S. Typhi*) and *S. enterica* subsp. *enterica* Paratyphi A, B and C (*S. Paratyphi* A, B and C), are human-restricted pathogens that cause the invasive, systemic disease known as enteric fever. The remaining *Salmonella* serovars are referred to as non-typhoidal *Salmonella* (NTS) serovars. The NTS serovars, which include *S. Typhimurium* and *S. enterica* subsp. *enterica* Enteritidis (*S. Enteritidis*), amongst others, are broad-host-range, zoonotic pathogens capable of infecting both humans and animals. In immunocompetent humans, the NTS serovars typically cause a self-limiting gastrointestinal disease. The NTS serovars are, however, capable of causing invasive, disseminated infections known as invasive NTS (iNTS) in immunocompromised individuals, which can often be fatal if left untreated (Gordon, 2011).

1.3.2 The Typhoidal *Salmonella* serovars and Enteric fever

Enteric fever is the collective name for typhoid and paratyphoid fever, which are life-threatening, systemic diseases caused by the Typhoidal *Salmonella* serovars *S. Typhi* and *S. Paratyphi* A, B, and C, respectively (Crump and Wain, 2017; Feasey and Gordon, 2013; Thompson *et al.*, 2018). These serovars are host-adapted to humans, with no other natural hosts or environmental reservoirs having been identified to date (Dougan and Baker, 2014; Gal-Mor *et al.*, 2014). The disease is relatively rare in developed countries, where public health measures such as good sanitation and the effective treatment of drinking water have effectively reduced the transmission of food-borne pathogens. The disease is, however, endemic in many parts of the world where access to proper sanitation facilities and potable water is limited (Lathrop *et al.*, 2015; Sánchez-Vargas *et al.*, 2011). The majority of cases of enteric fever occur in low- to middle-income countries located in either Asia/Oceania (85.9 % of all global cases) or sub-Saharan Africa (12.1 % of all global cases) (Stanaway *et al.*, 2019a). According to the most recent estimates, ~ 14.3 million cases of the disease occurred globally in 2017, of which 10.9 and 3.4 million were attributable to *S. Typhi* and *S. Paratyphi* infections, respectively (Stanaway *et al.*, 2019a). The mortality associated with infections caused by both organisms was ~ 135, 900 (Stanaway *et al.*, 2019a).

1.3.2.1 Clinical manifestations of enteric fever

Enteric fever is acquired via the ingestion of food or water contaminated with the faecal matter of individuals with either acute or chronic *S. Typhi* and *S. Paratyphi* infections (Crump and Wain, 2017; Feasey and Gordon, 2013). Following ingestion, the bacteria pass through the gastric cavity

to reach the intestinal tract, which they can occupy transiently without inducing a significant inflammatory response. The incubation period for enteric fever is dependent on the infecting *Salmonella* serovar and size of the inoculum but typically ranges from 10 - 20 days. The onset of enteric fever is initially characterised by non-specific symptoms, such as high and prolonged fever, headaches, malaise, abdominal pain, nausea, and vomiting (Farrar *et al.*, 2013; Gal-Mor *et al.*, 2014). If left untreated, the symptoms can become more severe, leading to inflammation of the small intestinal lymphoid tissues, bacteraemia, and hepato- and splenomegaly. In severe cases, the symptoms can include life-threatening symptoms such as intestinal perforation and peritonitis, gastrointestinal haemorrhage, septic shock, encephalopathy, meningitis, and delirium. Acute enteric fever infections can last for up to 4 weeks and can have a case fatality ratio as high as 10-30 % (Farrar *et al.*, 2013). This fatality rate can, however, be reduced to 1 - 4 % if antimicrobial therapy is administered promptly (see **Section 1.4**). Following recovery, ~ 2 - 5 % of individuals may remain chronically infected and continue to shed the bacteria in their stool for extended periods (Crump and Wain, 2017; Gonzalez-Escobedo *et al.*, 2011).

1.3.3 The Non-typhoidal *Salmonella* serovars

All *S. enterica* serovars other than *S. Typhi* and *S. Paratyphi* are classified as NTS serovars. These serovars are broad-host-range, zoonotic pathogens capable of infecting both animals and humans (Crump and Wain, 2017; Gordon, 2011; Gordon *et al.*, 2008). Disease in humans is, however, caused by a relatively few NTS serovars, with *S. Typhimurium* and *S. Enteritidis* accounting for > 50 % of all infections. Animals are the primary reservoir of the NTS serovars and the majority of NTS infections are acquired following the ingestion of contaminated foods of animal origin, such as poultry, eggs, or dairy products (Acheson and Hohmann, 2001). Transmission can also occur by direct contact with infected animals and their environments, or with infected humans (Wikswa *et al.*, 2015). Infection of immunocompetent individuals with NTS serovars typically produces a mild to moderate, self-limiting form of gastroenteritis (Crump and Wain, 2017; Thompson *et al.*, 2018). In 2017, the NTS serovars were collectively responsible for ~ 95.1 million cases of gastrointestinal disease globally, which were associated with ~ 51, 000 deaths (Stanaway *et al.*, 2019b). In addition to gastroenteritis, the NTS serovars are also capable of causing invasive, extraintestinal disease in immunocompromised individuals, referred to as “invasive NTS disease” (iNTS disease) (Crump and Wain, 2017; Gilchrist and MacLennan, 2019; Gordon, 2011; Lê-Bury *et al.*, 2020; Lê-Bury and Niedergang, 2018). In 2017, ~ 535, 000 cases of iNTS diseases were identified globally. The majority of these cases (~ 80 %) occurred in regions in sub-Saharan Africa,

where the disease is endemic (Stanaway *et al.*, 2019b). In contrast to NTS-induced gastroenteritis, iNTS infections are often life-threatening, with ~ 11 % (59,100) of all infected individuals succumbing to the disease in 2017.

1.3.3.1 Clinical manifestations of NTS infections

Infection of immunocompetent humans with the NTS serovars typically present as a mild to moderate gastroenteritis, which is localised to the terminal ileum, colon, and mesenteric lymph nodes (Hume *et al.*, 2017; LaRock *et al.*, 2015; Lê-Bury *et al.*, 2020; Lê-Bury and Niedergang, 2018). Following an incubation period of approximately 4 to 72 h, the disease is characterised by the acute onset of fever, nausea, vomiting, and abdominal pain (Farrar *et al.*, 2013). The NTS serovars also induce significant inflammation in the intestinal lumen and surrounding lymphoid tissues, which elicits diarrheal symptoms. In the majority of instances, the disease resolves after three to seven days, without the need for antimicrobial therapy or any other medical interventions besides fluid replenishment. Some patients may, however, develop long-term symptoms following recovery, which primarily include irritable bowel syndrome (IBS) or reactive arthritis (Keithlin *et al.*, 2015).

In contrast to the localised NTS infections described above, iNTS infections present as non-specific, febrile bacteraemia with few symptoms of gastrointestinal disease (Crump and Wain, 2017; Haselbeck *et al.*, 2017). The primary risk factors for iNTS infections include extremes of age, malnutrition, and the presence of immunosuppressive conditions or other co-morbidities (Stanaway *et al.*, 2019b). Individuals that fall within these risk groups are thought to have reduced immune responses in the gastrointestinal mucosa and associated lymphoid tissues that impede their ability to restrict the NTS serovars to the intestinal tract, resulting in their spread to systemic sites (Lathrop *et al.*, 2015; Lê-Bury *et al.*, 2020; Lê-Bury and Niedergang, 2018). The bacteria can subsequently establish focal infections at systemic sites, resulting in diseases such as meningitis, abscesses, septic arthritis, osteomyelitis, thoracic empyema, and pneumonia (Gal-Mor *et al.*, 2014; Herrero-Fresno and Olsen, 2018; Hume *et al.*, 2017; Sánchez-Vargas *et al.*, 2011). As with gastrointestinal infections, *S. Enteritidis*, *S. Typhimurium* and *S. Dublin* are the most common serovars associated with iNTS infections (Uche *et al.*, 2017). Whole-genome sequencing studies have revealed that the majority of iNTS infections in sub-Saharan Africa are caused by *S. Typhimurium* sequence type ST313 (Crump and Wain, 2017; Uche *et al.*, 2017). The greater ability of this strain to cause extraintestinal infections has been attributed to ST313 having undergone several genome degradation events similar to that observed in the Typhoidal serovars

(Pulford *et al.*, 2021). This suggests that ST313 may be undergoing a similar process of human host-adaptation. The greater disease severity and multidrug resistance phenotypes of ST313 are likely to represent a significant challenge for the control and prevention of infections caused by iNTS serovars in the future.

1.4 Treatment and Prevention of *Salmonella* infections

Gastrointestinal infections caused by the NTS serovars are self-limiting and antimicrobial therapy is generally not recommended (Acheson and Hohmann, 2001). Antibiotics may, however, be beneficial to patients with severe NTS infections, especially where individuals have immunosuppressive conditions. The effective treatment of invasive *Salmonella* infections, by contrast, requires the administration of antimicrobial therapy to reduce both the severity of disease and the risk of death (Crump *et al.*, 2015; Manesh *et al.*, 2021). Historically, a combination of chloramphenicol, ampicillin, and co-trimoxazole (trimethoprim-sulfamethoxazole) was used to treat infections caused by *S. Typhi* and *Paratyphi* (Manesh *et al.*, 2021). Multidrug-resistant (MDR) strains, which possess resistance to all three of these drugs have however emerged in the last three decades, leading to their discontinued use as first-line agents for the treatment of enteric fever (Marchello *et al.*, 2020). MDR has also been observed in NTS serovars over the same period, reducing the efficacy of these drugs for treating iNTS infections (Haselbeck *et al.*, 2017). At present, *Salmonella* infections are treated using a combination of fluoroquinolones, such as ciprofloxacin and ofloxacin, and third-generation cephalosporins that include ceftriaxone. Resistance to these drug classes has been observed in MDR Typhoidal *Salmonella* serovars over the last decade, leaving azithromycin as the only treatment option available for treating these extremely drug-resistant (XDR) isolates (Carey *et al.*, 2021; Haselbeck *et al.*, 2017; Manesh *et al.*, 2021). The recent emergence of azithromycin resistance has raised the prospect of potentially untreatable Typhoidal *Salmonella* infections (Sajib *et al.*, 2021), further highlighting the need for new therapeutic options for treating the disease.

In addition to antibiotic therapy, the control of *Salmonella* infections can be achieved by control measures designed to reduce disease transmission. These include eliminating animal reservoirs of infection during outbreaks or withdrawing the sale of contaminated animal foods or beverages (Acheson and Hohmann, 2001; Crump and Wain, 2017). Improved public health infrastructure and sanitation, hygiene measures such as handwashing, and the provision of safe drinking water will also assist in reducing disease transmission. Since humans represent the only host for the

Typhoidal *Salmonella* serovars, vaccination represents a viable strategy for the control and eradication of enteric fever (Milligan *et al.*, 2018; Stanaway *et al.*, 2019a). Several Typhoid vaccines, including the oral, live-attenuated Ty21a and Vi capsular polysaccharide vaccine, are currently available for the prevention of enteric fever caused by *S. Typhi*. These vaccines, however, have variable efficacy when administered to adults and do not protect infants and young children. A newer, conjugated Vi capsular polysaccharide vaccine has been shown to possess improved immunological properties, conferring protection to infants and young children and providing more durable protection than other vaccines (Milligan *et al.*, 2018; Stanaway *et al.*, 2019a). The Typhoid Conjugate vaccine (TCV) is consequently recommended for use by the World Health Organisation in endemic countries where the incidence of Typhoid fever is high, particularly when these are caused by infection with MDR or XDR *S. Typhi* isolates (World Health Organization, 2019). These Typhoid vaccines do not confer protection against *S. Paratyphi* infections, however, leaving transmission interruption as the primary means of controlling Paratyphoid fever. Due to the antigenic variation that exists between the various NTS serovars, there are currently no effective vaccines that confer protection against iNTS infections (Haselbeck *et al.*, 2017; Tennant *et al.*, 2016). Since animals are frequently the sole reservoir of NTS infections, the vaccination of livestock may be a viable strategy for minimising transmission to humans (Berry and Wells, 2018).

1.5 *Salmonella* Infection and the host environment

Infections with both typhoidal and NTS serovars are initiated following the consumption of *Salmonella*-contaminated food or water. While a large part of the inoculum is killed by host defences such as gastric acid, bile, and intestinal antimicrobial peptides, a sub-population of bacteria survives to reach the intestinal tract. Depending on the serovar, *Salmonella* can replicate predominantly in the intestinal lumen to cause localised enteritis, or invade the intestinal epithelium and lymphoid tissue and proceed to cause systemic disease (Fabrega and Vila, 2013). To invade cells of the epithelium, *Salmonella* must first traverse the intestinal mucus layer, which it accomplishes using a combination of flagellar motility and chemotaxis (Elhadad *et al.*, 2015).

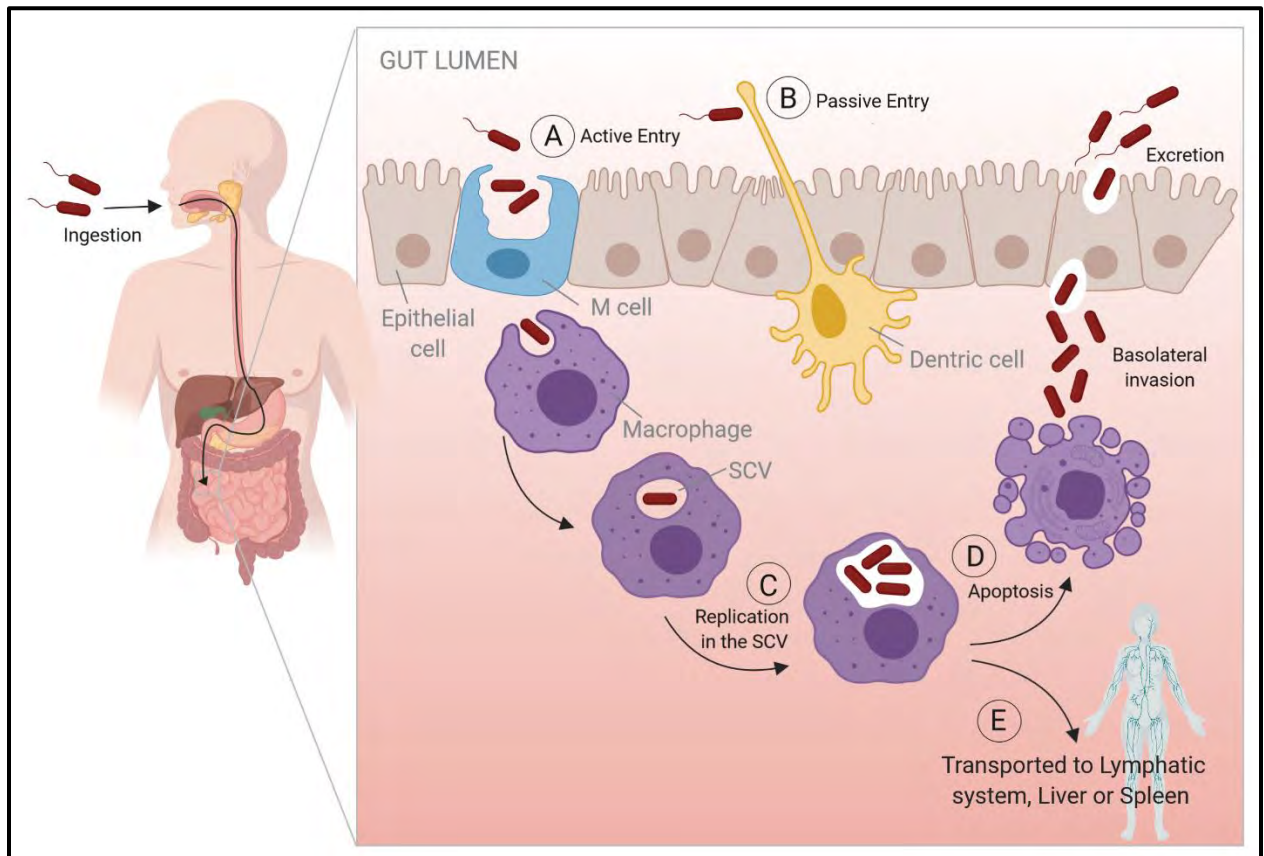


Figure 1.1: The infection scheme of pathogenic *Salmonella* species (Adapted from Gal-Mor, 2019, created with BioRender). See text for details.

Following its passage through the mucosal layer, *Salmonella* encounters several different types of host cells which it can enter using either active or passive uptake mechanisms (Ibarra and Steele-Mortimer, 2009). The primary mechanism of uptake involves the active invasion of either microfold cells (M-cells) in the Peyer's patch regions of the intestines, or non-phagocytic absorptive epithelial cells (enterocytes) (Haraga *et al.*, 2008; Jepson and Clark, 2001; Santos and Bäumlner, 2004), see **Figure 1.1 A**. The second mechanism of uptake involves passive entry into dendritic cells, which sample the intestinal lumen by projecting dendrites between the tight junctions of cells (Rescigno *et al.*, 2001), see **Figure 1.1 B**. The active invasion of cells by *Salmonella* requires the function of a Type Three Secretion System (TTSS), which is encoded by *Salmonella* Pathogenicity Island 1 (SPI1) on the *Salmonella* genome and is consequently known as the SPI1-TTSS (Galán, 1996; Kaniga *et al.*, 1995). The TTSSs are macromolecular syringe-like structures that are comprised of (i) a basal body composed of two ring-like structures that span the bacterial inner and outer membrane (ii) a needle complex that is attached to the basal body and extends away from the bacterial surface and (iii) a pore-forming translocon that inserts into the

host cell plasma membrane and delivers effector proteins into the host cells cytosol (Ellermeier and Slauch, 2007; Galán and Collmer, 1999). The expression of the SPI1-TTSS is up-regulated by the conditions *Salmonella* encounters in the intestinal environment, including high osmolarity, neutral pH and low O₂ tension, and the bacteria are consequently primed for invasion ahead of their encounter with intestinal epithelial cells (Galán, 2001). Following contact with host cells, the SPI1-TTSS is activated and translocates effector proteins from the bacteria into host cell cytosol, where they induce cytoskeletal rearrangements and plasma membrane ruffling (Fabrega and Vila, 2013; Hume *et al.*, 2017; Ibarra and Steele-Mortimer, 2009). These membrane ruffles extend around *Salmonella* leading to bacterial engulfment and their subsequent uptake into cells by macropinocytosis (LaRock *et al.*, 2015; Lê-Bury and Niedergang, 2018). Following internalisation, *Salmonella* is contained in a membrane-bound phagosomal compartment known as the *Salmonella*-containing vacuole (SCV) (Galán, 1996). The SCV serves as the primary niche for the growth and survival of *Salmonella* in the intracellular environment of both epithelial cells and phagocytic cells (see below) (Herrero-Fresno and Olsen, 2018; LaRock *et al.*, 2015; Rivera-Chávez and Bäumler, 2015; Thompson *et al.*, 2018). Immediately after its uptake into the host's cells, the SPI1-TTSS translocates several effector proteins across the SCV membrane whose function is to terminate the invasion process by reversing cytoskeletal rearrangements thereby returning the plasma membrane to its original state. The genes required for invasion, including those encoding the TTSS-1 and flagella, are subsequently repressed in the SCV, and the genes required for intracellular growth and survival are induced (Ellermeier and Slauch, 2007; Ibarra and Steele-Mortimer, 2009; Liu *et al.*, 2015; Park *et al.*, 2015b). Following the infection of cultured epithelial cells, a sub-population of bacteria may escape the SCV and enter the host cell cytosol (Knodler, 2015; Knodler *et al.*, 2014). These cytosolic bacteria replicate to higher numbers than vacuolar bacteria, a phenotype referred to as “hyper-replication”. The physiological significance of this population of bacteria is not currently known, and most intracellular bacteria remain housed within the SCV.

Once within the epithelial cells, *Salmonella* can alter the maturation process of the SCV to promote its intracellular growth and survival. This process is dependent on the expression of the second TTSS, known as the SPI2-TTSS, which is encoded on *Salmonella* Pathogenicity Island 2 (SPI2) (Hensel *et al.*, 1995; Hensel, 2000; Shea *et al.*, 1996). The expression of SPI2-T3SS genes are induced in response to the conditions encountered within the SCV, such as low pH and limited magnesium and phosphate availability (Deiwick *et al.*, 1999; Deiwick and Hensel, 1999). Once

formed, the SPI2–T3SS translocates approximately 30 effector proteins across the SCV membrane into the cytosol of the host cells. Several of these effector proteins alter vesicular trafficking to prevent fusion of the SCV with lysosomes or delivery of other antimicrobial effectors to the SCV (Chakravorty *et al.*, 2002; Jennings *et al.*, 2017). Approximately two hours after infection, the SCV migrates to a perinuclear region adjacent to the Golgi and microtubule organising centre, where the bacterium is capable of intercepting endocytic and exocytic vesicles (Abrahams *et al.*, 2006; Kuhle *et al.*, 2006; Salcedo and Holden, 2003). These are thought to provide *Salmonella* with a source of membranous material to expand the SCV during bacterial replication (Liss *et al.*, 2017; Ibarra and Steele-Mortimer, 2009). The membranous material is also used to form a network of tubular structures (Liss and Hensel, 2015), which are referred to as *Salmonella*-induced tubules or filaments (SITs or SIFs, respectively) (Knuff and Finlay, 2017). These SIFs extend away from the SCV and may provide *Salmonella* with increased access to endocytosed material, including nutrients while residing in the SCV (Krieger *et al.*, 2014; Liss *et al.*, 2017). While the precise mechanisms by which many of the SPI2-TTSS modulate the host function remain to be determined (Knuff-Janzen *et al.*, 2020), their combined action is essential for *Salmonella* growth and survival in the intracellular environment.

Following its invasion and replication within cells of the intestinal epithelium, some SCV bound *Salmonella* migrate from the apical to the basolateral side of infected cells and are released into the sub-mucosal space. Here, *Salmonella* encounters resident mononuclear phagocytes such as macrophages and dendritic cells, which are capable of internalising *Salmonella* by phagocytosis (**Figure 1.1**) (Tam *et al.*, 2008). Following their uptake by phagocytic cells, *Salmonella* is again contained within an SCV, which has many of the properties listed for epithelial cells above. The subsequent course of disease usually follows two trajectories, depending on the infecting *Salmonella* serovar (Fabrega and Vila, 2013; Gal-Mor *et al.*, 2014). During infection with NTS serovars, the invasion and entry of bacteria into the sub-mucosal space activates pattern recognition receptors present on phagocytic cells, eliciting an inflammatory response. This results in the recruitment of neutrophils, which are usually capable of efficiently killing any NTS serovars present in the intestinal lumen or sub-mucosal space. The intracellular replication of these serovars in epithelial cells may also activate inflammasomes and induce pyroptosis (Crowley *et al.*, 2016), which contributes to intestinal inflammation. The inflammatory response and damage caused by neutrophils promote water loss into the intestinal lumen, producing the symptoms of enteritis and diarrhoea. The antibacterial activity of neutrophils, together with several other innate immune

effector mechanisms, are nevertheless sufficient to prevent dissemination of the infecting NTS serovars beyond the intestinal lumen and associated lymphoid tissues.

The typhoidal *Salmonella* serovars, by contrast, do not activate a significant inflammatory response while present in the intestinal lumen or following their invasion of intestinal epithelium cells and entry into the submucosal space. This lack of inflammation during infection is thought to be attributable to the presence of the Vi capsular polysaccharide, which may mask the lipopolysaccharide and other surface antigens present on the bacterial surface and prevent neutrophil recruitment. Following their uptake by mononuclear phagocytes, the Typhoidal *Salmonella* serovars can enter the mesenteric lymph nodes and disseminate systemically to gain access to various organs, including the liver, spleen, and bone marrow, where they are capable of replicating within both epithelial cells and phagocytes. From the liver, the bacteria can gain access to the gallbladder, where they can establish chronic infections. The bacterium can subsequently re-enter the intestinal lumen via the bile ducts and be shed in the faeces to be transmitted to the next host.

The pathogen used in this study, *S. Typhimurium* (*S. Tm*), causes disease in humans and animals. While the NTS serovar causes gastrointestinal infections in humans, it can also cause a Typhoid-like systemic infection in susceptible mice strains, such as the C57BL/6 and BALB/c strains (Fabrega and Vila, 2013). This, together with its simple growth requirements, make it a good model organism for conducting studies of the pathogenesis of both gastrointestinal infections in humans, as well as systemic disease using the murine model of infection.

1.6 *Salmonella* metabolism in the host

Infections caused by drug-sensitive *Salmonella* strains can be successfully treated with existing classes of antibiotics. The increase in antibiotic drug resistance has, however, led to the need to identify drugs that inhibit targets that have not yet evolved resistance mechanisms. During infection, *Salmonella* must acquire nutrients to survive and replicate, while also withstanding the antimicrobial effects of the host's innate immune system (Dandekar *et al.*, 2015; Haraga *et al.*, 2008; Tam *et al.*, 2008). While the mechanisms by which *Salmonella* achieves the latter has been an area of active investigation, relatively little is known about how the bacterium adjusts its metabolism to survive in the various environments it inhabits during infection (Dandekar *et al.*, 2015; Tam *et al.*, 2008). The identification of metabolic pathways required for the growth of *Salmonella* under nutrient limiting conditions may facilitate the identification of antibacterial

compounds that target either the biosynthesis or uptake of essential nutrients. The nutritional profile encountered by *Salmonella* residing in the intestinal lumen differs significantly from that encountered during systemic infections, however, and these will be briefly discussed below.

1.6.1 The nutritional environment in the intestinal lumen

The intestinal lumen is a relatively nutrient-rich environment due to the large amounts of dietary carbohydrates, proteins, and lipids that enter the environment. While *S. Tm* does not produce any secreted proteases or glycosidases, it can utilise peptides, oligosaccharides, and fatty acids released from these macromolecules following their hydrolysis by saccharolytic and proteolytic members of the microbiota (Thiennimitr *et al.*, 2012). Commensal microorganisms also produce large amounts of short-chain fatty acids (SCFA) such as acetate, propionate, and butyrate as end products of the fermentation of carbohydrates, which can be utilised as a carbon-source by *Salmonella* when present at low concentrations. *S. Tm* can also utilise microbiota-generated hydrogen, formate, and lactate by anaerobic respiration when suitable electron acceptors such as nitrate, tetrathionate, and thiosulphate are available (Nuccio and Bäumlér, 2014). Many of these electron acceptors are produced during the inflammatory response to *Salmonella* infection, and the ability to utilise these are thought to provide *Salmonella* with a competitive advantage over commensal microorganisms thus promoting its growth and transmission. The inflammatory response has also been shown to reduce the levels of butyrate-producing members of the microbiota (Rivera-Chávez *et al.*, 2016). The decrease in butyrate levels that ensues causes host-cells to increase the concentrations of lactate and oxygen in the intestinal lumen (Gillis *et al.*, 2018). As a facultative anaerobe, *S. Tm* can switch to metabolising lactate by aerobic respiration under these conditions, which allows it to outcompete the commensal bacteria in the intestinal lumen, the majority of which are strict anaerobes.

In addition to carbohydrates of dietary origin, *S. Tm* can also utilise host-derived macromolecules such as mucins as a nutrient source (Best and Kwaik, 2019; Drecktrah *et al.*, 2006; Ng *et al.*, 2013; Tailford *et al.*, 2015). Mucins contain several fermentable sugar groups including galactose, fucose, sialic acid, N-acetyl-galactosamine, and N-acetyl-glucosamine which *S. Tm* can utilise following their release by saccharolytic bacteria, or via the production of native sialidases and sialic acid uptake systems (Arabyan *et al.*, 2016; Ng *et al.*, 2013; Severi *et al.*, 2010). Phospholipids such as phosphatidylcholine and phosphatidylethanolamine can also be utilised by *Salmonella* after their conversion to trimethylamine and ethanolamine by lipolytic bacteria, respectively. *S. Tm* can ferment both 1,2-propanediol, which is produced by the fermentation of fucose or

rhamnose by saccharolytic bacteria, and ethanolamine under anaerobic conditions in a vitamin B₁₂-dependent manner (Faber *et al.*, 2017; Thiennimitr *et al.*, 2011). Ethanolamine is converted to ammonia, acetaldehyde, and acetyl-coA and *S. Tm* can consequently use it as the sole source of carbon and nitrogen (Thiennimitr *et al.*, 2011). Due to the high concentration and diverse range of nutrients available, the growth of *Salmonella* is thought to be seldomly constrained in the intestinal environment and the bacterium can consequently replicate to high levels to promote its onward transmission into the environment.

1.6.2 The nutritional environment in the SCV

The nutrients available to *Salmonella* during intracellular growth in the SCV are far more limited than that within the intestinal environment (Kehl *et al.*, 2020; Satiaputra *et al.*, 2016; Sprenger *et al.*, 2018). Due to the technical challenges associated with determining the nutritional composition of isolated phagosomal compartments, the nutritional profile of the SCV has not been directly measured to date (Holtkötter and Hensel, 2016). The majority of information regarding the nutritional environment encountered within the SCV has therefore been extrapolated from transcriptional or proteomic profiling of *Salmonella* isolated from infected cells, animal hosts, or by the phenotypic analysis of the growth of mutant strains during infection.

Glucose is thought to be the primary carbon source utilised by *S. Tm* in the intracellular environment since bacterial mutants defective for glucose uptake, glycolysis, and the TCA cycle are attenuated during the infection of cultured cells and murine infections (Bowden *et al.*, 2009; Lundberg *et al.*, 1999; Noster *et al.*, 2019a; Noster *et al.*, 2019b). In contrast to the intestinal environment, anaerobic respiration and fermentation are dispensable for *Salmonella* replication in macrophages and epithelial cells (Garcia-Gutierrez *et al.*, 2016). The activity of ATP synthase and other respiratory components are required in cultured cells, suggesting that *S. Tm* may meet its energy requirements by either oxidative or substrate-level phosphorylation during systemic infections (Garcia-Gutierrez *et al.*, 2016). Fatty acids appear to play a limited role in supporting the growth of *Salmonella* in the SCV, since mutants defective for gluconeogenesis, the glyoxylate bypass, and fatty acid metabolism are not required for systemic infections (Tchawa Yimga *et al.*, 2006). *Salmonella* has the biosynthetic capacity to synthesise all amino acids from precursors derived from the central metabolic pathways. The biosynthetic operons for several amino acids have been shown to be upregulated following infection of host cells (Kröger *et al.*, 2013; Shi *et al.*, 2006; Shi *et al.*, 2009a; Srikumar *et al.*, 2015), suggesting that the SCV environment has limited access to host-cell amino acids. This is supported by the observation that several amino

acid auxotrophs, including those for aspartate, arginine, proline, and the aromatic amino acids, are attenuated for growth in cultured cells and during murine infections (Fields *et al.*, 1986; Hölzer and Hensel, 2012; Park *et al.*, 2011, 2015a; Popp *et al.*, 2015). The growth defects associated with the amino acids auxotrophy may, however, be restored by supplementation with exogenous amino acids suggesting that *S. Tm* may have access to these nutrients in infected hosts (Hölzer and Hensel, 2012; Park *et al.*, 2011, 2015a; Popp *et al.*, 2015). The attenuation observed for *Salmonella* uptake mutants lacking the transporters for methionine and arginine would support this idea (Das *et al.*, 2010). The study of Becker *et al.* (2006) revealed that *Salmonella* may also be capable of acquiring nucleosides and vitamins during infection of the murine host, which is supported by the reduced growth observed for catabolic and transporter mutants involved in these pathways (Becker *et al.*, 2006).

In addition to organic compounds, host cells often attempt to reduce the availability of transition metals and other inorganic compounds such as Fe^{2+} , Zn^{2+} , Mg^{2+} , and phosphate from pathogens during infection in a phenomenon referred to as nutritional immunity (Hennigar and McClung, 2016). The expression of the genes for several metal-uptake systems, including those for iron, manganese, magnesium, and zinc are upregulated in the SCV environment (Kröger *et al.*, 2013; Röder *et al.*, 2020; Röder and Hensel, 2020; Srikumar *et al.*, 2015), indicating that these metals are present in limited amounts in this environment. While potassium is readily available in the SCV and cytosol of host cells, phosphate is present in limiting amounts and the expression of a phosphate transporter is consequently required to sustain the growth of *S. Tm* in the SCV (Röder *et al.*, 2020). The latter study also showed that the genes for the *de novo* biosynthesis of biotin were induced in the SCV of both epithelial cells and macrophages, confirming the findings of several previous studies (Hautefort *et al.*, 2008; Kröger *et al.*, 2013; Shi *et al.*, 2006; Srikumar *et al.*, 2015). The role of the biotin uptake in sustaining the growth of *S. Tm* in the SCV has not, however, been investigated to date and serves as the topic of the current study.

1.7 Biotin Metabolism

Biotin (vitamin B7 or H) is a water-soluble member of the B-complex group of vitamins and is essential for the viability of organisms present in all three domains of life (McMahon, 2002; Polyak and Chapman-Smith, 2013; Zemleni, 2005; Zemleni *et al.*, 2009). The cofactor is required for the activity of several biotin-dependent enzymes that participate in the transfer of CO_2 in metabolic pathways such as fatty acid biosynthesis, amino acid catabolism, and gluconeogenesis (Zemleni,

2005). In microorganisms, biotin can either be supplied by the *de novo* biosynthesis of the vitamin, or by its transport from the extracellular growth environment (Salaemae *et al.*, 2016). While some microorganism can meet their biotin requirements through either of these pathways, others can only supply biotin through its biosynthesis or uptake. Humans and other mammals, by contrast, lack the enzymes required for the *de novo* biosynthesis of biotin and must acquire the vitamin from their diet and/or their intestinal microbiota (McMahon, 2002; Zempleni, 2005). The absence of the biotin biosynthetic pathways in humans, nevertheless, makes biotin biosynthesis an attractive target for the development of new antimicrobial drugs (Carfrae *et al.*, 2020; Salaemae *et al.*, 2016).

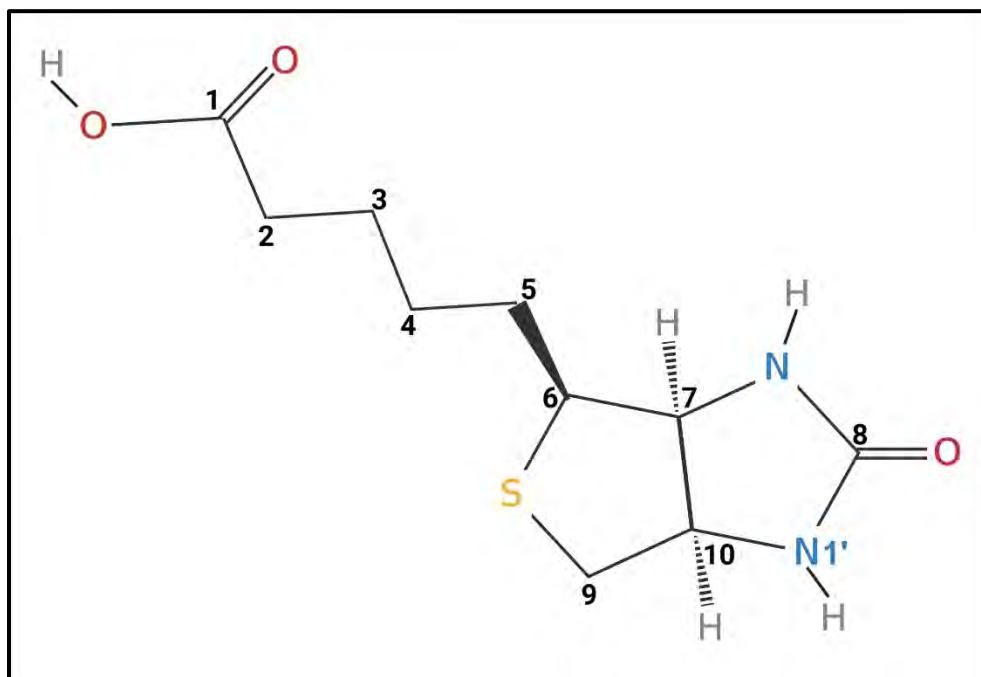


Figure 1.2: Chemical structure of biotin (adapted from Cronan, 2014, created with BioRender). The biotin molecule has a bicyclic ring structure comprised of a fused ureido and sulphur-containing tetrahydrothiophene ring. The tetrahydrothiophene ring is attached to a valerate side chain. The first seven carbon atoms (C1 to C7) of biotin are derived from pimelic acid (see text for details). During CO₂ transfer reactions the N1' atom of biotin, located between C8 and C10, is carboxylated to form carboxybiotin.

1.7.1 Biological roles of biotin

The primary role of biotin is to serve as a covalently bound cofactor for enzymes that catalyse carboxylation reactions in eukaryotic and prokaryotic cells, as well as some decarboxylation or transcarboxylation reactions in bacteria and fungi (Tong, 2013; Waldrop *et al.*, 2012). Biotin-

dependent enzymes are synthesized as enzymatically inactive apoenzymes that become active holoenzymes following the covalent attachment of biotin (Tong, 2013). The attachment of biotin to the biotin-dependent apoenzymes is mediated by holocarboxylase synthetases (also known as biotin-protein ligase) and occurs via the formation of an amide bond between a conserved lysine residue in the apoenzymes and the valerate moiety of biotin. Mammalian cells contain five biotin-dependent carboxylases; two acetyl-CoA carboxylases (ACCs, ACC1 and ACC2), propionyl-CoA carboxylase (PCC), β -methyl-crotonyl CoA carboxylase (MCC), and pyruvate carboxylase (PC). Here, the enzymes play major roles in fatty acid metabolism (ACC and PCC), amino acid catabolism (MCC), and gluconeogenesis (PC) (Zempleni *et al.*, 2009).

While several exceptions exist, microorganisms generally encode fewer biotin-dependent enzymes than mammals (Cronan, 2014; Salaemae *et al.*, 2016; Zempleni *et al.*, 2009). *E. coli*, for instance, contains ACC as its only biotin-dependent enzyme (Cronan, 2014). ACC catalyses the conversion of acetyl-CoA to malonyl-CoA, the first committed step in fatty acid biosynthesis. The activity of ACC is required for phospholipid biosynthesis and membrane biogenesis and it is therefore essential for the viability of *E. coli* and most other microbes under all growth conditions. In addition to ACC, *S. Tm* contains a second biotin-dependent enzyme, oxaloacetate decarboxylase (ODC), a transmembrane protein involved in citrate transport (Cronan, 2014). Unlike ACC, ODC is only required for the growth of *S. Tm* under anaerobic growth conditions when citrate is present as the sole carbon source. Other microorganisms may also contain additional biotin-dependent decarboxylases and transcarboxylases (Waldrop *et al.*, 2012). Like ODC, the activities of these enzymes are typically restricted to certain groups of microorganisms where they typically have specialised functions, and they will therefore not be discussed here further.

1.7.2 Biotin Metabolism

Microorganisms meet their biotin requirements through biosynthesis *de novo* or via transport from the environment. The mechanisms known to be utilised by microorganisms for each of these processes will be briefly discussed in the following section, and compared to that found in other species, where relevant.

1.7.2.1 Biotin biosynthesis

In enteric bacteria such as *E. coli* and *S. Tm*, the biotin atoms are derived from acetate, CO₂, alanine, S-adenosyl-L-methionine, and sulphide (Cronan, 2014; Salaemae *et al.*, 2016; Sirithanakorn and Cronan, 2021). Biotin biosynthesis from these precursors occurs in two clearly

defined stages: the “early stage” and “late stage”. The early stage is responsible for the synthesis of a thioester-activated form of pimelate [i.e. either pimelate-acyl carrier protein (ACP) or pimeloyl-coA], a seven carbon dicarboxylate used to form the valerate side chain and first two thiophene ring carbons of the biotin molecule (Sirithanakorn and Cronan, 2021). The late stage of biotin biosynthesis is involved in the completion of the ureido and thiophene heterocyclic rings. While the reactions of the late stage are performed by enzymes and metabolic pathways that are conserved in the majority of microorganisms studied to date, the synthesis of pimelate can be generated by several different means, depending on the microorganism.

1.7.2.1.1 The early stage of biotin biosynthesis

The pimeloyl-ACP generated by enteric bacteria during the early stage of biotin biosynthesis is derived from 3 molecules of acetate, which is used to form malonyl-ACP and CO₂. Its synthesis requires the activity of two biotin biosynthetic enzymes, BioC and BioH (Cronan, 2018; Lin and Cronan, 2011). The former enzyme, BioC, is S-adenosyl-L-methionine (SAM)-dependent O-methyltransferase that initiates the synthesis of pimeloyl-ACP by methylating the free carboxyl group of malonyl-ACP (Lin *et al.*, 2010). This results in the formation of a malonyl-ACP methyl ester, which can serve as a substrate for elongation by the fatty acid biosynthetic enzymes, FabG, FabZ, and FabI (Lin *et al.*, 2010). Following two rounds of elongation by these enzymes, a pimeloyl-ACP methyl ester is produced. The end of the early stage is reached when BioH, a short-chain fatty acid esterase, removes the methyl group of the pimeloyl-ACP methyl ester to produce pimeloyl-ACP (**Figure 1.3**). The pimeloyl-ACP released subsequently enters the lower pathway for conversion into biotin by BioF, as described below (**Section 1.7.2.1.2**). In certain bacterial species, the activity of BioH can be replaced by six structurally distinct pimeloyl-ACP methyl esterases, which include BioG, BioJ, BioK, BioV, BtsA, and BioU_h (reviewed by Sirithanakorn and Cronan, 2021). While the BioG enzyme appears to be widely distributed amongst different bacterial species, the remaining biosynthetic enzymes appear to be limited to only a few bacterial species. The activity of BioC can also be replaced by BioW, BioI, or BioZ in some bacterial species. These enzymes convert pimelate into either pimelate-CoA or pimeloyl-ACP, which can subsequently be recognised as a substrate by the enzyme BioF in the late stage of biotin biosynthesis (Manandhar and Cronan, 2017).

1.7.2.1.2 The late stage of biotin biosynthesis

During the late stage of biotin biosynthesis, the pimelate thioester is converted into biotin by four biotin biosynthetic enzymes that are highly conserved in the majority of biotin-producing

microorganisms (**Figure 1.3**). These enzymes include 7-keto-8-aminopelargonic acid (KAPA) synthase (BioF), 7,8-diaminopelargonic acid (DAPA) synthase (BioA), dethiobiotin synthetase (BioD) and biotin synthase (BioB) (Knowles, 1989; Sirithanakorn and Cronan, 2021). The late-stage is initiated by BioF, which catalyses the condensation of pimeloyl-ACP or pimeloyl-CoA and alanine to produce KAPA. The aminotransferase BioA then transaminates KAPA to yield DAPA, using SAM as an amino group donor. BioD then mediates the completion of the ureido ring by catalysing the ATP-dependent carboxylation of the nitrogen atoms of DAPA to generate dethiobiotin. In the final step of the biotin biosynthesis, BioB catalyses the SAM-dependent closure of the thiophene ring by inserting a sulphur atom between the methyl and methylene carbons of dethiobiotin. BioB is an iron-sulphur cluster protein that contains two different clusters: an air-sensitive [4Fe-4S] and air-insensitive [2Fe-2S] cluster. A sulphur atom within the [2Fe-2S] cluster is believed to provide the sulphur atom required for biotin synthesis. The loss of this sulphur atom results in the inactivation of the BioB enzyme and its continuous expression is therefore required to maintain sufficient levels of biotin biosynthesis.

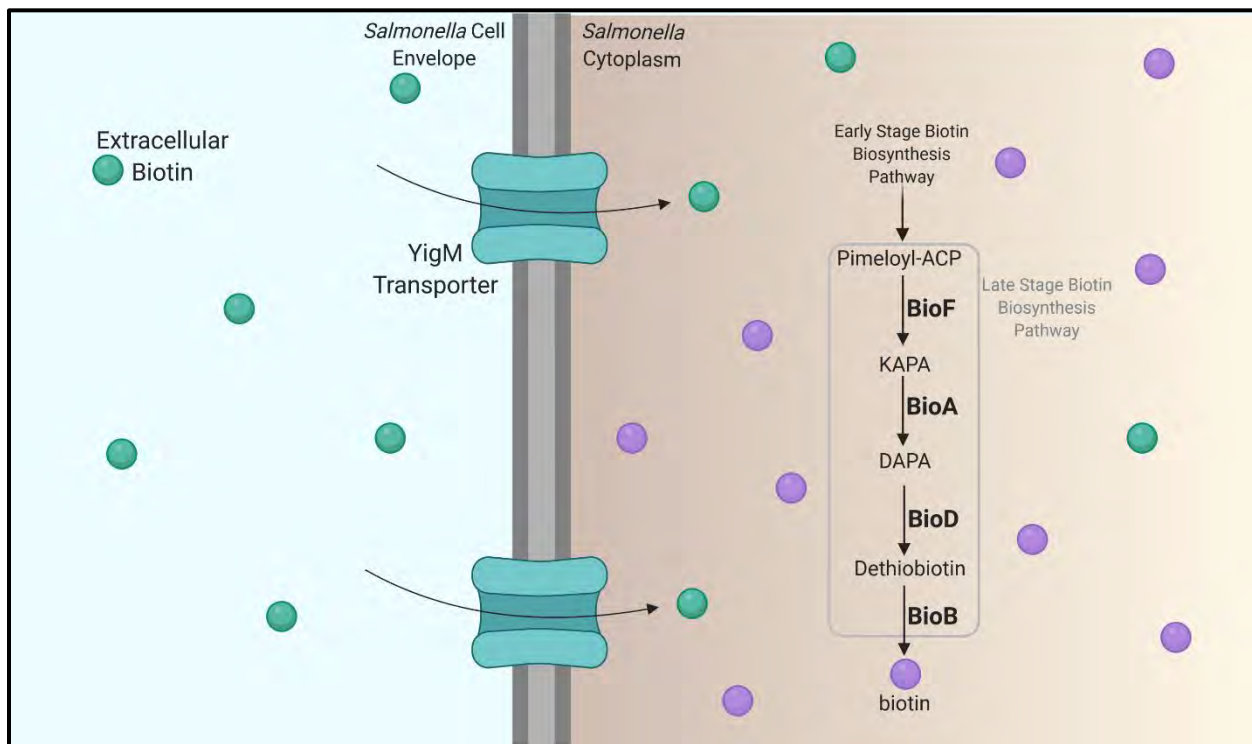


Figure 1.3: Schematic diagram of the late stage biotin biosynthesis pathway and putative biotin transporter YigM (adapted from Finkenwirth, Kirsch and Eitinger, 2013, created with BioRender). See text for details.

1.7.2.1.3 The *bio* operon and its regulation

In enteric bacteria, the genes encoding the biotin biosynthetic enzymes are clustered in a bi-directional operon known as the “*bio* operon” (Rodionov *et al.*, 2002; Sirithanakorn and Cronan, 2021). As depicted in **Figure 1.4**, the region of the operon oriented to the right includes the genes that encode four of the biotin biosynthetic enzymes, *bioB*, *bioF*, *bioC*, and *bioD*. The operon oriented to the left includes the *bioA* gene and an additional, downstream open reading frame of unknown function. While the *bioH* gene is often found upstream of *bioC* in many bacterial species, it is encoded outside of the *bio* operon in both *E. coli* and *S. Tm*. Transcription of the *bio* operon occurs from two divergently oriented promoters located within the *bioA-bioBFCD* intergenic region. These promoters share a common 40 bp operator site known as *bioO*, which serves as a binding site for a bifunctional regulatory protein, BirA (for biotin retention protein A).

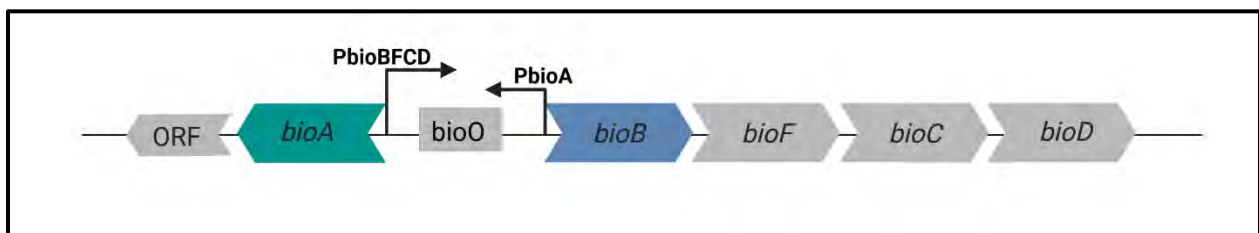


Figure 1.4: Schematic diagram of the bi-directional *bio* operon (adapted from Streit and Entcheva, 2003, created with BioRender)

In enteric bacteria, BirA serves as both the transcriptional repressor of the *bio* operon and as a biotin-protein ligase. The ability of BirA to serve as a transcriptional repressor of the *bio* operon is dependent on the formation of a complex between BirA and biotin-AMP, which is initiated by binding of biotin and ATP to the monomeric form of BirA. Under biotin replete conditions, the formation of the BirA-biotin-AMP complex is favoured. BirA can subsequently transfer the biotin to the conserved lysine residues of biotin-dependent apoenzymes to form the active holoenzyme. The formation of the BirA-biotin-AMP complex under biotin replete conditions also promotes the formation of a dimeric form of BirA, which enables the protein to bind to *bioO* and repress expression of the biotin biosynthetic genes. In the absence of biotin, the levels of the BirA-biotin-AMP complex decreases, promoting the formation of the monomeric form BirA, which is unable to bind to *bioO*. This results in the de-repression of the *bio* operon in the absence of biotin, and an increase in the levels of the biotin biosynthetic enzymes. Overall, the regulation of the *bio* operon by BirA ensures that the *bio* operon is maximally expressed when the supply of biotin is limited and the corresponding levels of monomeric, BirA-biotin-AMP complex low. Conversely, *bio* operon expression is repressed when the supply of biotin, as well as levels of dimeric BirA-biotin-

AMP complex, are high. This mode of regulation ensures that the synthesis of biotin, which is energetically expensive, does not occur when sufficient levels of exogenous biotin are available to meet cellular needs.

1.7.2.2 Biotin Transport

As discussed above, some organisms are biotin auxotrophs that lack the capacity to synthesise biotin *de novo*. To acquire biotin, these organisms possess transport mechanisms that facilitate the binding and import of extracellular biotin from into the cell. Since biotin biosynthesis is energetically costly, expending up to 19 ATP equivalents per molecule, many biotin prototrophs also possess biotin transporter proteins to circumvent the need to synthesise the vitamin when it is readily available in the environment (Jaehme and Slotboom, 2015).

1.7.2.2.1 Biotin transport in mammals

Since mammals lack the enzymes for biotin biosynthesis, they must acquire biotin from exogenous sources (McMahon, 2002; Zempleni *et al.*, 2009). The primary biotin transporter in mammalian cells is the sodium-dependent multivitamin transporter (SMVT) (Prasad *et al.*, 1998). The SMVT protein contains twelve membrane-spanning helices and is expressed in cells and tissues found throughout the body. The transporter mediates the active transport of biotin, as well as that of two other water-soluble vitamins, pantothenate and lipoate. A second transporter, the monocarboxylate transporter 1 (MCT1), can also transport biotin as well as other monocarboxylic acids. MCT1's role in biotin transport is, however, limited to cells of the lymphoid lineage and potentially mitochondria (Daberkow *et al.*, 2003). Once inside the cell, biotin can be covalently attached to the mammalian biotin-dependent carboxylases discussed in **Section 1.7.1**.

1.7.2.2.2 Biotin transport by bacteria

Biotin transport in bacteria is mediated primarily by members of the energy coupling factor (ECF) family of transporters (Hebbeln *et al.*, 2007), a sub-class of the energy-dependent ATP-binding cassette transporters (Finkenwirth and Eitinger, 2019; Thomas and Tampé, 2020). The ECF transporters are comprised of a membrane-bound, substrate-binding component (the S-component), which can interact with an “energising module” composed of a transmembrane component (the T-component) and pair of ATPase components (the A-components, A1, and A2). The ECF components may be encoded in the same operon (Class I ECF transporters), or the S-component may be encoded on the genome apart from the operon encoding the energising module's T and A components (Class II ECF transporters). The Class II biotin transporter of

Rhodobacter capsulatus has been extensively characterised and is composed of BioY, BioM, and BioN as the S, A, and T components, respectively (Finkenwirth *et al.*, 2013; Finkenwirth and Eitinger, 2019). Studies have shown that BioY can function as a low-affinity biotin transporter when expressed in *E. coli* in the absence of the BioMN energising module (Finkenwirth *et al.*, 2013). Following its interaction with the BioMN components, however, BioY is converted into a high-affinity biotin transporter (Finkenwirth and Eitinger, 2019; Hebbeln *et al.*, 2007). The Class I ECF biotin transporters of other organisms have been shown to function similarly to the *R. capsulatus* BioMNY (Finkenwirth and Eitinger, 2019). Interestingly, some organisms that encode BioY have been shown to lack homologues of BioM and BioN, or any other AT modules. This suggests that the BioY proteins of these organisms may only be capable of mediating low-affinity biotin transport.

Many microorganisms lack homologues of BioY and biotin transport has to be mediated by an alternative transporter. Biotin transport in *E. coli* was recently confirmed to be performed by YigM, a transmembrane protein belonging to the carboxylate/amino acid/amine family of secondary transporters (Finkenwirth *et al.*, 2013; Ringlstetter, 2010). The transporter consists of 299 amino acids and is predicted to contain ten transmembrane helices (Finkenwirth *et al.*, 2014; Salaemae *et al.*, 2016). In *E. coli*, the inactivation of YigM results in dramatically reduced rates of biotin uptake (Finkenwirth *et al.*, 2013), while its overexpression leads to increased rates of biotin uptake (Ringlstetter, 2010). The simultaneous disruption of biotin biosynthesis and YigM, furthermore, produced a strain that is unable to grow in the presence of trace amounts of biotin (<100 nM) (Finkenwirth *et al.*, 2013, 2014). While homologues of YigM have been identified in a wide range of Gamma- and Epsilon-proteobacteria (Carfrae *et al.*, 2020), the biological role of relatively few of these homologues in biotin transport have been experimentally validated to date (Xiao *et al.*, 2020). The precise mechanism of YigM-mediated biotin transport has not yet been established to date, although it is thought to occur via a facilitated diffusion or proton-coupled symport mechanism (Jaehme and Slotboom, 2015).

1.8 Rationale

S. Tm is a biotin prototroph and contains all the genes required for the biosynthesis of biotin (Cronan, 2014). The configuration of the biotin biosynthetic genes in the *bio* operon is identical to that described for *E. coli*, and the genes are similarly regulated by BirA in response to the availability of biotin in the environment (Cronan, 2014). Several lines of evidence have suggested that biotin is important for the intracellular growth of *S. Tm* during infection. Firstly, a combination of transcriptomic and proteomic studies have shown that the biotin biosynthesis pathway is induced following infection of HeLa epithelial cells and RAW264.7 macrophages *ex vivo*, suggesting that biotin may be limited in the intracellular environment (Denkel *et al.*, 2013; Eriksson *et al.*, 2003; Hautefort *et al.*, 2008; Liu *et al.*, 2015; Shi *et al.*, 2009a). Studies designed to investigate the importance of biotin biosynthesis during infection *ex vivo* or *in vivo* have, however, yielded contradictory results. The study of Denkel *et al.*, (2013), for instance, showed that a $\Delta bioB$ auxotrophic mutant was attenuated following infection of RAW264.7 macrophages (Denkel *et al.*, 2013). Genetic inactivation of the biotin biosynthetic pathway, by contrast, did not affect the ability of *S. Tm* to replicate within HeLa epithelial cells, or during the murine model of infection (Chaudhuri *et al.*, 2009; Hautefort *et al.*, 2008; Husna *et al.*, 2019). These contrasting observations may be attributable to *S. Tm*'s ability to transport biotin under certain growth conditions encountered during infection, which would enable the requirement for the *de novo* biosynthetic pathway to be circumvented. The molecular mechanisms used by *S. Tm* to transport biotin has, however, not been determined to date. The current study was therefore designed to (i) confirm the identity of the biotin transporter in *S. Tm* and (ii) determine the relative importance of the biotin biosynthetic and transport pathways for the growth and survival of *S. Tm* in the intracellular environment. Understanding how biotin synthesis and transport in *S. Tm* is regulated may provide insights into potential targets for the development of antimicrobials to combat infections caused by this organism.

1.9 Aims and objectives

The specific objectives for this study were, therefore:

- 1) To generate *S. Tm* $\Delta bioB$ and $\Delta yigM$ single mutant strains that are deficient in the biotin biosynthetic and putative transport pathways, respectively.
- 2) To generate an *S. Tm* $\Delta bioB \Delta yigM$ double mutant that is deficient in both the biotin biosynthetic and putative transport pathways.

- 3) To generate genetically complemented versions of the *S. Tm* mutant strains for phenotypic analysis *in vitro*.
- 4) To generate *S. Tm* $\Delta bioB$ $P_{BAD}::\Delta yigM$ promoter replacement strain for evaluating YigM function.
- 5) To confirm the role of YigM in biotin transport by evaluating the effect of silencing *yigM* expression in the promoter replacement strain.
- 6) To confirm the role of YigM in biotin transport by evaluating the effect of chemically inhibiting biotin biosynthesis with a BioA inhibitor.
- 7) To evaluate the growth phenotypes of the biotin biosynthesis and transport mutants during the growth of *S. Tm* *in vitro*.
- 8) To evaluate the growth phenotypes of the biotin biosynthesis and transport mutants following infection of HeLa epithelial cells and RAW264.7 macrophages.
- 9) To examine the vulnerability of the biotin biosynthetic pathway to chemical inhibition in the intracellular environment.

Chapter 2: Materials and Methods

2.1 Bacterial strains

A complete list of the strains used and generated in this study is listed in **Table 2.1**. *Salmonella enterica* subsp. *enterica* serovar Typhimurium 14028s was obtained from the *Salmonella* Genetic Stock Center (SGSC) at the University of Calgary and was used as the wild-type (WT) and parental strain for the construction of all mutants during this study. *Escherichia coli* BW25113 was acquired from the *E. coli* Genetic Stock Center (CGSC) at Yale University. *E. coli* DH5 α , Mach1-T1^R, and Omnimax Mach1-T1^R were purchased from ThermoFisher Scientific and used for the routine maintenance and propagation of plasmids.

2.2 Bacterial media, growth and storage conditions

Bacterial strains were routinely grown under aerobic conditions at 37 °C in Luria broth (LB) [1 % tryptone, 0.5 % yeast extract, and 1 % NaCl (w/v)] with shaking (180 rpm), or on the surface of LB agar (LA) medium [LB broth supplemented with 1.5 % agar (w/v)], unless otherwise specified. Evans Blue Uranine (EBU) agar [LA supplemented with 0.25 % glucose, 0.25 % K₂HPO₄, 0.00125 % Evans Blue, and 0.0025 % sodium fluorescein (w/v)] was used for confirming the removal of phage P22 from *S. Tm* transductants. Mueller-Hinton Agar [1.75 % casein hydrolysate, 0.2 % beef extract, 0.2 % starch, 1.5 % agar (w/v)] was used to enumerate *S. Tm* following infection of mammalian cells.

For growth in chemically defined media, bacteria were grown in M9 minimal medium (MM) broth [48 mM NaH₂PO₄, 22 mM K₂HPO₄, 8.6 mM NaCl, 19 mM NH₄Cl, 2.0 mM MgSO₄, 0.1 mM CaCl₂], or on MM agar medium [MM broth supplemented with 1.5 % agar (w/v)]. The MM was supplemented with either 0.2 % glucose (1.11 mM) or 0.2 % glycerol (2.17 mM) as a carbon source and 1 to 1000 nM biotin (Sigma) and/or 0.2 % L-arabinose (13.3 mM) as specified in the Results. The growth media was supplemented with 100 μ g/ml ampicillin, 50 μ g/ml kanamycin, 34 μ g/ml chloramphenicol, and 20 μ g/ml gentamicin for the selection and maintenance of plasmids or genomic markers when required.

Table 2.1: Bacterial strains and plasmids used and generated in this study

Strain	Relevant genotypes / phenotypes	Source / Reference
<i>E. coli</i>		
DH5a	<i>ΔrecA1398 endA1 φ80Δ(lacZ)M15 ΔlacX74 hsdR(rk-mK+) fluA</i>	ThermoFisher Scientific
Mach1 T1 ^R	<i>ΔrecA1398 endA1 F φ80(lacZ)ΔM15 ΔlacX74 hsdR(rk-mK+) tonA</i>	ThermoFisher Scientific
OmniMAX 2 T1 ^R	<i>recA1 endA1 φ80(lacZ)ΔM15 Δ(lacZYA-argF)U169 gyrA96(Nal^R) relA1 F[proAB+ lacIq Tn10(TetR) Δ(ccdAB)] mcrA Δ(mrr-hsdRMS-mcrBC) glnV44 tHI-1 panD tonA</i>	ThermoFisher Scientific
BW25113 (WT)	<i>Δ(araD-araB)567, ΔlacZ4787(::rmB-3), λ, rph-1, Δ(rhaD-rhaB)568, hsdR514</i>	CGSC 7636
<i>S. Typhimurium</i>		
WT	ATCC 14028s	SGSC 2262
<i>ΔbioB::Km^R</i>	single, marked, in-frame deletion mutant of <i>bioB</i> ; growth is biotin-dependent, Km ^R	This study
<i>ΔbioB</i>	single, unmarked, in-frame deletion mutant of <i>bioB</i> , growth is biotin dependent	This study
<i>ΔbioB::Km^R pBioB</i>	<i>ΔbioB::Km^R</i> mutant genetically complemented with pBioB; Km ^R , Amp ^R	This study
<i>ΔyigM::Km^R</i>	single, marked, in-frame deletion mutant of <i>yigM</i> ; Km ^R	This study
<i>ΔyigM</i>	single, unmarked, in-frame deletion mutant of <i>yigM</i>	This study
<i>ΔyigM::Km^R pYigM</i>	<i>ΔyigM::Km^R</i> mutant genetically complemented with pYigM; Km ^R , Amp ^R	This study
<i>ΔbioB::Km^R ΔyigM</i>	double mutant with marked, in-frame deletion of <i>bioB</i> and unmarked, in-frame deletion of <i>yigM</i> , growth is biotin dependent, Km ^R	This study
<i>P_{BAD}::yigM::Km^R</i>	marked promoter replacement mutant, <i>yigM</i> expression inducible by arabinose from the P _{BAD} promoter; Km ^R	This study
<i>P_{BAD}::yigM</i>	unmarked P _{BAD} :: <i>yigM::Km^R</i> mutant	This study
<i>ΔbioB::Km^R P_{BAD}::yigM</i>	marked, in-frame deletion mutant of <i>bioB</i> in the P _{BAD} :: <i>yigM</i> genetic background; growth is arabinose and biotin-dependent; Km ^R	This study
Plasmids	Description	Source / Reference
pKD46	Expresses λ red proteins, temperature-sensitive, Amp ^R	Datsenko and Wanner (2001)
pKD4	Template plasmid containing FRT-Flanked Km ^R cassette, Km ^R , Amp ^R	Datsenko and Wanner (2001)
pKD13	Template plasmid containing FRT-Flanked Km ^R cassette, Km ^R , Amp ^R	Datsenko and Wanner (2001)
pRL128	Template plasmid containing FRT-Flanked Km ^R cassette and P _{BAD} promoter, Km ^R , Amp ^R	Gueguen and Cascales (2013)
pE-FLP	FLP-recombinase expressing vector, temperature-sensitive, Amp ^R	St. Pierre <i>et al.</i> , (2013)
pJET 1.2/blunt	Positive selection cloning vector for PCR products, Amp ^R	ThermoFisher Scientific
pWSK29	Low copy number cloning vector, Amp ^R	Wang and Kushner (1991)
pBioB	pWSK29 vector harbouring the <i>S. Tm bioB</i> gene between <i>Bam</i> HI and <i>Hind</i> III sites	This study
pYigM	pWSK29 vector harbouring the <i>S. Tm yigM</i> gene between <i>Bam</i> HI and <i>Hind</i> III sites	This study

For the long-term storage and maintenance, glycerol stocks of all bacterial strains used in the study were made as follows. Bacteria were grown to late exponential phase in LB and 0.5 ml of the bacterial suspension transferred to a cryopreservation vial containing an equal volume of 50 % glycerol as a cryopreservant. The cells were allowed to equilibrate in the glycerol for 15 minutes and the cryopreservation vial was transferred to a - 80 °C freezer. Working stocks of the strains were prepared by scraping cells from the surface of the glycerol stocks onto the surface of the LA medium, followed by streak plating for single colonies. The LA plates were incubated at 37 °C for 16 h before their transfer and storage at 4 °C. A single colony from the LA plates was used to initiate liquid cultures within two weeks of their initial isolation from long-term storage.

2.3 Growth assays

2.3.1 Growth assays in liquid medium

Bacterial cultures for growth assays were grown overnight at 37 °C with shaking in either LB or MM supplemented with 100 nM biotin. The cells were harvested by centrifugation at $12\ 100 \times g$ and washed three times with an equal volume of biotin-free MM. The washed cultures were diluted ten-fold in biotin-free MM and grown at 37 °C with shaking for an additional 16 h to deplete intracellular reservoirs of biotin. The OD_{600} of the overnight cultures was measured, and the starting inoculum of each culture was standardized to an OD_{600} of 0.02. The OD_{600} values were measured at the indicated time points using a Jenway 7200 spectrophotometer. The data plotted are the average of at least three biological replicates, with error bars indicating the standard deviation of the replicates.

2.3.2 Growth assays on solid medium

Bacterial cultures for growth assays were incubated with shaking in LB at 37 °C for 16 h, harvested by centrifugation at $12\ 100 \times g$, and washed three times with an equal volume of biotin-free MM. The washed cells were diluted ten-fold in biotin-free MM and incubated at 37 °C for 16 h to deplete any intracellular reservoirs of biotin. The OD_{600} of cultures was adjusted to ~ 1.0 ($\sim 8 \times 10^8$ CFU/ml) and serially diluted ten-fold in sterile saline (0.85 % NaCl in dH₂O). 10 μ l of each serial dilution was spotted onto the surface of MM agar plates, supplemented with biotin and/or arabinose as indicated in the Results. The spots were allowed to dry, and the plates were incubated at 37 °C for 24 to 48 h before quantification and imaging.

2.3.3 Bacterial viability assays

Bacterial cultures were cultured at 37 °C for 16 h with shaking, harvested by centrifugation at 12 100 × g, and washed three times with an equal volume of biotin-free MM. The cells were diluted ten-fold in biotin-free MM and incubated at 37 °C for an additional 16 h to deplete any intracellular reservoirs of biotin. The cells were diluted to an OD₆₀₀ of 0.000001 (~ 2 × 10² CFU/ml) in MM in the presence or absence of 10 nM biotin and grown for a further 24 h at 37 °C with shaking. The number of bacteria present at the start and end of the assay (t = 0 and t = 24 h, respectively) was enumerated by spotting 10 µl of a ten-fold dilution series of cells onto the surface of an LB agar plate. The fold-change from 0 to 24 h was calculated using the following equation:

$$\text{Fold Change} = \frac{\text{CFU at 24 h}}{\text{CFU at 0 h}}$$

The data was plotted and represent the average of at least three independent biological replicates, with error bars indicating the standard error of the mean (SEM).

2.3.4 Broth microdilution assays

Broth microdilution assays to determine minimal inhibitory concentrations (MIC) were performed as described by El Zahed and Brown, (2018). Bacterial cultures were grown overnight at 37 °C with shaking in LB for 16 h. The cells were harvested by centrifugation at 12 100 × g and washed three times with an equal volume of biotin-free MM. The washed cells were diluted 1:50 in biotin-free MM and grown with shaking at 37 °C to an OD₆₀₀ of 0.5 to deplete intracellular reservoirs of biotin. The cells were diluted 1:1000 to OD₆₀₀ = 0.0005 in MM, supplemented as described in **Section 3.3**. 50 µl of the cells were transferred into the wells of a 96 well, U-bottomed microtiter plate (Nunc) containing a two-fold serial dilution of the BioA inhibitor MAC-13772 (Zlitni et al., 2013). The plates were incubated for 18 h at 37 °C and bacterial growth was measured by the addition of 10 µl resazurin to each well. The plates were incubated at 37 °C for 1 to 4 h and the levels of fluorescence were measured using a SpectraMax M3 (Molecular Devices) microplate reader at 560/590 nm. From these readings, the levels of fluorescence were calculated using the formula $F = F_R - F_B$, where F_B represents the background fluorescence measured in the wells immediately after the addition of resazurin, and F_R represents the fluorescence measured in the wells after 1 to 4 h of incubation with resazurin. The relative fluorescence (% F) was calculated using the formula $\% F = F_T / F_U$, where F_T represents the fluorescence in the 11 wells treated with MAC-13772, and F_U representing the growth in the wells lacking MAC-13772. The concentration that resulted in a percentage residual growth of ≤ 10 % was deemed to be the MIC.

2.4 Chemicals and reagents

All chemicals used in this study were obtained from Sigma Aldrich, Merck, or Alfa Aesar. All DNA restriction and modification enzymes used were obtained from ThermoFisher Scientific or New England Biolabs. For a detailed list of chemicals and reagents used in the study, refer to **Appendix A**.

2.5 DNA isolation and purification

All nucleic acid isolation and purification procedures were performed using kits obtained from ThermoFisher Scientific. Genomic DNA extraction and purification were performed using the GeneJET Genomic DNA Purification Kit. Small- and large-scale plasmid purification were performed using the GeneJet MiniPrep or MidiPrep Kit, respectively. PCR products were purified using the GeneJet PCR Purification Kit. When required, restriction enzyme digests or PCR products were subjected to agarose gel electrophoresis and DNA fragments of the desired size excised using a scalpel blade following visualisation with a long-wave UV (UVP; 365 nm) or blue light transilluminator (IORodeo; 470 nm). The DNA was subsequently purified from the excised gel fragments using the GeneJet Gel Purification Kit.

2.6 DNA quantification

The purity and concentration of DNA samples were determined by measuring the sample absorbance at a wavelength of 260 nm using a Nanodrop ND-100 Spectrophotometer (ThermoFisher Scientific) and a conversion factor of 50 ng and 33 ng for single and double-stranded DNA, respectively. The purity of the samples was assessed by assessing the absorbance ratios at 260/280 or 230/260 nm, which indicates contamination with RNA or organic salts, respectively. The concentration of DNA samples was also assessed by comparing the intensity of ethidium-bromide-stained DNA samples relative to that of known quantities of DNA present in the molecular weight marker following agarose gel electrophoresis and visualisation under UV light (see **Section 2.8** below).

2.7 General recombinant DNA procedures

Recombinant DNA and molecular biology techniques were performed according to standard protocols (Ausubel et al., 2012; Russell and Sambrook, 2001) unless otherwise specified. All plasmids listed in this study are listed in **Table 2.1**.

2.7.1 Restriction Enzyme Digestion

Restriction enzyme digests were performed using FastDigest or Anza restriction enzymes purchased from ThermoFisher Scientific or New England Biolabs. Analytical scale digests were used to confirm the identity of plasmids and were performed in 30 μ l volumes containing 0.2 - 1.0 μ g of DNA, 3 μ l 10 \times restriction enzyme buffer, 1 μ l of each restriction enzyme (10 U/ μ l), and UltraPure nuclease-free dH₂O (Gibco). Reactions were incubated for 1 - 16 h at 37 $^{\circ}$ C before analysis by agarose gel electrophoresis. Preparative scale digests of plasmid DNA or PCR products for use in cloning reactions were performed in 50 μ l reaction volumes containing 1.0 - 5.0 μ g of DNA, 5 μ l 10 \times restriction enzyme Buffer, 1 μ l of each restriction enzyme (10 U/ μ l) per μ g DNA, and UltraPure nuclease-free dH₂O (Gibco). Reactions were incubated for 1 - 16 h at 37 $^{\circ}$ C before analysis by agarose gel electrophoresis and/or purification for use in downstream applications.

2.7.2 Dephosphorylation reactions

The re-circularisation of cloning vectors during ligations was reduced by treating restriction enzyme digested vectors with FastAP Thermosensitive Alkaline Phosphatase (ThermoFisher Scientific), as per the manufacturer's instructions. Reactions were performed by adding 1 μ l FastAP (1 U/ μ l) per μ g DNA directly to restriction enzyme digests, followed by incubation at 37 $^{\circ}$ C for 10 min. The dephosphorylated vector was purified prior to use in ligation reactions.

2.7.3 Ligation reactions

Ligation reactions were performed using a 1:1 and 3:1 insert: vector ratio in 20 μ l reaction volumes containing 2 μ l 10 \times T4 ligase buffer (ThermoFisher Scientific), 2 μ l T4 ligase (ThermoFisher Scientific), the appropriate volume of vector and insert DNA, and UltraPure nuclease-free dH₂O (Gibco). The amount of insert DNA required in each reaction was calculated using the following equation: the required amount of insert DNA (ng) = [(Desired molar ratio of insert: vector) \times (Amount of vector DNA (ng))] \times (Ratio of the insert to vector lengths). Reactions lacking a DNA insert were included as controls. Ligation reactions were incubated at room temperature overnight.

For transformation reactions, 2 µl of each ligation was introduced into competent *E. coli* cells as described in **Section 2.11.2**.

2.7.4 Polymerase Chain Reaction (PCR)

The oligonucleotide primers used in this study are listed in **Table 2.2** below. Primer sequences were based on the complete genome sequences of *S. Tm* 14028s (GenBank Accession Number CP001363.1) or *E. coli* BW25113 (GenBank Accession Number CP009273.1) and synthesised by Inqaba Biotec (South Africa) or ThermoFisher Scientific (UK). All PCR reactions were performed using the Applied Biosystems SimpliAmp (ThermoFisher Scientific) or MultiGene Mini Personal (Labnet International) thermal cyclers.

2.7.4.1 Preparative PCR reactions

PCR amplification of DNA fragments used for the generation of recombinant plasmids or allelic replacement cassettes were performed using the Phusion High Fidelity PCR Kit (ThermoFisher Scientific). PCR reactions were performed according to the manufacturers' recommendations in 50 µl reaction volumes containing 10 µl 5 × HF reaction buffer, 0.3 µM forward and reverse primers, 200 µM deoxynucleotide triphosphates (dNTPs), 10 - 100 ng of template DNA, 0.5 µl of Phusion DNA polymerase, and the remaining volume (to 50 µl) with ultrapure nuclease-free water (Gibco). The following cycling conditions were used: initial denaturation at 98 °C for 3 min, followed by 30 cycles of denaturation (98 °C for 20 s), annealing (the appropriate annealing temperature for primer pair for 30 s), extension (72 °C for 30 s/kb), and a final extension at 72 °C for 7 min. The annealing temperatures were calculated according to the melting temperatures of the forward and reverse primers, as per the manufacturer's recommendations.

Table 2.2: List of oligonucleotide primers used in this study

Primer Name	Sequence	Amplicon properties/ region targeted
Oligonucleotides used for PCR-based genotyping		
bioB-US-Check	ATGATAACCGTGGCGAAACG	Forward primer located 521 bp upstream of <i>bioB</i>
bioB-DS-Check	CTTCTGTCACCACCAGTTGC	Reverse primer located 522 bp downstream of <i>bioB</i>
yigM-US-Check	ACTCGCTGTTTGAGCCTG	Forward primer located 490 bp upstream of <i>yigM</i>
yigM-DS-Check	ACTGGGTGGTGGAAAGCGTT	Reverse primer located 126 bp downstream of <i>yigM</i>
K1-Rev-Check	CAGTCATAGCCGAATAGCCT	Forward primer located in Km ^R cassette
K2-For-Check	CGGTGCCCTGAATGAACTGC	Reverse primer located in Km ^R cassette
M13-For	GTAAAACGACGGCCAGT	Forward primer upstream of the multiple cloning site in pWSK29
M13-Rev	CAGGAAACAGCTATGAC	Forward primer upstream of the multiple cloning site in pWSK29
pBAD-For	ATGCCATAGCATT TTTATCC	Forward primer upstream of the multiple cloning site in pBAD30
pBAD-Rev	GATTTAATCTGTATCAGGCTG	Forward primer downstream of the multiple cloning site in pBAD30
Oligonucleotides used for generation on Km^R cassettes for gene or promoter replacements ^a		
bioB-Del-For	CATATCAAAAACAAACAACATATTTTGGAGAAAGCCCGATGATT CCGGGGATCCGTCGACC	Forward primer for amplification of the Km ^R cassette from pKD13. 40 bp homology to the first codon and 37 nt upstream of the <i>bioB</i> gene.
bioB-Del-Rev	ACGCGTTGTTGCCAACTCATAAGGCTGCCGCGTTGTAATATGTA GGCTGGAGCTGCTTCG	Reverse primer for amplification of the Km ^R cassette from pKD13. 40 bp homology to last seven codons and 19 nt downstream of the <i>bioB</i> gene.
yigM-Del-For	TAAGAGACATCCATTGTGGCGCTACTCATCATTACCACTATCCT GGTGCAGGCTGGAGCTGCTTC	Forward primer for amplification of the Km ^R cassette from pKD4. 45 bp homology to first 10 codons and 15 nt upstream of the <i>yigM</i> gene.
yigM-Del-Rev	GGTAGCGCCATAGTTCCACATAAAGTAGCCAATGCCTGACGCCA CCATATGAATATCCTCCTTAG	Reverse primer for amplification of the Km ^R cassette from pKD4. 45 bp homology to codons 213 to 227 of the <i>yigM</i> gene.
yigM-Pro-For	TCTTTTCTTACGCTGATGTGATTGTTTGTAGTTGACCAGGTGTA GGCTGGAGCTGCTTC	Forward primer for amplification of the Km ^R -P _{BAD} cassette from pRL128. Homology to the last 18 nt, and 22 nt downstream of the <i>yigL</i> gene.
yigM-Pro-Rev	ATAGTGGTAATGATGAGTAGCGCCACAATGGATGTCTCTTGGGT ATGGAGAAACAGTAGA	Reverse primer for amplification of the Km ^R -P _{BAD} cassette from pRL128. Homology to the first 26 nt, and 14 nt upstream of the <i>yigM</i> gene.
Oligonucleotides used for genetic complementation vector construction ^b		
bioB-BamHI-For	AAT <i>GGATCC</i> ACATGACATGCGACATGG	Forward primer located 324 bp upstream of the <i>S. Tm bioB</i>
bioB-HindIII-Rev	ACTA <i>AAGCTT</i> CACGGAATAACCGCTGAT	Reverse primer located 251 bp downstream of the <i>S. Tm bioB</i>
yigM-BamHI-For	AG <i>GGATCC</i> AATGAACGACGCTGAAATGC	Forward primer located 237 bp upstream of the <i>S. Tm bioB</i>
yigM-EcoRI-Rev	GCT <i>GAATTC</i> CCAGCGAAACGCTGTTGATT	Reverse primer located 288 bp downstream of the <i>S. Tm bioB</i>
Oligonucleotides used for Sanger sequencing of PCR amplified inserts		
M13-For	GTAAAACGACGGCCAGT	Forward primer upstream of the multiple cloning site in pWSK29
M13-Rev	CAGGAAACAGCTATGAC	Forward primer upstream of the multiple cloning site in pWSK29
pBAD-For	ATGCCATAGCATT TTTATCC	Forward primer upstream of the multiple cloning site in pBAD30
pBAD-Rev	GATTTAATCTGTATCAGGCTG	Forward primer downstream of the multiple cloning site in pBAD30

^a Sequences complementary to the FRT-flanked, Km^R cassettes in pKD13, pKD4, and pRL128 are in bold.

^b Restriction enzyme sites are in bold, italics.

2.7.4.2 Analytical PCR Reactions

PCR analysis for the identification of recombinant plasmids and strains were performed using 2 × DreamTaq PCR Master Mix (Thermo Scientific) or KAPA Taq DNA polymerase Ready Mix (Sigma). Cell lysates for use in PCR reactions were prepared as described by Woodman (2008). In brief, antibiotic-resistant transformants were inoculated into 100 µl of LB broth supplemented with appropriate antibiotics prior to incubation at 37 °C with shaking at 180 rpm for 4 - 16 h. The cells were centrifuged at 12 100 x g for 1 min in a MiniSpin Microfuge (Eppendorf), the supernatant removed, and the cell pellet resuspended in 100 µl nuclease-free dH₂O (Gibco). The cells were boiled at 100 °C for 10 min and centrifuged at 12 100 × g for 1 min to remove cell debris. The resulting cell-free supernatant containing DNA was transferred to a sterile microfuge tube and used in PCR reactions. The PCR reactions were performed in 25 µl reaction volumes containing 12.5 µl 2 × DreamTaq Master Mix or KAPA Taq Ready Mix, 0.3 µM forward and reverse primers, 2.5 µl cell-free supernatant, and 7.5 µl nuclease-free dH₂O. The following cycling conditions were used: initial denaturation at 95 °C for 4 min, followed by 30 cycles of denaturation (95 °C for 30 s), annealing (the appropriate annealing temperature for primer pair for 30 s), extension (72 °C for 60 s / kb) and a final extension at 72 °C for 7 min. The annealing temperature was calculated according to the melting temperatures of the forward and reverse primers, as per the manufacturer's recommendations.

2.8 Agarose gel electrophoresis

Agarose gels were prepared by melting TopVision Agarose Tablets (0.8 to 2 % w/v; ThermoFisher Scientific) in 1 × TAE buffer (40 mM Tris, 20 mM acetic acid, 1 mM EDTA, pH 8.0) and 0.5 µg/ml ethidium bromide to facilitate the visualisation of DNA. DNA samples were mixed with 6 × TriTrack Loading Dye (ThermoFisher Scientific) before loading on gels. The Kapa Universal Ladder (Sigma) or GeneRuler 1 kb Plus DNA Ladder (ThermoFisher Scientific) was used to estimate the size of the larger DNA fragments. The GeneRuler 50 bp DNA ladder (ThermoFisher Scientific) was used to estimate the size of DNA fragments smaller than 1 kb (**Appendix B, Figure B1**). Gels were electrophoresed at 80 to 100V for 45 to 60 min using a Mini-Sub Cell GT horizontal electrophoresis chamber (Bio-Rad) and Universal PowerPac Power Supply (Bio-Rad). Gels were visualised under UV-light using the ChemiDoc XRS+ Imaging System (Bio-Rad) and digital images acquired using the accompanying Image Lab Software.

Table 2.3: Expected PCR product sizes when amplifying WT and mutant strains with the indicated primer pairs

Primer pairs	Gene/Allele	Expected PCR product size
yigM-Del-For yigM-Del-For	pKD4 Km ^R cassette	1595 bp (Figure 3.3)
yigM-US-Check yigM-DS-Check	<i>S. Tm yigM</i>	1516 bp (Figure 3.4 and 3.5)
	<i>S. Tm ΔyigM::Km^R</i>	2384 bp (Figure 3.4 and 5)
	<i>S. Tm ΔyigM</i>	944 bp (Figure 3.6)
	<i>S. Tm P_{BAD}::yigM::Km^R</i>	4132 bp (Figure 3.17)
	<i>S. Tm P_{BAD}::yigM</i>	2910 bp (Figure 3.17)
yigM-US-Check K1-Rev-Check	<i>S. Tm yigM</i>	Lacks K1 binding site. No PCR product expected. (Figure 3.4 and 3.5)
	<i>S. Tm ΔyigM::Km^R</i>	1019 bp (Figure 3.4 and 3.5)
	<i>S. Tm ΔyigM</i>	Lacks K1 binding site. No PCR product expected.
yigM-DS-Check K2-For-Check	<i>S. Tm yigM</i>	Lacks K2 binding site. No PCR product expected. (Figure 3.4 and 3.5)
	<i>S. Tm ΔyigM::Km^R</i>	1279 bp (Figure 3.4 and 3.5)
	<i>S. Tm ΔyigM</i>	Lacks K2 binding site. No PCR product expected
bioB-Del-For bioB-Del-For	pKD13 Km ^R cassette	1568 bp (Figure 3.7)
bioB-US-Check bioB-DS-Check	<i>S. Tm bioB</i>	2084 bp (Figure 3.9 and 3.17)
	<i>S. Tm ΔbioB::Km^R</i>	2374 bp (Figure 3.9 and 3.17)
	<i>S. Tm ΔbioB</i>	1105 bp
bioB-US-Check K1-Rev-Check	<i>S. Tm ΔbioB</i>	Lacks K1 binding site. No PCR product expected. (Figure 3.10)
	<i>S. Tm ΔbioB::Km^R</i>	996 bp (Figure 3.10)
	<i>S. Tm ΔbioB</i>	Lacks K1 binding site. No PCR product expected. (Figure 3.10)
bioB-DS-Check K2-For-Check	<i>S. Tm bioB</i>	Lacks K2 binding site. No PCR product expected. (Figure 3.10)
	<i>S. Tm ΔbioB::Km^R</i>	1241 bp (Figure 3.10)
	<i>S. Tm ΔbioB</i>	Lacks K2 binding site. No PCR product expected. (Figure 3.10)
bioB-Del-For bioB-Del-For	pRL128 Km ^R -pBAD cassette	2626 bp (Figure 3.15)
bioB-BamHI-For bioB-HindIII-Rev	<i>S. Tm bioB</i>	1613 bp (Appendix C1)
yigM-BamHI-For yigM-EcoRI-Rev	<i>S. Tm yigM</i>	1425 bp (Appendix C2)

2.9 DNA sequencing

All PCR-generated amplicons were DNA sequenced to confirm that no mutations had been introduced into the amplicons. Sanger sequencing was outsourced to the inqaba Biotech and performed using the BigDye terminator v3.1 Cycle Sequencing kit. The resulting chromatograms and sequence data were analysed using the SnapGene software program (GSL Biotech; <https://www.snapgene.com>).

2.10 Bioinformatic tools and software

Several bioinformatic tools were used for the viewing and analysis of DNA and protein sequences. The genome sequences of *E. coli* BW25113 (GenBank Accession Number CP009273.1) and *S. Tm* 14028s (GenBank Accession Number CP001363.1) were obtained from the National Centre for Biotechnology Information (NCBI). Whole-genome sequences were imported and viewed using the Benchling (www.benchling.com) software program. Primer design and analysis were performed using Benchling or SnapGene (GSL Biotech; <https://www.snapgene.com>). Plasmid maps were generated, analysed, and exported using SnapGene. Graphs and statistical analysis were performed with GraphPad Prism 8.4 (www.graphpad.com).

2.11 Bacterial transformation

DNA was introduced into bacterial strains via transformation of chemically competent cells (for the introduction of plasmid DNA or ligation reactions into *E. coli*) or electrocompetent cells (for the introduction of plasmid DNA or allelic replacement substrates into *S. Tm*).

2.11.1 Preparation of chemically competent cells

Chemical competent cells were prepared according to the method of Inoue *et al.* (1990). *E. coli* cultures were grown overnight at 37 °C (16 h) and diluted 1 in 100. The cultures were incubated with shaking at 37 °C until an OD₆₀₀ of ~ 0.6 was reached. These cultures were transferred into ice for 10 min and then centrifuged at 2 500 × g (Beckman Coulter Allegra X-22R Centrifuge) for 10 min at 4 °C. The supernatant was discarded, and the cell pellet resuspended in 1/3rd of the initial volume of ice-cold transformation buffer [55 mM MnCl₂, 15 mM CaCl₂, 250 mM KCl, 10 mM PIPES, pH 6.7]. The cells were kept on ice for 10 min and then centrifuged at 2 500 × g for 10 min at 4 °C. The supernatant was discarded, and the cell pellet resuspended in a tenth of the initial volume of ice-cold transformation buffer. The cells were divided into 50 µl aliquots and used in transformation reactions immediately or stored at - 80 °C for later use.

2.11.2 Transformation of chemically competent cells

Transformation reactions were performed by mixing 1 - 10 ng of plasmid DNA, or 2 μ l ligation reactions, with 50 μ l of thawed competent cells. The cells were incubated on ice for 10 min and then transferred to 42 °C for 45 s to allow for the uptake of the plasmid DNA. The cells were incubated on ice for an additional 2 min. 950 μ l of outgrowth medium (LB) was added to the cells and incubated for 1 h at 37 °C to allow for the expression of the antibiotic resistance genes. 100 μ l cells were plated on LA plates that were supplemented with antibiotics and 20 μ g/ml X-Gal and 0.1 mM IPTG when required.

2.11.3 Preparation of electrocompetent cells

S. Tm cultures were grown in LB at 37 °C (or 30 °C when harbouring plasmids with temperature-sensitive replicons) for 16 h and then diluted 1 in 100 in low-salt LB [1 % tryptone, 0.5 % yeast extract, and 0.5 % NaCl (w/v)]. The cultures were incubated with shaking at the appropriate growth temperature (30° or 37° C) until an OD₆₀₀ of ~ 0.6 was reached. The cultures were centrifuged at 4 °C for 10 min at 7 000 \times g and washed three times with an equal volume of 10 % glycerol. After the final wash, the supernatant was discarded, and the cell pellet resuspended in 10 % glycerol at 1/100th of the initial culture volume. The electrocompetent cells were kept on ice before performing the electroporation reactions or stored at - 80 °C for later use.

2.11.4 Transformation of electrocompetent cells

For electroporation, 50 μ l of electrocompetent cells were mixed with 100 - 800 ng DNA in a pre-cooled microfuge tube. The mixture was transferred into a sterile, pre-cooled 0.2 cm gap electroporation cuvette (Bio-Rad or Sigma-Aldrich) and electroporation performed in a Bio-Rad GenePulser using the following settings: 25 μ F, 200 Ω , 2.5 kV. 950 μ l of pre-warmed outgrowth medium (LB) was added to the cells immediately after electroporation. The cells were transferred to a sterile microfuge tube and incubated at 30 ° or 37 °C with shaking for 1.5 to 3 h. 100 μ l of these cells were streaked onto LA plates which were supplemented with Amp, Km, or Cm. These plates were then incubated at 30 ° or 37 °C and the antibiotic-resistant transformants were identified after 16 - 24 h.

2.12 Generation of mutant strains

2.12.1 Generation of *S. Tm* $\Delta bioB$ and $\Delta yigM$ deletion mutant strains

Allelic replacement of *bioB* and *yigM* was achieved using the λ -red-mediated recombination method of Datsenko and Wanner (2000), which relies on the plasmid-based expression of the phage λ proteins Exo, Gam, and Bet to mediate recombination between short (> 40 bp) sequences present at the ends of linear PCR products and homologous regions on the bacterial chromosome. The PCR primers (60-mers) for the allelic replacement of *bioB* were designed to contain 40 bp homologous to regions located at the 5' and 3' ends of the *bioB* coding sequence (*bioB*-Del-For and *bioB*-Del-Rev, respectively), upstream of 20 bp regions homologous to the Km^R-cassette on pKD13 (Datsenko and Wanner, 2000) (**Table 2.2**). PCR primers for allelic replacement of *yigM* contained 45 bp homologous to regions located at the 5' end and codons 213 - 227 of the *yigM* coding sequence, (*yigM*-Del-For and *yigM*-Del-Rev, respectively), upstream of a 20 bp region homologous to the Km^R-cassette of pKD4 (**Table 2.2**). PCR reactions to generate the Km^R resistance cassettes specific for replacement of *bioB* and *yigM* (*bioB*::Km^R and *yigM*::Km^R, respectively) were performed as described in **Section 2.7.4.1**, using ~ 10 ng plasmid DNA as a template. This generated linear ~ 1.4 kb PCR products containing the FLP recombination target (FRT)-flanked *bioB*::Km^R and *yigM*::Km^R cassettes flanked by 45 nucleotide termini to facilitate recombination at the corresponding, homologous genomic location. Following PCR, the samples were treated with *DpnI* at 37 °C for 1 h to remove the template DNA. The PCR products were then purified and used to generate deletion mutants as described below.

The temperature-sensitive helper plasmid pKD46 (Datsenko and Wanner, 2000) expresses the λ -red recombinase Exo, Bet, and Gam from the arabinose-inducible P_{BAD} promoter was introduced into *S. Tm* by electroporation. Transformants were selected for on LA plates supplemented with Amp and incubated at 30°C to maintain the temperature-sensitive plasmid. The *S. Tm* strain harbouring pKD46 was subsequently cultured to OD₆₀₀ of ~ 0.6 at 30 °C in low-salt LB supplemented with Amp and 0.2 % arabinose for induction of the λ -red recombinase. 100 ng of the purified *bioB*::Km^R and *yigM*::Km^R PCR products were introduced into the recipient strain via electroporation, as described above (**Section 2.11.4**). The cells were plated on LA/Km and the Km^R transformants were identified following overnight incubation at 37 °C. Transformants were re-streaked on LA/Km and the plates were incubated at 42 °C to ensure the loss of pKD46. This procedure was repeated twice and the loss of pKD46 confirmed by the replica plating onto LA and

LA/Amp plates, followed by incubation at 37 °C overnight. The genotypes of suspected mutants were confirmed via PCR using primers that bind upstream (US) and downstream (DS) of the *bioB* and *yigM* genes (Table 2.3; BioB-US-Check and BioB-DS-Check or YigM-US-Check and YigM-DS-Check, respectively), either as primer pairs or in conjunction with primers that bind to the Km^R resistance gene (Table 2.3; K1-Rev-Check and K2-For-Check).

2.12.2 Generation of *S. Tm yigM* promoter-replacement mutant (P_{BAD}*yigM*)

To generate a promoter-replacement mutant in which the *yigM* promoter is replaced by the arabinose-regulatable *araBAD* promoter (P_{BAD}), forward and reverse primers were designed to contain a 40-nucleotide region of homology to the 3' - and 5' -ends the *yigL* and *yigM* genes (*yigM*-Pro-For and *yigM*-Pro-Rev, respectively), upstream of a 3' -terminal 20 nucleotide extension with homology to the FRT-flanked Km^R-*araC*-P_{BAD} cassette present in pRL128 (Gueguen *et al.*, 2013). The PCR reactions to generate the Km^R resistance cassette were performed as described in Section 2.7.4.1, using 10 ng pRL128 as a template. This resulted in the amplification of a 2.5 kb PCR product containing the FRT-flanked Km^R cassette (FRT-Km^R-*araC*-P_{BAD}-FRT) with 40 bp termini to facilitate recombination at the homologous genomic location, thus replacing the *yigM* promoter located in the *yigL*-*yigM* intergenic region with P_{BAD}. Following PCR, the samples were treated with *DpnI* at 37 °C for 1 h to remove the template DNA. The PCR product was then purified and electroporated into electrocompetent *S. Tm* strain harbouring pKD46 as described above.

2.12.3 Phage P22 mediated transduction of mutant alleles

The transfer of marked mutant alleles into a clean WT genetic background, or mutant strains when combining several different mutations, was accomplished by generalised transduction using phage P22HT/int, as described by Thierauf *et al.* (2009).

2.12.3.1 Preparation of donor phage lysates

Donor phage lysates were generated by combining 4 ml of P22 broth [LB supplemented with 1.66 mM MgSO₄, 9.5 mM citric acid monohydrate, 57 mM K₂HPO₄, 16.7 mM NaNH₃PO₄, 0.4 % (w/v) glucose, and ~ 1 × 10⁶ P22 HT/int pfu/ml] with 3 ml of a mid-exponential phase culture of an antibiotic resistance marked donor strain. The culture was co-incubated with the phage at 37 °C with shaking (180 rpm) for 4 - 8 h, or until bacterial cell lysis was observed. 1.5 ml of the lysed bacterial culture was transferred to a microfuge tube, which was then centrifuged at 12 100 × g for 1 min to remove cell debris. The phage-containing supernatant was transferred to a fresh tube and

50 µl chloroform was added to lyse any remaining cells and to prevent bacterial growth. The resulting P22/int phage lysates were stored at 4 °C until further use.

2.12.3.2 Phage transduction and selection

The transfer of alleles into a different genetic background was accomplished by growing 3 ml of the recipient strain in LB at 37 °C with shaking overnight (16 h). 100 µl of the strain was combined with 1, 5, or 10 µl of the donor phage lysate and incubated at 37 °C for 15 to 30 min to allow for phage absorption. 900 µl of phage outgrowth medium (LB supplemented with 10 mM EGTA) was added to each of the tubes and the cells were incubated with shaking at 37 °C for 1 h to allow for the expression of antibiotic resistance markers. 100 µl of the cells were streaked onto LA plates supplemented with 10 mM EGTA and Km for incubation at 37 °C overnight. Km^R transductants were streak purified an additional two times on LA plates supplemented with 10 mM EGTA and Km, to prevent the formation of lysogenic strains.

The transductants were confirmed to be phage-free by streaking on Evans Blue Uranine (EBU) agar plates [LA supplemented with 0.2 % glucose, 0.5 % K₂HPO₄, 0.0025 % Evans Blue, and 0.0025 % sodium fluorescein (w/v)], which differentiates between colonies containing or lacking phage based on their dark-green and white colours, respectively. White colonies were subsequently confirmed to be phage-free by demonstrating their sensitivity to re-infection with phage P22 on EBU agar plates. The genotype of phage-free, antibiotic-resistant transductants was subsequently verified by colony PCR as described in **Section 2.7.2.2** with allele-specific primers (**Table 2.3**).

2.12.4 Generation of unmarked mutant strains

Where required, the Km^R cassette present in the marked *S. Tm* $\Delta bioB::Km^R$, $\Delta yigM::Km^R$, and P_{BAD}:: $\Delta yigM::Km^R$ mutants were removed via electroporation with pE-FLP (**Table 2.2**), a temperature-sensitive plasmid encoding the FLP recombinase under the control of the pE promoter (St-Pierre *et al.*, 2013). Electrocompetent *S. Tm* $\Delta bioB::Km^R$, $\Delta yigM::Km^R$ and P_{BAD}:: $\Delta yigM::Km^R$ cells were prepared as described in **Section 2.11.3** and transformed with 100 ng pE-FLP. 100 µl of cells was plated on LA/Amp plates and incubated at 37 °C overnight. Several Amp^R transformants were selected and re-streaked on LA/Amp plates, which were then incubated at 42 °C to promote the loss of the temperature-sensitive pE-FLP. This procedure was repeated twice and the loss of pE-FLP and the Km^R cassette was confirmed by replica plating mutant strains onto LA, LA/Amp, and LA/Km plates and incubation at 37 °C overnight. The genotype of mutants sensitive to both Amp and Km, suggesting loss of both pE-FLP and the Km^R cassette, were

screened by colony PCR using primers that bind upstream and downstream of the *bioB* and *yigM* genes, as described in **Section 2.4.2.1**.

2.12.5 Generation of *S. Tm* $\Delta bioB \Delta yigM$ double mutant

For the generation of an *S. Tm* $\Delta bioB \Delta yigM$ double mutant, the $\Delta yigM::Km^R$ mutant strain was first unmarked, using the protocol described in **Section 2.11.4**. The $\Delta bioB::Km^R$ allele was then transferred into the unmarked $\Delta yigM$ strain via P22-mediated transduction. The genotype of the strain was confirmed via colony PCR with the (i) *yigM*-US-Check/*yigM*-US-Check and (ii) *bioB*-US-Check/*bioB*-DS-Check primer pairs (**Table 2.3**).

2.12.6 Generation of *S. Tm* $\Delta bioB::P_{BAD}::yigM$ mutant

For the generation of an *S. Tm* $\Delta bioB::P_{BAD}::yigM$ double conditional mutant, the $P_{BAD}::yigM::Km^R$ mutant was first unmarked, using the protocol described in **Section 2.11.4** above. The marked $\Delta bioB::Km^R$ mutant allele was then transferred into the unmarked $P_{BAD}::yigM$ mutant via P22-mediated transduction. The genotype of the strain was confirmed via colony PCR with the (i) *yigM*-US-Check/*yigM*-US-Check and (ii) *bioB*-US-Check/*bioB*-DS-Check primer pairs (**Table 2.3**).

2.13 Generation of plasmids for genetic complementation of *bioB* and *yigM*

Plasmids for the genetic complementation of the $\Delta bioB$ and $\Delta yigM$ mutants were constructed by PCR amplification of the coding sequences of each gene, together with their native promoters and terminators. The *bioB* specific primers *bioB*-BamHI-For and *bioB*-HndIII-Rev were designed to anneal 286 bp upstream and 294 bp downstream of the *bioB* coding sequence, respectively, while the *yigM* specific primers *yigM*-BamHI-For and *yigM*-EcoRI-Rev were designed to anneal 237 bp upstream and 288 bp downstream of the *yigM* gene. PCR amplification was performed with 100 ng genomic DNA as described in **Section 2.7.4.1**. The PCR products harbouring *bioB* or *yigM* were purified and digested with *Bam*HI and *Hind*III or *Bam*HI and *Eco*RI, respectively, and ligated into the multiple cloning site of the low-copy number vector pWSK29 (Wang and Kushner, 1991), which had been digested with the same enzymes. The ligation reactions were introduced into *E. coli* DH5 α competent cells and transformants selected on LA/Amp plates supplemented with 40 μ g/ml X-Gal and 0.1 mM IPTG. Colony PCR with gene-specific primers, as well as plasmid purification and restriction enzyme digestion with *Xho*I and *Xba*I were used to verify the successful construction of recombinant plasmids. The regions of plasmids constructed by PCR were verified via Sanger sequencing as described in **Section 2.10**. The confirmed constructs for genetic

complementation of the marked and/or unmarked *bioB* and *yigM* mutant alleles, (designated as pBioB and pYigM, respectively) were electroporated into their respective *S. Tm* mutant backgrounds for subsequent phenotypic analysis *in vitro*.

2.14 Growth and maintenance of mammalian cells

HeLa and RAW264.7 cells were obtained from Cellonex (South Africa) and cultured in BenchStable DMEM (Gibco) supplemented with 4.5 g/litre glucose, 4 mM Glutamax, sodium pyruvate, and 10 % heat-inactivated FBS (Gibco) (subsequently referred to as “complete DMEM”) at 37 °C in a humidified incubator supplemented with 5 % CO₂.

2.14.1 Intracellular survival assay using HeLa cells

HeLa epithelial cells were seeded in 24-well cell culture plates at a density of 1×10^5 cells per well 24 h before infection. *S. Tm* strains were grown at 37 °C in 3 ml of LB without shaking (i.e., oxygen-limited, “invasive” conditions) to induce the expression of the SPI-1 invasion associated TTSS. The cultures were diluted to OD₆₀₀ = 0.2 in DPBS and added to the wells at a multiplicity of infection (MOI) of 100 in DMEM lacking FBS. After 30 min of incubation at 37 °C, the cells were washed three times with pre-warmed complete DMEM to remove extracellular bacteria, followed by a 1 h incubation in the same medium supplemented with 100 µg/ml of gentamicin (Gm). The medium was subsequently removed and replaced with complete DMEM with 10 µg/ml for the remainder of the experiment. The number of bacteria present in the HeLa cells was assessed at 2 h and 16 h post-infection (p.i) by washing the cells with PBS three times followed by lysis in 1 ml of 0.1 % Triton × 100. The cell lysates were diluted using ten-fold serial dilutions and 10 µl spotted on the surface of Muller-Hinton plates supplemented with 1 µM biotin to ensure the recovery of single and double mutants. The plates were incubated at 37 °C for 24 h and the bacterial strains were enumerated. The bacterial invasion was calculated by dividing the colony counts at 2 h post-infection by the colony counts for the inoculum used to initiate infection. Bacterial replication was calculated by dividing the colony counts at 16 h post-infection by the colony counts at 2 h post-infection. All experiments were performed in triplicate.

2.14.2 Intracellular survival assay using RAW264.7 cells

RAW264.7 macrophages were seeded in 24- well plates at a density of 2×10^5 per well 24 h prior to infection. *S. Tm* strains were inoculated into 3 ml LB broth and grown to stationary phase at 37 °C with shaking (i.e., oxygen replete, “non-invasive” conditions). The cultures were diluted to OD₆₀₀ = 0.2 and added to the wells at a multiplicity of infection (MOI) of 10 in DMEM lacking

FBS. After 30 min of incubation at 37 °C, the cells were washed three times with pre-warmed complete DMEM to remove extracellular bacteria, followed by a 1 h incubation in the same medium supplemented with 100 µg/ml of gentamicin (Gm). The medium was subsequently removed and replaced with complete DMEM with 10 µg/ml for the remainder of the experiment. The number of bacteria present in the RAW264.7 cells was assessed at 2 h and 16 h post-infection by washing the cells with PBS three times, followed by lysis in 1 ml of 0.1 % Triton × 100. The cell lysates were diluted using ten-fold serial dilutions and 10 µl spotted on the surface of Muller-Hinton plates supplemented with 1 µM biotin to ensure the recovery of single and double mutants. The plates were incubated at 37 °C for 24 h and the bacterial strains were enumerated. The bacterial invasion was calculated by dividing the colony counts at 2 h post-infection by the colony counts for the inoculum used to initiate infection. Bacterial replication was calculated by dividing the colony counts at 16 h post-infection by the colony counts at 2 h post-infection. All experiments were performed in triplicate.

2.14.3 Chemical inhibition of biotin biosynthesis in mammalian cells

Bacterial survival following treatment with the BioA inhibitor MAC-13772 was performed as described above except that 320 µg/ml MAC-13772 was added to DMEM containing 10 µg/ml gentamicin immediately after the 1 h incubation step with 100 µg/ml gentamicin. All experiments were performed in triplicate.

Chapter 3: Results

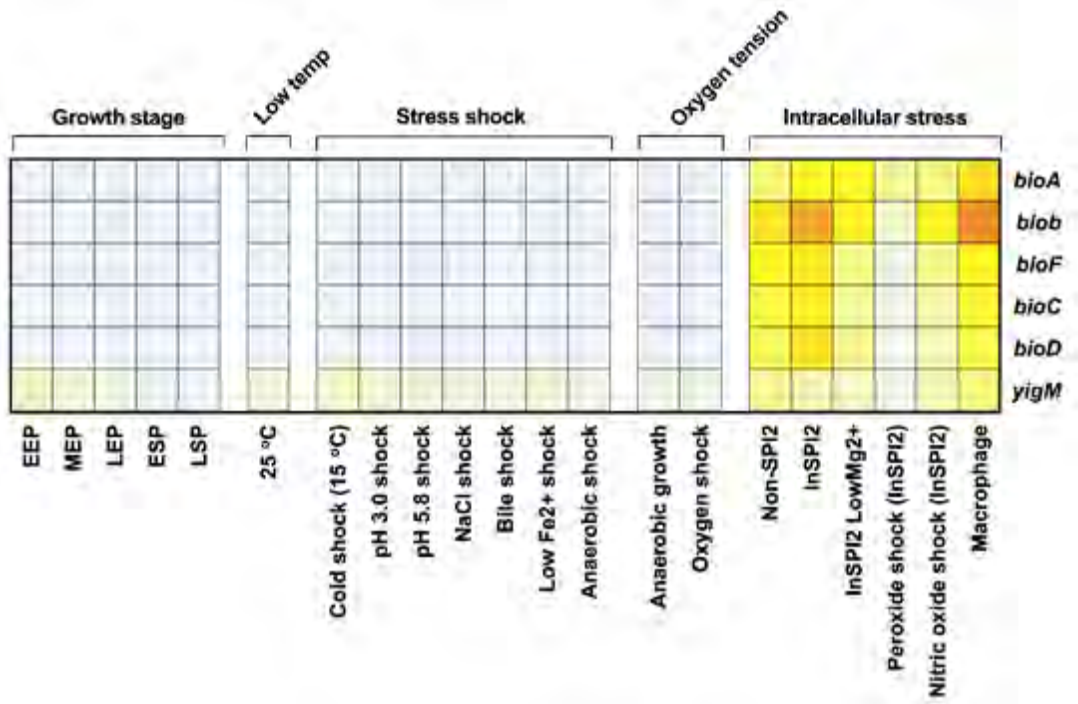
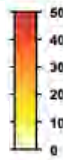
3.1 Introduction

To gain initial insights into the relative contributions of the biotin biosynthetic and transport pathways for the intracellular growth of *S. Tm*, we compared the transcriptional profiles of the *bio* operon and *yigM* genes using data available from the *S. Tm* Gene Expression Compendium (<http://tinyurl.com/SalComMac>) (Kroger *et al.*, 2013; Srikumar *et al.*, 2015). This database contains the expression data for all *S. Tm* genes during growth in 21 different environmental conditions *in vitro* or following the infection of macrophages *ex vivo* (reviewed by Perez-Sepulveda and Hinton, 2018). As shown in **Figure 3.1 A and B**, the genes of the *bio* operon (*bioA*, *bioB*, *bioC*, *bioD*, and *bioF*) are expressed at relatively low levels during growth in rich media (LB) at all growth stages (early, mid, and late exponential phase, early and late stationary phase). Their expression is, however, increased during growth in biotin-free PCN minimal medium (see Non-SPI2 medium and InSPI2 medium) and is maximal when *S. Tm* is grown in macrophages, an observation that likely reflects the nutrient-limited conditions encountered within the SCV. The expression of *yigM*, which encodes a putative biotin transporter, was also analysed. The gene is constitutively expressed during growth in LB, but its expression is repressed as growth proceeds from early exponential to late stationary phase. Similar to the observations for the biosynthetic genes, *yigM* expression levels are greatest during growth in macrophages, which suggests that *S. Tm* may employ both the biosynthetic and transport pathways to ensure an adequate supply of biotin to support growth in the intracellular environment. To obtain experimental evidence to support or refute this hypothesis we compared the effects of genetically inactivating each of these pathways, either individually or in combination, on bacterial growth *in vitro* and *ex vivo* as described in the following sections.

Figure 3.1 (overleaf). Expression of selected genes involved in biotin metabolism in *S. Tm*. Transcriptional data was obtained from the SalComMac database (<http://tinyurl.com/SalComMac>) Heat-maps were drawn using the GraphPad Prism Software program. **A)** Absolute expression levels of the indicated genes under each condition in transcripts per million (TPM). **B)** Relative expression levels of the indicated genes under each condition (log 2-fold change). Gene expression is shown relative to the first column (designated “reference condition”) present in each sample block. Growth conditions indicated are: EEP (early exponential phase), MEP (mid-exponential phase), LEP (late-exponential phase), ESP (early stationary phase), LEP (late stationary phase), NonSPI2 (growth in PCN media pH 7.4), InSPI2 (growth in PCN medium pH 5.8), InSPI2 low Mg²⁺ (InSPI2 with 10 mM MgSO₄). Macrophage (infection of RAW264.7 macrophages for 8 h). For “shock” conditions, bacteria were exposed to the indicated stressors in LB medium for 10 min, as described in (Kroger *et al.*, 2013).

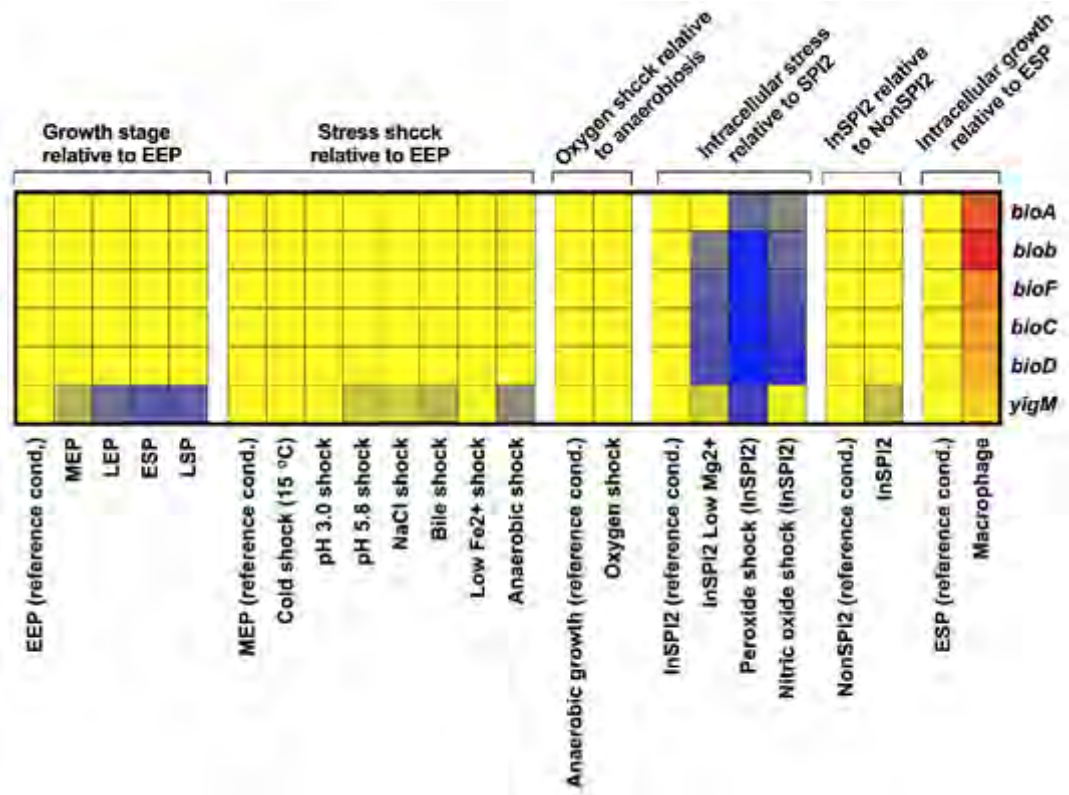
A

High-expression
> 500 TPM
Scale (TPM)
Low-expression
> 500



B

Up-regulated
> 20-fold
No change
Down-regulated
> 20-fold



3.2. Generation and genotypic confirmation of *S. Tm* single mutant strains

3.2.1 Generation and confirmation of the *S. Tm* $\Delta yigM$ mutant

To identify proteins that could serve as a biotin transporter in *S. Tm*, the organism's genome was screened for homologues of known bacterial biotin transporters using the *E. coli* YigM and *R. capsulatus* BioY as reference sequences. This analysis revealed that the bacterium does not possess a homologue of the *R. capsulatus* BioY protein, either as a solitary transporter or together with BioM and BioN as part of a ClassI or ClassII ECF transport system. The organism does, however, possess a coding DNA sequence (STM3963) predicted to encode a 299 amino acid protein with 92 % identity and 96 % similarity to the *E. coli* YigM biotin transporter. The *S. Tm* YigM protein is predicted to contain 10 transmembrane regions and has a domain structure typical of the carboxylate/amino acid/amine family of transporters (Ringlsetter, 2010). The *yigM* gene of *S. Tm* has a 113 bp overlap with the downstream *metR* gene, which is transcribed in the opposite direction (**Figure 3.2**). The *metR* gene encodes a transcriptional activator that induces the expression of several genes involved in methionine biosynthesis, including those encoding the vitamin B12 - dependent and -independent methionine synthases, MetE and MetH.

To provide experimental evidence for the biotin transport activity of YigM, we genetically inactivated the *yigM* gene using the λ Red recombination system of Datsenko and Wanner (2000). To accomplish this, primers YigM-US-Del and YigM-DS-Del were used to amplify the FRT-flanked Km^R cassette from pKD4 (see **Figure 3.2**). To prevent the simultaneous inactivation of the *metR* gene, the reverse primer (YigM-DS-Del) was designed 106 bp downstream of the stop codon of *metR*. The use of these primers should result in the retention of the first 10 and last 88 codons (i.e. codons 1 - 10 and 213 - 300, respectively) of the *yigM* gene, together with the entire *metR* coding sequence, following homologous recombination. As shown in **Figure 3.3** (Lane 2), PCR amplification with YigM-US-Del and YigM-DS-Del produced an amplicon of ~ 1.6 kb, which corresponds to the expected size of the *yigM*-specific Km^R cassette (see **Table 2.3** for all predicted amplicon sizes). No PCR amplicon was, however, observed in the reaction that lacked the pKD4 DNA template (**Figure 3.3**, Lane 3).

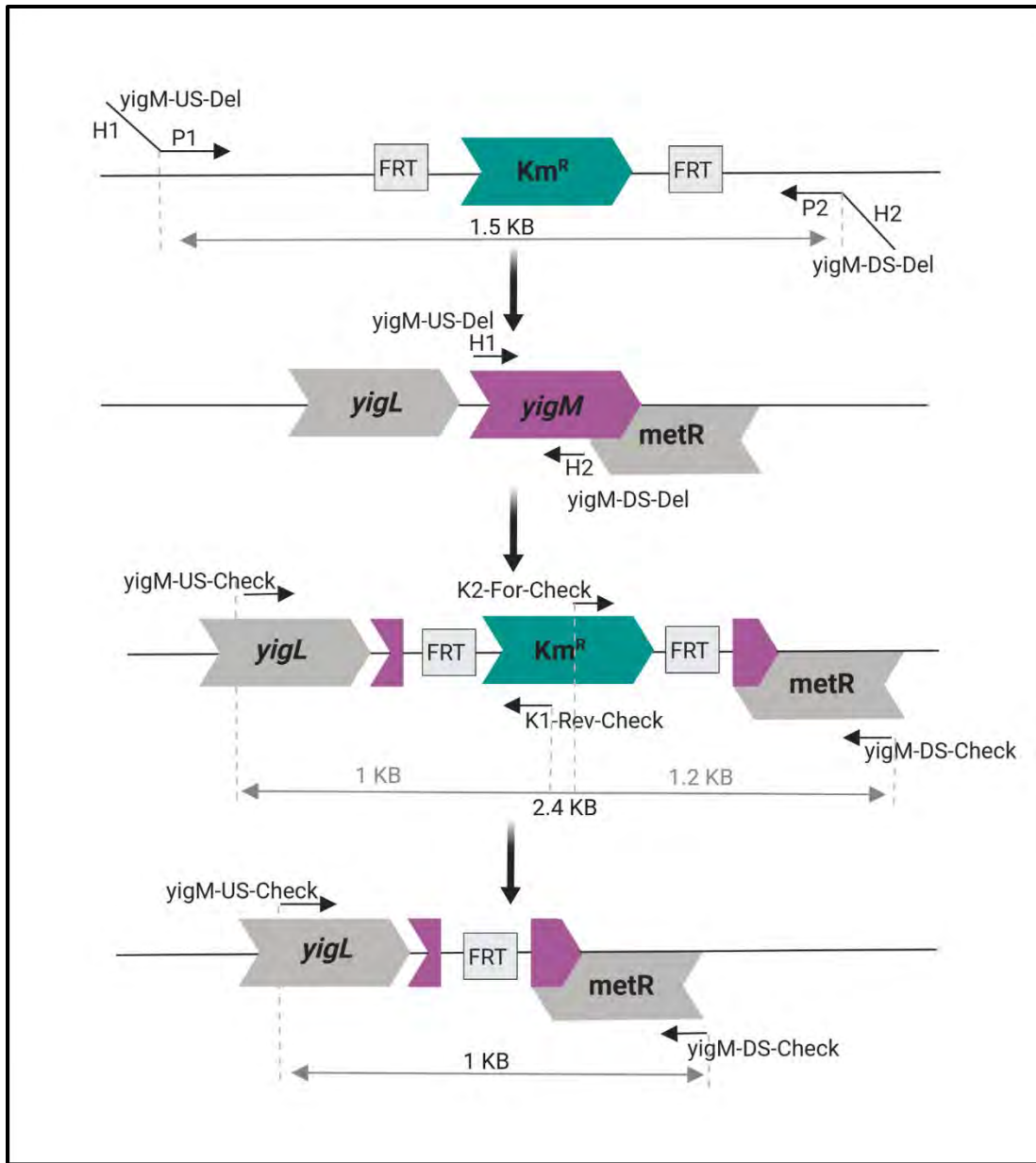


Figure 3.2: Schematic representation of the targeted deletion of the *bioB* and *yigM* genes of *S. Tm* and subsequent removal of the Km^R cassette (adapted from Baba *et al.*, 2006, created with BioRender). The 65 bp YigM-US-Del and YigM-DS-Del primers consist of 45 bp regions homologous to the 5' and 3' ends of the *yigM* gene (designated H1 and H2, respectively), and 20 bp regions homologous to the FLP recombination target (FRT)-flanked Km^R cassette of pKD4 (Datsenko and Wanner, 2000). Primers YigM-US-Check and YigM-DS-Check positioned ~ 457 bp upstream and 322 bp downstream of the region that underwent homologous recombination were either used in combination, or with primers K1-Rev-Check and K2-For-Check primers, to confirm gene inactivation.

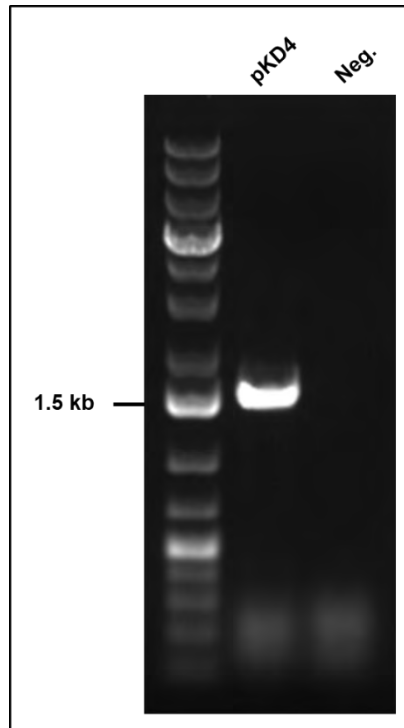


Figure 3.3: PCR amplification of the *yigM*-specific Km^R cassette from pKD4. PCR amplification reactions were performed using the *yigM* deletion primers, YigM-Del-For/YigM-Del-Rev, and pKD4 plasmid DNA as a template. The products of the PCR reactions were electrophoresed on a 0.8 % agarose gel at 80V for 50 min before being visualised under UV light. **Lane 1:** MW marker, **Lane 2:** PCR product with pKD4 DNA template, **Lane 3:** PCR product for no DNA, negative control.

The purified *yigM::Km^R* cassette was subsequently electroporated into wild-type *S. Tm* and transformants selected on LA plates supplemented with Km. The genotypes of two randomly selected Km^R transformants were verified by PCR amplification with 3 different primer pair combinations (US/DS, K1/US, and K2/DS). As shown in **Figure 3.4**, PCR products corresponding to the predicted sizes of ~ 2.4, 1.2, and 1 kb were identified for both the putative $\Delta yigM::Km^R$ transformants (Lanes 5, 6, 7 and 8, 9, 10, respectively). By contrast, a single PCR product of ~1.6 kb was identified for the WT strain when using primers US/DS (**Figure 3.4**, Lane 2), which is consistent with the expected size. No products were visible in **Figure 3.4**, Lanes 3 and 4, given the lack of binding sites for the Km^R specific primers in the WT strain. Taken together, these results confirm the successful generation of the *S. Tm* $\Delta yigM::Km^R$ mutant strain.

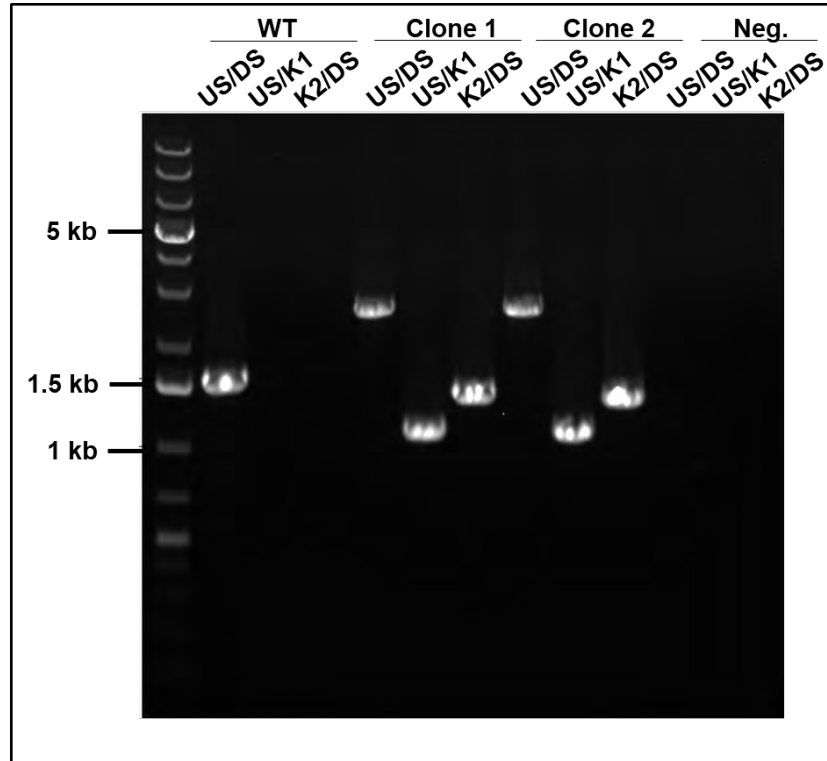


Figure 3.4. PCR confirmation of the genotype of the putative *yigM::Km^R* mutant clones. PCR reactions were performed using genomic DNA isolated from WT or putative $\Delta yigM::Km^R$ *S. Tm* mutant strains using primers YigM-US-Check/YigM-DS-Check (US/DS), YigM-US-Check/K1-Rev-Check (US/K1), and YigM-DS-Check/K2-For-Check (K2/DS). The products of the PCR reactions were electrophoresed on a 0.8 % agarose gel at 80 V for 50 min. The genomic DNA used as a template in the PCR reactions were as follows: **Lanes 2-4:** WT genomic DNA, **Lanes 5-7:** $\Delta yigM::Km^R$ Clone 1 genomic DNA, **Lane 8-10:** $\Delta yigM::Km^R$ Clone 2 genomic DNA, **Lane 11-13:** No DNA, negative controls.

Following confirmation of the genotypes of the Km^R -marked mutants, the strains were first cured of the temperature-sensitive pKD46, which encodes the λ red recombination enzymes. Since the use of these enzymes can occasionally introduce off-target mutations (Murphy *et al.*, 2016), the *yigM::Km^R* allele was subsequently transduced into a “clean” WT genetic background using phage P22 (Thierauf *et al.*, 2009). The successful transduction of the allele into the chromosome of the WT *S. Tm* recipient strain was verified by colony PCR performed on four independent Km^R transductants. As shown in **Figure 3.5.** (Lanes 2- 5), a single band of ~ 2.4 kb was observed for each of the transductants analysed, confirming the successful transfer of the marked *yigM* allele.

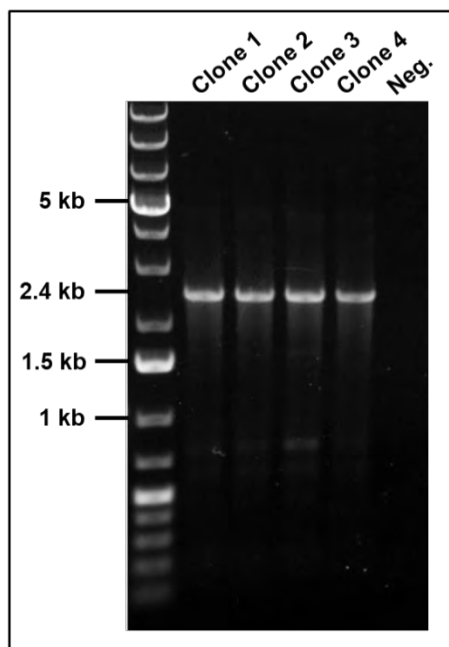


Figure 3.5: PCR confirmation of the successful transduction of the *yigM::Km^R* allele into a clean WT *S. Tm* background. Colony PCR reactions were performed on the lysates obtained from four putative transductants (Clones 1-4) using primers YigM-US-Check/YigM-DS-Check. The reaction products were subjected to electrophoresis on 0.8 % agarose at 80 V for 50 min. **Lane 1: MW Marker, Lanes 2-5: Colony PCR products from Clones 1-4, Lane 6: Colony PCR product from no lysate, negative control.**

To facilitate the construction of the $\Delta bioB::Km^R \Delta yigM$ double mutant required to confirm the role of *yigM* in biotin transport (see **Section 3.2.3**), we next removed the FRT-flanked Km^R cassette from the marked $\Delta yigM$ mutant by introducing pE-FLP into the strain. The FLP recombinase-mediated excision of the Km^R cassette was confirmed by colony PCR analysis. As shown in **Figure 3.6**, an amplicon of ~ 1 kb was observed for each of the four transformants analysed (Lanes 2-5), which is consistent with the expected size of the unmarked *yigM* allele following removal of the Km^R cassette. These observations confirm the successful removal of the Km^R cassette to yield an unmarked *S. Tm* $\Delta yigM$ mutant.

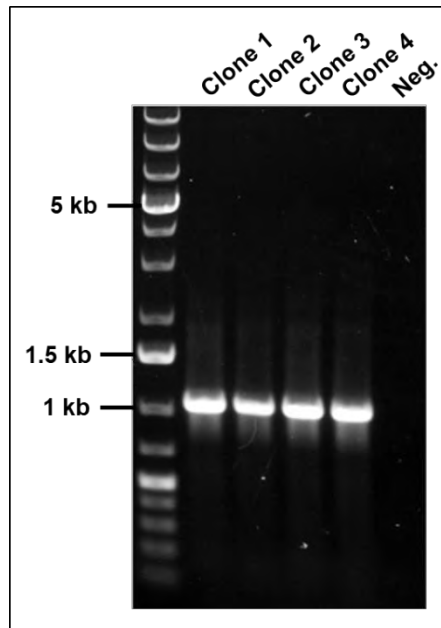


Figure 3.6: PCR Confirmation of the removal of the Km^R marker from the *S. Tm* $\Delta yigM::Km^R$ strain. The *S. Tm* $\Delta yigM::Km^R$ strain was transformed with pE-FLP and colony PCR performed on transformants using the YigM-US-Check and YigM-DS-Check primers. The products of the PCR reaction were electrophoresed on a 0.8 % agarose at 80 V for 50 min. **Lane 1:** MW Marker, **Lanes 2-5:** Colony PCR products from Clones 1-4, **Lane 6:** Colony PCR product from no lysate, negative control.

Following removal of the temperature-sensitive pE-FLP from the strain by growth at elevated temperatures, the verified Amp^S and Km^S $\Delta yigM$ mutant was used in the construction of the *S. Tm* $\Delta bioB::Km^R \Delta yigM$ double mutant as described below.

3.2.2 Generation and confirmation of an *S. Tm* $\Delta bioB$ mutant

To confirm the role of YigM in biotin transport, we next generated a biotin auxotroph by genetically inactivating the gene encoding biotin synthase (BioB), which catalyses the final step in the *de novo* biotin biosynthetic pathway. To accomplish this, a Km^R cassette targeting the *bioB* gene was generated by PCR amplification using primers BioB-Del-For/BioB-Del-Rev and pKD13 as a template. Agarose gel electrophoresis of the reaction products revealed the presence of a single amplicon of ~ 1.3 kb, which corresponds with the predicted size of the *bioB::Km^R* cassette (**Figure 3.7, Lane 2**)

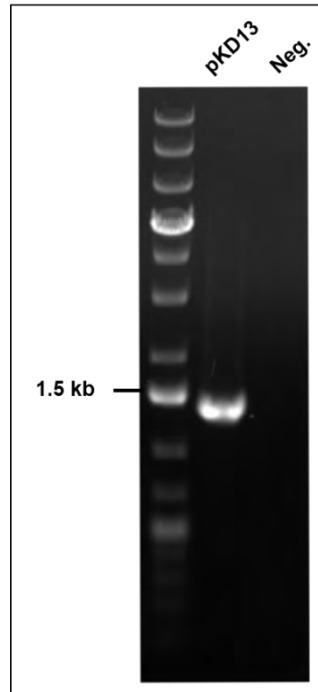


Figure 3.7: PCR amplification of the *bioB*-specific Km^R cassette from pKD13. The Km^R cassette present on pKD13 was amplified by PCR with primers BioB-Del-For/BioB-Del-Rev. The products of the reactions analysed by electrophoresed on a 0.8 % agarose gel at 80 V for 50 min and visualised under UV light. **Lane 1:** MW marker, **Lane 2:** PCR product with pKD13 DNA template, **Lane 3:** PCR product for no DNA, negative control.

To inactivate the genomic copy of the gene, the purified *bioB*:: Km^R cassette was introduced into WT *S. Tm* by electroporation. The genotype of two randomly selected Km^R transformants was analysed by PCR amplification using the primers BioB-US-Check/BioB-DS-Check (**Figure 3.8 and 3.9**). While PCR analysis of the WT control strain yielded an amplicon of ~ 2.0 kb (**Figure 3.9, Lane 2**), the *bioB*:: Km^R mutants yielded an amplicon of ~ 2.5 kb (Lanes 3 and 4), which corresponds to the predicted sizes of the marked *bioB*: Km^R allele.

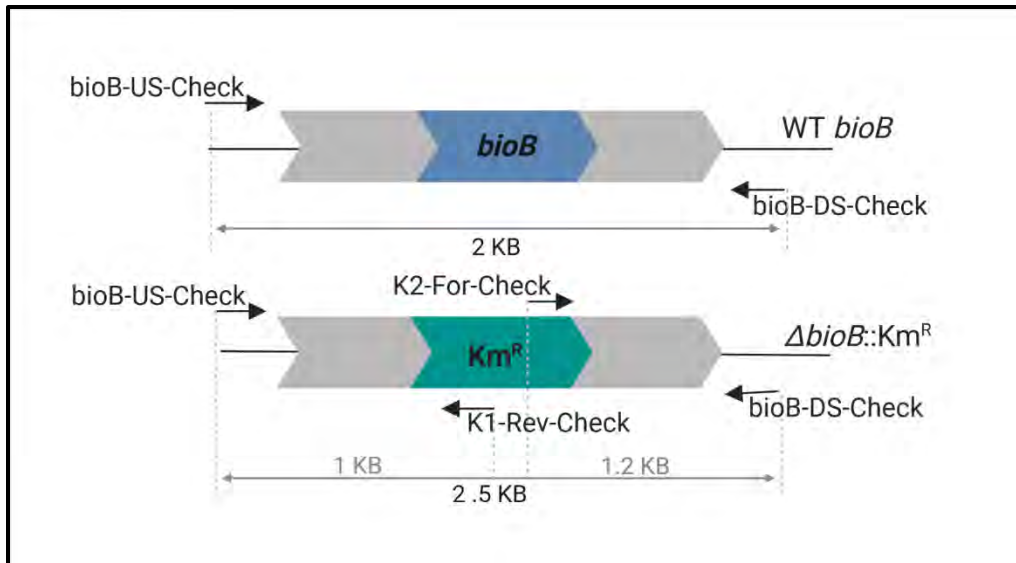


Figure 3.8: Schematic representation of the *bioB* gene of *S. Tm* (created with BioRender). The expected sizes following PCR amplification with primers bioB-US-Check/bioB-DS-Check, bioB-US-Check/K1-Rev-Check, and bioB-DS-Check/K2-For-Check for the (A) WT and (B) mutant *bioB* genotypes. Km^R: Kanamycin resistance marker.

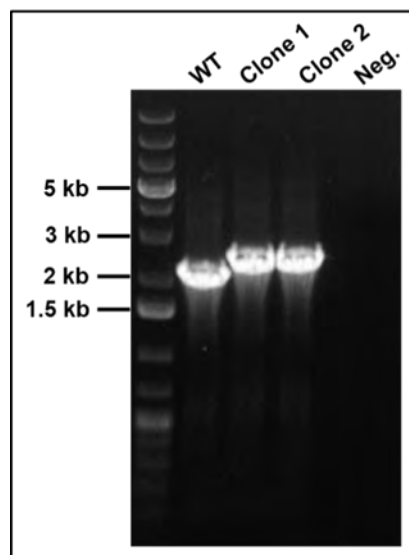


Figure 3.9: PCR confirmation of the genotype of the putative $\Delta bioB::Km^R$ mutant clones. PCR reactions were performed using genomic DNA isolated from WT or two putative $\Delta bioB::Km^R$ *S. Tm* mutant strains using the BioB-US-Check/BioB-DS-Check primers. The products of the PCR reactions were electrophoresed on a 0.8 % agarose gel at 80 V for 50 min. **Lane 1:** MW Marker, **Lane 2:** Colony PCR products from WT *S. Tm*, **Lane 3- 4:** Colony PCR from mutant Clones 1 and 2, **Lane 5:** PCR product from no lysate, negative control.

Following confirmation of the $\Delta bioB::Km^R$ genotype, the strain was first cured of pKD46, as described for *yigM* above. The $\Delta bioB::Km^R$ allele was then transduced into a clean genetic background to generate a strain that could be used in the phenotypic analysis of the strains (Sections 3.2.5 and 3.2.6). The successful transduction of the Km^R -marked alleles into the chromosome of the WT *S. Tm* recipient strain was confirmed by colony PCR using both *bioB* and Km^R -cassette specific primers. As expected, amplicons of ~ 2.5, 1.0, and 1.2 kb were observed for the *bioB::Km^R* transductant analysed (Figure 3.10, Lane 5, 6 and 7, respectively), while a single band of ~ 2.0 kb was observed for WT *S. Tm*, which confirms the genetic identity of the newly generated biotin auxotroph.

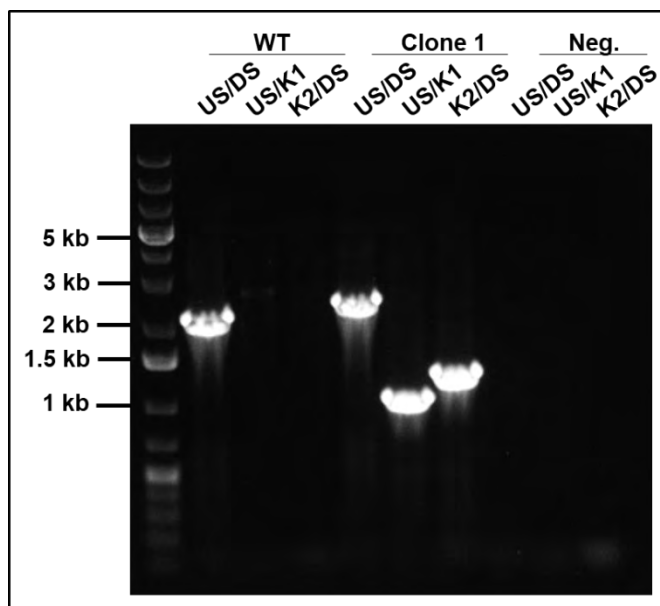


Figure 3.10: Confirmation of the genotype of the putative $\Delta bioB::Km^R$ mutant clones by PCR. PCR reactions were performed using genomic DNA isolated from WT or putative $\Delta bioB::Km^R$ *S. Tm* mutant strains using primers *bioB*-US-Check/*bioB*-DS-Check (US/DS), *bioB*-US-Check/K1-Rev-Check (US/K1), and *bioB*-DS-Check/K2-For-Check (K2/DS). The products of the PCR reactions were electrophoresed on a 0.8 % agarose gel at 80 V for 50 min. The genomic DNA used as a template in the PCR reactions were as follows: **Lanes 2-4:** WT genomic DNA, **Lanes 5-7:** Clone 1 genomic DNA, **Lanes 8-10:** No DNA, negative control.

3.2.3 Construction and confirmation of an *S. Tm* $\Delta bioB::Km^R \Delta yigM$ double mutant

To generate the *S. Tm* $\Delta bioB::Km^R \Delta yigM$ double mutant, we next transduced the $\Delta bioB::Km^R$ allele into the $\Delta yigM$ mutant. To maintain the viability of the double mutants, which contain disruptions in both the biotin biosynthetic and putative transport pathways, the growth medium was supplemented with excess (1 μ M) biotin during both the recovery and selection of the recombinant strains. Using this methodology, numerous Km^R transductants were recovered following overnight incubation at 37° C. To confirm the genotypes of the strains, colony PCR was performed on 3 randomly selected transductants using gene-specific *bioB* and *yigM* primers (**Table 2.3**). Analysis of the resulting PCR products revealed the presence of DNA fragments of ~ 2.5 kb and ~1 kb in each of the transductants (**Figure 3.11**; Lanes 8 - 13), which correspond to the predicted sizes of the marked and unmarked $\Delta bioB::Km^R$ and $\Delta yigM$ alleles, respectively. These results confirmed the successful generation of the *S. Tm* $\Delta bioB::Km^R \Delta yigM$ double mutant, referred to as $\Delta bioB \Delta yigM$ from now on.

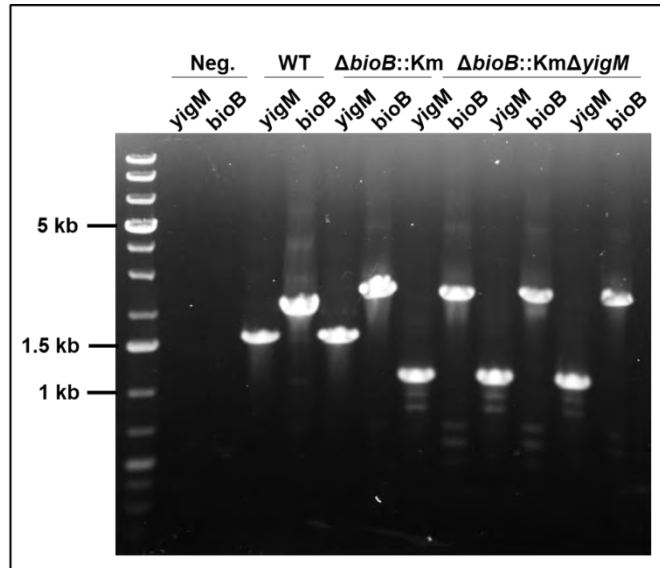


Figure 3.11: Genotypic analysis of the *yigM* and *bioB* alleles present in putative *S. Tm* $\Delta bioB::Km^R \Delta yigM$ double mutant strains. PCR reactions were performed using the bioB-US-Check/bioB-DS-check and yigM-US-Check/yigM-DS-primer for either the *bioB* or *yigM* allele, respectively. PCR reaction products were subjected to electrophoresis on 0.8 % agarose for ~ 50 min at 80 V. **Lane 1:** MW marker, **Lanes 2- 3:** PCR product from no DNA template, negative control, **Lanes 4- 5:** PCR product from WT DNA template, **Lanes 6-7:** PCR product from $\Delta bioB::Km^R$ DNA template, **Lanes 8-13:** PCR products from the DNA templates of $\Delta bioB::Km^R \Delta yigM$ clones 1-3.

3.2.4 Generation of complementation vectors pBioB and pYigM

To generate plasmids capable of genetically complementing the growth phenotypes of the single deletion mutants, the coding sequence and native promoters of the *bioB* and *yigM* genes were PCR amplified and cloned into the low copy number vector pWSK29, to generate pBioB and pYigM, respectively. The genetic integrity of the vectors was confirmed by restriction analysis and the results of these analyses are reported in **Appendix C**. Following confirmation of the PCR-generated segments of the plasmids by Sanger sequencing, the plasmids were electroporated into the *S. Tm* $\Delta bioB::Km^R$, $\Delta yigM$ and $\Delta bioB \Delta yigM$ backgrounds for phenotypic analysis as described below (**Section 3.2.5 - 3.2.7**).

3.2.5 Growth analysis of *S. Tm* mutants in liquid minimal medium

Having confirmed the mutant strain's genotypes, we next proceeded to characterise their growth phenotypes in both liquid and solid media. To establish a role for YigM in biotin transport, the growth kinetics of the $\Delta bioB::Km^R$ and $\Delta bioB \Delta yigM$ mutants were compared to the wild-type strain in M9 minimal medium, in either the presence or absence of exogenously supplied biotin (**Figure 3.12, A and B**, respectively). In contrast to WT *S. Tm*, the $\Delta bioB::Km^R$ mutant failed to grow in the absence of exogenous biotin, which is consistent with the known role of the gene in *de novo* biotin biosynthesis (Lin and Cronan, 2011). The $\Delta bioB::Km^R$ mutant grew at a similar rate to the WT strain in the presence of biotin, however, indicating that the strain's biotin auxotrophy can be overcome by the transport of exogenous biotin (**Figure 3.12 A, B**). As expected, the $\Delta yigM$ mutant grew in M9 media in the absence of biotin supplementation, indicating that YigM is not essential for growth provided that the *de novo* pathway is intact (data not shown; see **Figure 3.13** for growth on solid media). The simultaneous disruption of both the biosynthetic and putative transport pathways in the $\Delta bioB \Delta yigM$ double mutant, by contrast, yielded a strain that was unable to grow in the presence or absence of exogenously supplied biotin (**Figure 3.12 A, B**). The expression of the *yigM* gene in the genetically complemented strain ($\Delta bioB \Delta yigM::pYigM$), restored the ability of the double mutant to grow in the presence, but not the absence of biotin. The observation that the biotin auxotroph is unable to grow in the presence of biotin unless YigM is expressed from either its native location on the chromosome or an episomal plasmid suggests that its activity is required for the uptake of biotin by *S. Tm* during growth *in vitro* (**Figure 3.12 A, B**).

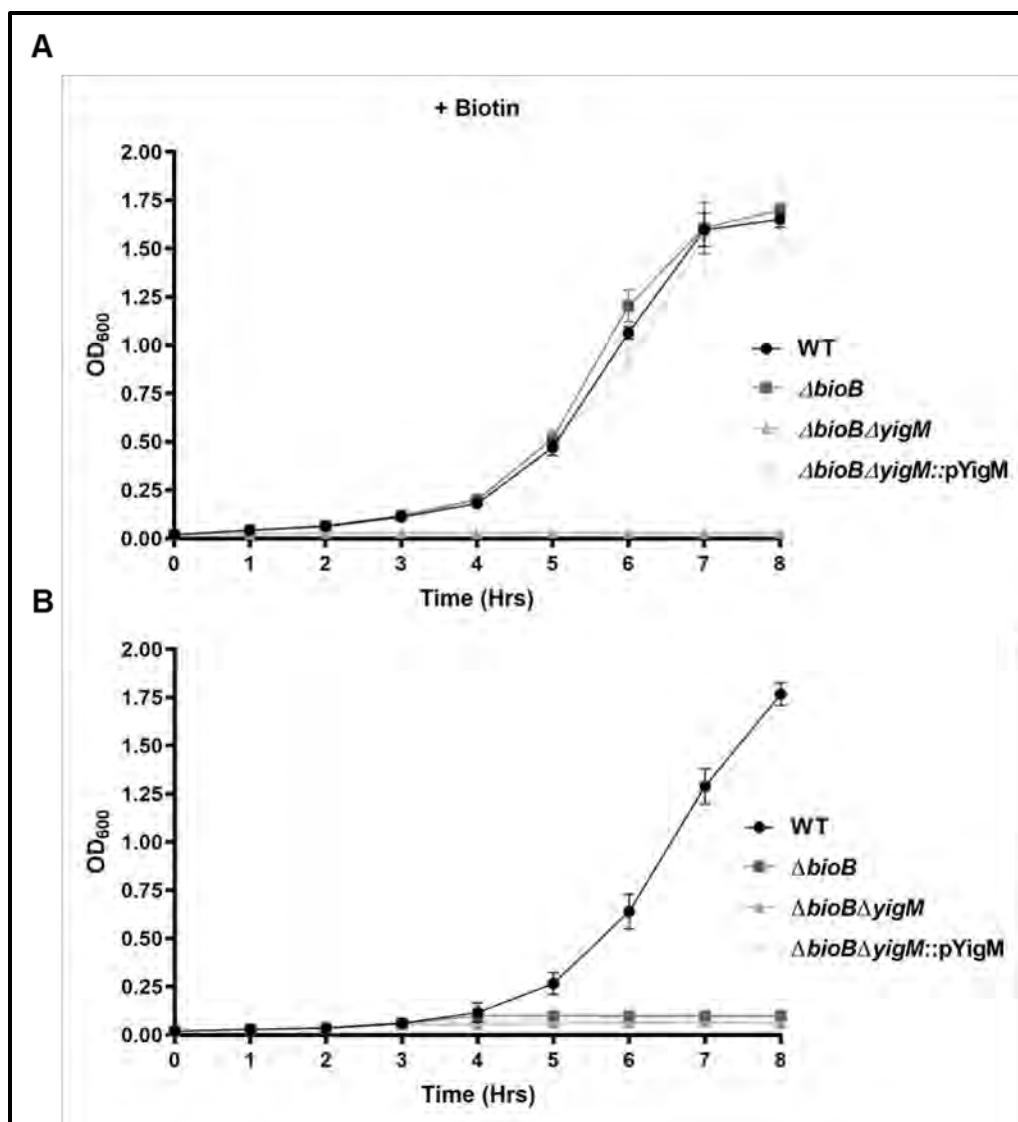


Figure 3.12: *S. Tm* mutants deficient in both the *de novo* biosynthesis and transport of biotin are defective for growth in M9 minimal media broth. The growth kinetics of *S. Tm* WT and indicated mutant strains were measured over 8 hours with OD₆₀₀ measurements taken at 1 h intervals. **(A)** Growth kinetics of the indicated strains in medium supplemented with 10 nM biotin; **(B)** Growth kinetics of the indicated strains in the absence of biotin. The average of three experiments repeated in triplicate is shown with \pm SD.

3.2.6 Growth kinetics of the *S. Tm* mutants on solid minimal medium

The dependence on YigM for biotin transport in *S. Tm* was subsequently analysed on solid M9 medium supplemented with increasing concentrations of biotin. Consistent with the results described above, the $\Delta bioB$ mutant was unable to grow when biotin was omitted from the growth

medium (**Figure 3.13 A, 0 nM**). The growth of the strain, however, increased in a dose-dependent manner when the biotin concentration was elevated from 1 to 100 nM. The biotin auxotrophy of this strain could be attributed to the lack of the BioB enzyme since the in trans expression of the *bioB* gene from the complementation vector, pBioB, restored the mutant's growth in the absence of biotin.

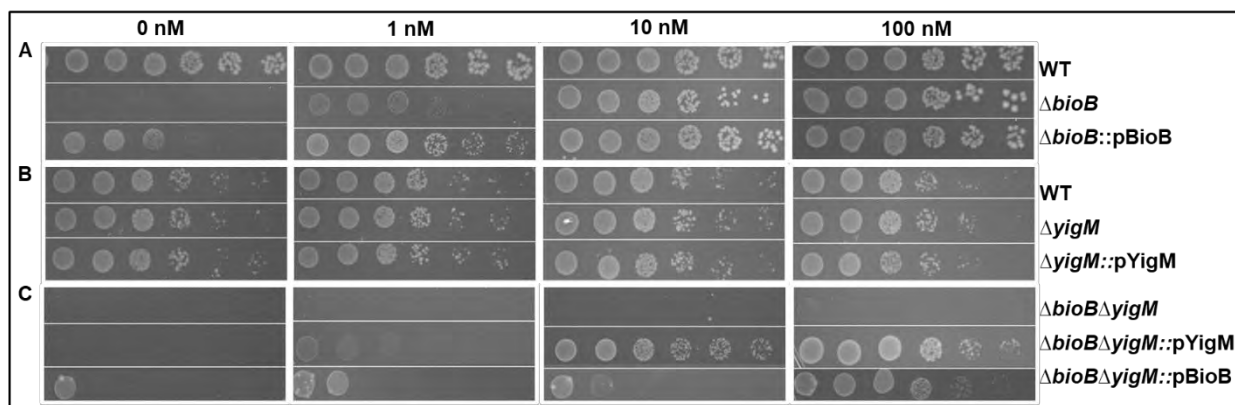


Figure 3.13: *S. Tm* mutants deficient in both the *de novo* biosynthesis and transport of biotin are defective for growth on solid M9 minimal media. Comparison of the growth of WT strain and (A) $\Delta bioB$ mutant and genetically complemented strains (B) $\Delta yigM$ mutant and genetically complemented strains (C) $\Delta bioB\Delta yigM$ mutant and genetically complemented strains. 10-fold serial dilutions of the indicated strains were prepared grown as described in the Materials and Methods (Section 2.3.2) and spotted on M9 agar plates supplemented with the indicated concentrations of biotin. The agar plates were imaged following 24 h incubation at 37°C.

The growth of the $\Delta yigM$ mutant, as well as its genetically complemented derivative, was not dependent on the inclusion of biotin in the growth medium due to the presence of an intact *de novo* biotin biosynthetic pathway in the strain (**Figure 3.13 B**). The simultaneous disruption of the biotin biosynthesis and transport in the $\Delta bioB \Delta yigM$ double mutant, by contrast, inhibited bacterial growth at all biotin concentrations examined. As was observed for the mutants grown in liquid medium, genetic complementation with pYigM restored the ability of the double mutant to grow in medium supplemented with biotin, but not in medium lacking the vitamin (**Figure 3.13 C**). The expression of the *bioB* gene from pBioB could similarly restore the growth of the $\Delta bioB \Delta yigM$ double mutant in the absence of biotin, although the levels of growth appeared to be reduced relative to that observed for the genetically complemented $\Delta bioB::pBioB$ strain (see **Figure 3.13, Panel A and C, Row 3**). The reason for differences in growth between the strains is, however, not

currently known, since both strains should possess a functional biotin biosynthetic pathway. These results, nevertheless, support the previous findings that the activity of YigM is required for the uptake of biotin by *S. Tm* when the biosynthetic pathway is absent.

3.2.7 *De novo* biotin biosynthesis is essential for *S. Tm* viability in M9 minimal media

The growth and survival of the WT and mutant strains were next examined following growth in minimal medium in the absence and presence of 10 nM biotin. As shown in **Figure 3.14**, WT *S. Tm* displayed a seven to eight log-fold increase in bacterial numbers following 24 h growth in both biotin-supplemented and non-supplemented minimal medium (**Figure 3.14**). The growth of the $\Delta bioB$ mutant was, by contrast, dependent on the presence of biotin with an approximately six log-fold increase observed over the same period. When biotin was omitted from the growth medium, however, the viability of the $\Delta bioB$ mutant was reduced (~ 0.5 log-fold decrease, relative to starting inoculum). The $\Delta yigM$ mutant's growth was not dependent on the presence of biotin, due to it containing an intact biotin biosynthetic pathway. The combined inactivation of the *bioB* and *yigM* genes, by contrast, decreased bacterial survival in both the presence and absence of biotin. These observations indicate that biotin supplementation is capable of rescuing the growth of the $\Delta bioB$ mutant only when YigM is present and supports the notion that the protein functions as the sole or primary biotin transporter in *S. Tm*, as has been shown for *E. coli*.

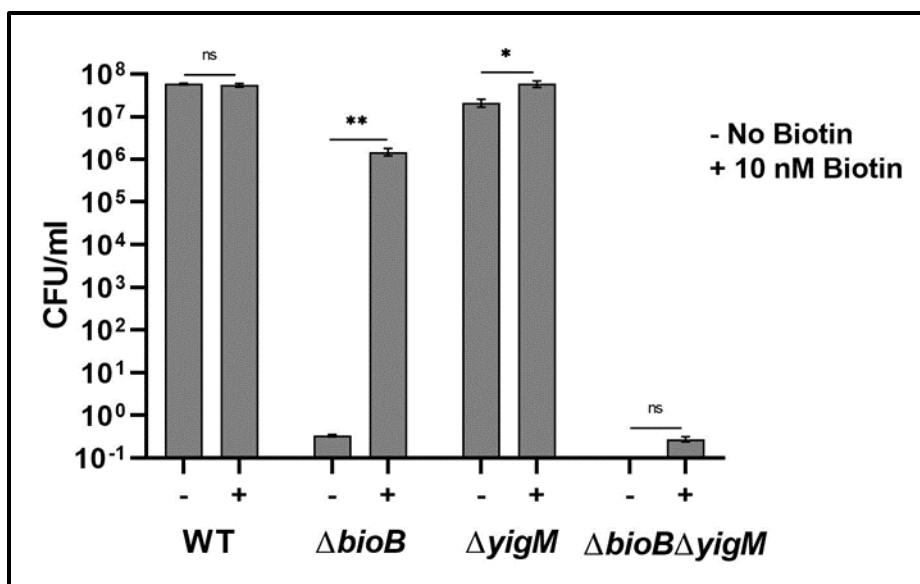


Figure 3.14: *S. Tm* mutants lacking BioB are dependent on YigM-mediated biotin transport for growth. The indicated strains were grown at 37°C in M9 minimal media in the presence and absence of 10 nM biotin (+ and -, respectively) and the number of viable bacteria (CFU/ml) enumerated after 24 h. The mean of three experiments repeated in triplicate is shown (\pm SEM). Two-way ANOVA with Sidak's post-test was used for statistical analysis, ns, $p > 0.05$; *, $p \leq 0.05$; **, $p \leq 0.01$.

3.2.8 Generation of a $\Delta bioB::Km^R P_{BAD}::yigM$ conditional mutant

As a complementary means of verifying the role of YigM in biotin transport in *S. Tm*, we also constructed an *S. Tm* conditional mutant in which the native promoter of the *yigM* gene was replaced with an arabinose inducible, P_{BAD} promoter (Gueguen and Cascales, 2013). Since the expression of YigM in the generated $P_{BAD}::yigM$ strain is expected to be arabinose-inducible, the growth of $\Delta bioB::Km^R P_{BAD}::yigM$ double mutant should only be possible in the presence of both arabinose and biotin. The promoter of *yigM* was initially replaced with the Km^R cassette of pRL128, which contains an FRT-flanked Km^R gene upstream of the *araC* repressor and the P_{BAD} promoter (Gueguen and Cascales, 2013). This was accomplished by utilising primers with sequences homologous to of the 3'- and 5'-ends of the *yigL* and *yigM* genes, respectively (**Figure 3.15**). The resulting ~2.5 kb PCR product (**Figure 3.16**) was purified and electroporated into wild-type *S. Tm* expressing the λ -Red recombinase proteins, as described for the creation of the single mutant strains above.

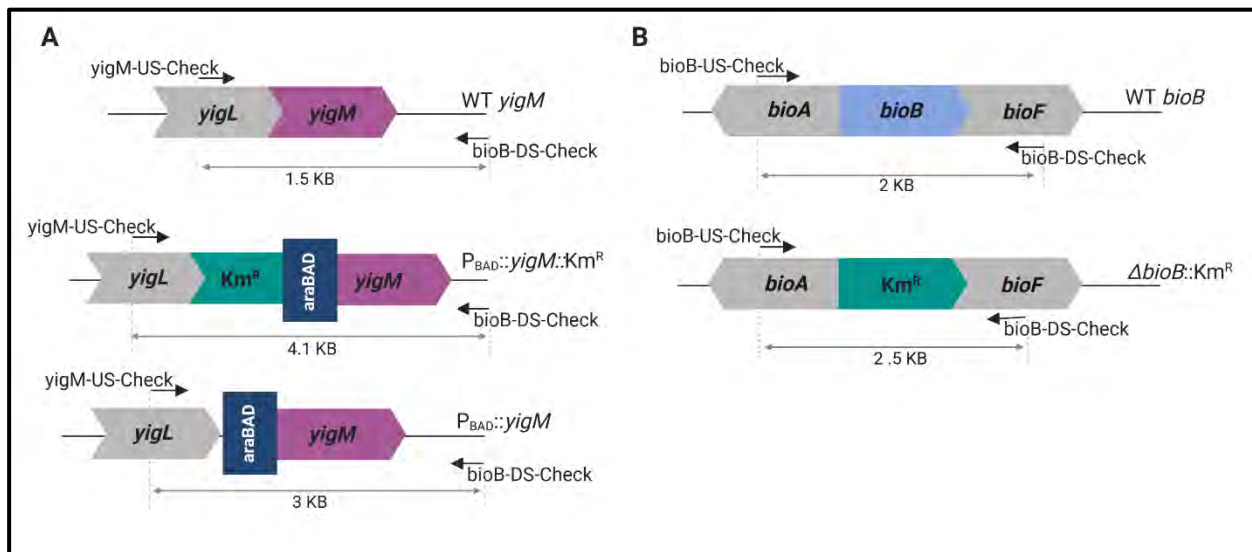


Figure 3.15: Schematic representation of the WT *yigM* locus of *S. Tm* and expected sizes of the marked and unmarked $P_{BAD}::yigM$ alleles. The location of the US and DS primers specific for (A) *yigM* and (B) *bioB* are represented by inward-facing arrows. The following features are depicted: Km^R : Kanamycin resistance cassette. *araBAD*: arabinose inducible promoter. Created with BioRender.

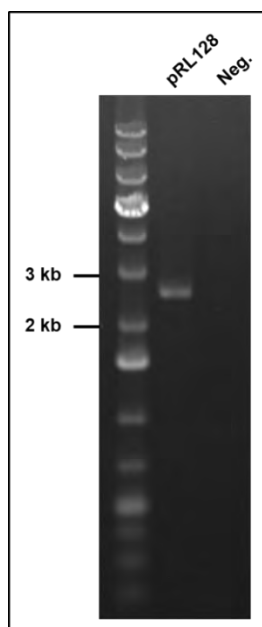


Figure 3.16: Generation of the *yigM* promoter-specific Km^R cassette by PCR amplification. PCR amplification reactions were performed using the primers YigM-Pro-For/YigM-Pro-Rev and pRL128 as a template. The PCR reaction products were electrophoresed on a 0.8 % agarose gel at 80V for 50 min before being visualised under UV light. Lane 1: MW marker, Lane 2: PCR product with pRL128 DNA template, Lane 3: PCR product for no DNA template, negative control.

The genotype of the selected $P_{BAD}::yigM$ transformant was confirmed by the identification of a ~ 4.1 kb amplicon following PCR amplification with primers *yigM*-US-Check/*yigM*-DS-Check, which corresponds to the size of the Km^R -marked $P_{BAD}::yigM$ allele (**Figure 3.17**, Lanes 7). The allele was subsequently transduced into a clean WT genetic background and the Km^R cassette removed by FLP-recombinase, as previously described for the *S. Tm* single mutant strains. To generate a biotin auxotroph in which the function of YigM could be assessed, the $\Delta bioB::Km^R$ allele previously generated was transduced into the unmarked $P_{BAD}::yigM$ strain and transformants selected under growth-permissive conditions (i.e. LB medium supplemented with arabinose). The genotype of the resulting $P_{BAD}::yigM \Delta bioB::Km^R$ strain was confirmed by the identification of amplicons of ~ 2.5 and 3.0 kb (**Figure 3.17**, Lane 4 and 5), which are consistent with the expected sizes of the $\Delta bioB::Km^R$ and unmarked $P_{BAD}::yigM$ alleles, respectively.

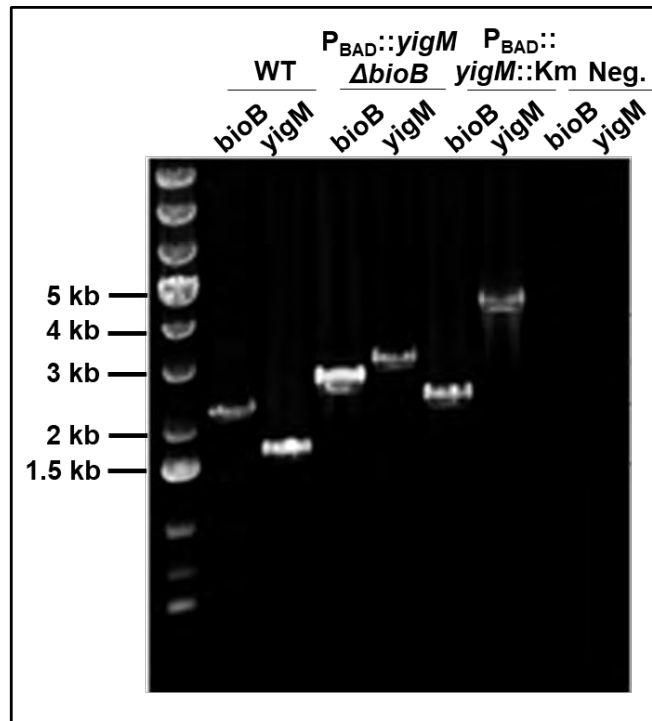


Figure 3.17: PCR confirmation of the genotypes of the *yigM* and *bioB* alleles present in the *S. Tm* WT and mutant strains. PCR reactions were performed on the *S. Tm* strains using primers specific for either *bioB* (*biob*-US-Check/*biob*-DS-check) or *yigM* (*yigM*-US-Check/*yigM*-DS-check) as listed above each lane. Reaction products were subjected to electrophoresis on 0.8 % Agarose for ~ 50 min at 80 V. Genomic DNA from the following strains were used as a template in the PCR reactions: **Lane 1:** MW marker, **Lanes 2-3:** WT genomic DNA, **Lanes 4-5:** $P_{BAD}::yigM \Delta bioB::Km^R$ genomic DNA, **Lanes 6-7:** $P_{BAD}::yigM::Km$ genomic DNA. **Lanes 8-9:** No DNA, Control

3.2.9 Growth analysis of the $\Delta bioB::Km^R$ $P_{BAD}::yigM$ promoter replacement mutant

The growth of the promoter replacement mutant was analysed by spotting the strain on M9 minimal medium agar plates, in the presence or absence of 0.2 % arabinose (**Figure 3.18**). In the absence of arabinose, the promoter replacement mutant was unable to grow, except when the growth medium was supplemented with excess (1 μ M) biotin. The induction of YigM expression by arabinose was similarly unable to restore bacterial growth in the absence of biotin (0 nM) but could do so when the medium was supplemented with 10 and 100 nM biotin. Surprisingly, no growth of the promoter replacement strain was observed on medium supplemented with 1 nM biotin. This contrasts with our previous observations where YigM was capable of restoring the growth of the $\Delta bioB$ biotin auxotroph when using this concentration of biotin (see **Figure 3.13**). This could be attributable to lower expression levels of *yigM* from the *E. coli* P_{BAD} promoter, relative to those achieved from the native *yigM* promoter on either the chromosome or the pYigM complementation vector. The dependence of the promoter replacement strain on both arabinose and biotin for growth, nevertheless, further supports the role of YigM in mediating biotin transport in *S. Tm*.

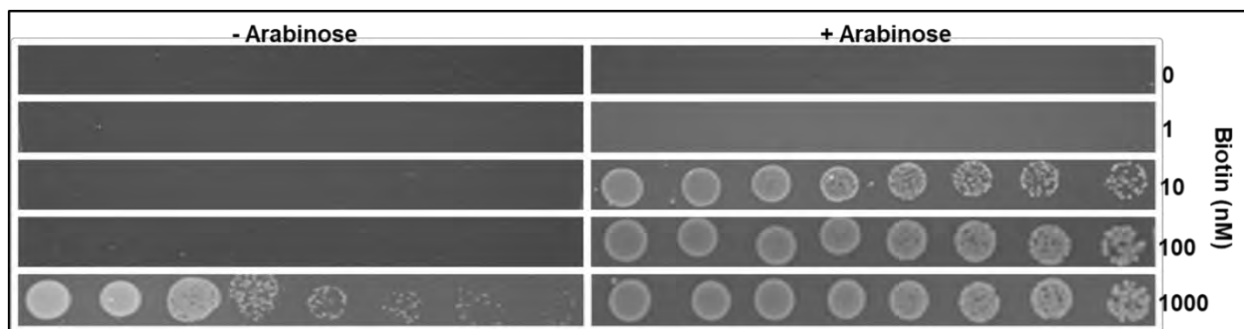


Figure 3.18: The growth of the *S. Tm* $\Delta bioB::Km^R$ $P_{BAD}::yigM$ promoter replacement mutant is dependent on the arabinose induced expression of YigM. The conditional mutant strain was starved for biotin as described in the Materials and Methods and ten-fold serial-dilutions spotted on M9 MM plates supplemented with the indicated biotin concentrations in the presence or absence of 0.2 % arabinose. The plates were incubated at 37°C for 24 h before imaging.

3.3 Chemical genetic studies to confirm the role of YigM in biotin transport

The genetic studies presented in the previous sections support a role for YigM in biotin transport in *S. Tm*. To complement these findings, we examined the effects of inhibiting biotin biosynthesis in the WT and $\Delta yigM$ mutant strain with the small molecule inhibitor of the BioA, MAC-13772 (Côté *et al.*, 2016; Zlitni *et al.*, 2013). To confirm whether MAC-13772 inhibits *S. Tm* growth, we first confirmed the compound's antibacterial activity against *E. coli* in biotin-supplemented and non-supplemented minimal medium. As shown in **Figure 3.19**, the minimal inhibitory concentration (MIC) of MAC-13772 against *E. coli* was ~ 16 and $1024 \mu\text{g/ml}$ when grown in the presence and absence of biotin, respectively. These MIC values are consistent with those obtained in previous studies (Côté *et al.*, 2016; Zlitni *et al.*, 2013; Carfrae *et al.*, 2020) and support the observation that the growth defect caused by the inhibition of biotin biosynthesis in the presence of MAC-13277 can be alleviated by the provision of exogenous biotin.

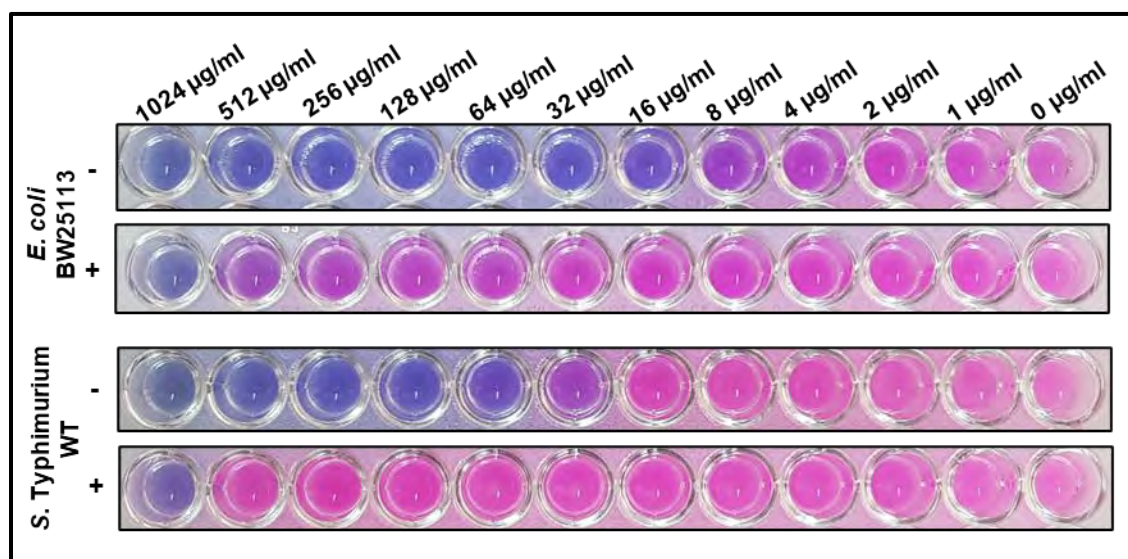


Figure 3.19: MAC-13772 inhibits biotin biosynthesis in both *E. coli* and *S. Tm*. The MICs of MAC-13772 were determined against *E. coli* and *S. Tm* in the presence (+) and absence (-) of 10 nM biotin. Bacterial growth was assessed via the addition of resazurin. A pink and blue colour indicates the presence or absence of growth, respectively.

To establish whether MAC-13772 possesses similar antibacterial activity against *S. Tm*, its activity against the WT strain was determined as described above for *E. coli*. As shown in **Figure 3.19**, the MIC of MAC-13772 against *S. Tm* was $\sim 64 \mu\text{g/ml}$ in the absence of biotin, which increased

to 1024 $\mu\text{g/ml}$ following supplementation with biotin. An identical two-fold difference in the MIC values of MAC-13277 against *S. Tm* and *E. coli* in biotin-free medium (64 $\mu\text{g/ml}$ vs. 16 $\mu\text{g/ml}$, respectively) was recently also observed by Carfrae *et al.* (2020). Our results, nevertheless, confirm that MAC-13772 inhibits the growth of WT *S. Tm* in a biotin-dependent manner, as has been demonstrated for *E. coli*.

To verify the role of YigM in biotin transport using this approach, we next examined the ability of biotin to reverse the growth inhibition caused by MAC-13772 in either the WT, ΔbioB , or ΔyigM strains. Consistent with our previous results, MAC-13772 inhibited the growth of the YigM-expressing (YigM⁺) WT strain in a biotin-dependent manner (**Figure 3.20**, MIC = 64 and >512 $\mu\text{g/ml}$ in the absence and presence of biotin, respectively). This reflects the strain's ability to overcome the chemical inhibition of biotin biosynthesis by MAC-13277 by transporting biotin from the growth medium. As expected, the YigM⁺ ΔbioB auxotrophic mutant was unable to grow in minimal medium in the absence of biotin (**Figure 3.20**). Similar to the WT strain, the ΔbioB strain was impervious to the antibacterial activity of MAC-13772 in the presence of biotin (MIC >512 $\mu\text{g/ml}$), presumably due to its ability to transport biotin from the media in a YigM-dependent manner. The growth of the ΔyigM mutant was inhibited to a similar extent as the WT strain in the absence of biotin (MIC= 64 $\mu\text{g/ml}$; **Figure 3.20**). In contrast to the observations for the YigM⁺ WT and ΔbioB strains (MICs >512 $\mu\text{g/ml}$), the growth inhibitory activity of MAC-13772 against the ΔyigM mutant could not be reversed by the inclusion of biotin in the growth medium (MIC= ~ 64 $\mu\text{g/ml}$). The synthetic lethal phenotype observed following chemical inhibition of biotin biosynthesis by MAC-13277 in the ΔyigM mutant supports our previous observations that YigM activity is essential for the uptake of biotin by *S. Tm*. Taken together, our findings in this and preceding sections support the assertion that YigM serves as the biotin transporter of *S. Tm* and should therefore be renamed BioP, as has been proposed for other members of this family of transporters (Cote *et al.*, 2016; Carfrae *et al.*, 2020).

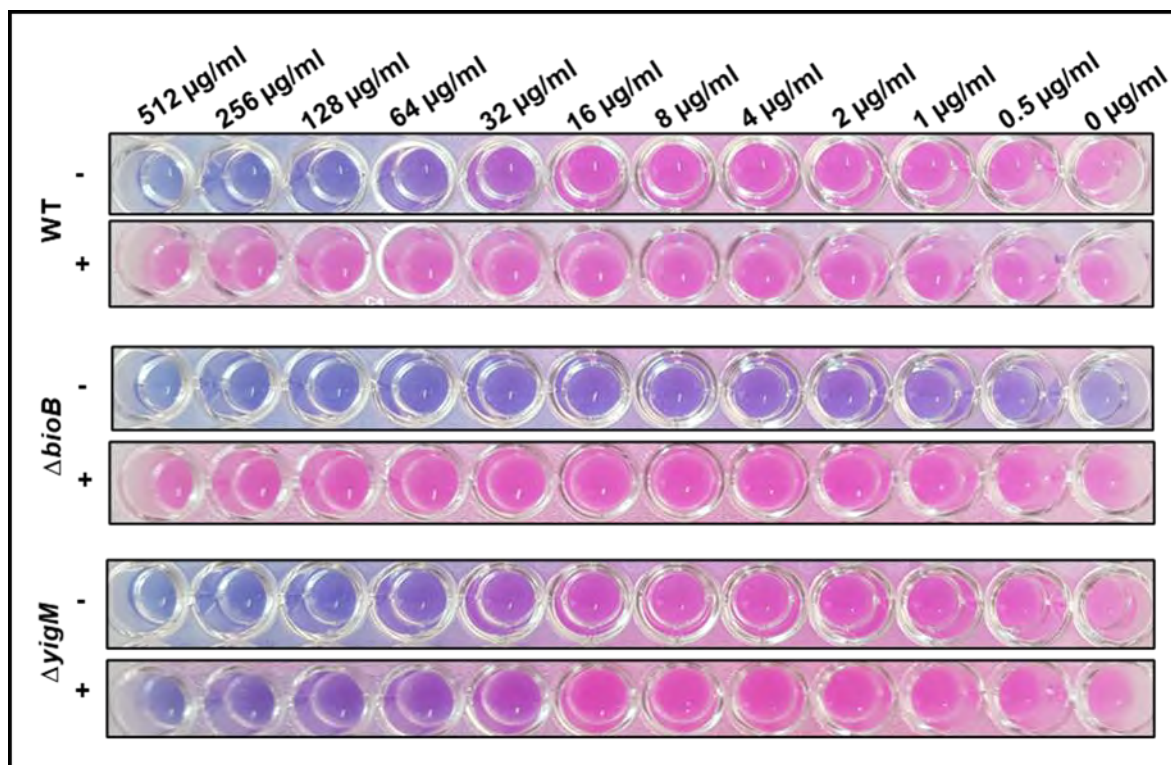


Figure 3.20: Chemical inhibition of *de novo* biotin biosynthesis in the $\Delta yigM$ mutant results in a synthetic lethal phenotype. The MICs of MAC-13722 were determined against the *S. Tm* WT, $\Delta bioB$, and $\Delta yigM$ strains in the presence (+) and absence (-) of 10 nM biotin. Growth was assessed via the addition of resazurin. A pink and blue colour indicates the presence or absence of growth, respectively.

3.4. Assessment of the role of biotin biosynthesis and transport in the intracellular growth and survival of *S. Tm*

To date, the role of the YigM has been investigated in *E. coli* during growth under biotin-limited and replete conditions *in vitro* (Cote *et al.*, 2016; Finkenwirth *et al.*, 2013; Ringlstetter, 2010). Relatively little is, however, known about the role of this family of transporters in supporting bacterial growth during infection of host cells. The gene expression data presented in **Section 3.1** suggests that *S. Tm* utilises both the biosynthetic and transport pathways to support its growth while residing within the nutrient-limited SCV. Epithelial cells and phagocytes are the primary host cells targeted by *Salmonella* during systemic infections and the ability to replicate within these cells is central to the organisms virulence and pathogenicity (see **Section 1.5**). To establish the relative importance of the biotin biosynthesis and transport pathways for the intracellular

growth and survival of *S. Tm*, we consequently compared the proliferation of the WT and biotin biosynthesis and transport deficient mutants following infection of each of these host cell types, as described below.

3.4.1. Intracellular replication of *S. Tm* in human HeLa epithelial cells.

The proliferation of the WT and mutant *S. Tm* strains was first compared following infection of the human HeLa epithelial cell line. An *S. Tm* Δ *ssaV* mutant, which is defective for intracellular replication due to its inability to translocate any SPI2-TTSS encoded effectors, was included as a negative control (Shea *et al.*, 1996). For these studies, all strains were grown under micro-aerophilic conditions prior to infection to induce the expression of the SPI1-TTSS, which is required for the invasion of non-phagocytic cells (Ibarra *et al.*, 2010). The intracellular bacteria were subsequently quantified at 2 and 16 h post-infection (p.i.). As shown in **Figure 3.21 A.**, the uptake of all strains was similar at 2 h p.i, with ~ 0.015, 0.015, 0.017, 0.024, and 0.026 % of the initial inoculum internalised for the WT, Δ *ssaV*, Δ *bioB*, Δ *yigM*, and Δ *bioB* Δ *yigM* strains, respectively. At 16 h p.i., the number of WT *S. Tm* increased by ~ 20-fold (**Figure 3.21 B**). The *S. Tm* Δ *ssaV* mutant strain, which is known to be attenuated for intracellular proliferation, displayed only a 3-fold change in bacterial numbers over the same period. The intracellular proliferation of the Δ *yigM* mutant was similar to the WT strain (~24-fold change). The Δ *bioB* mutant, by contrast, displayed a growth defect relative to the WT strain, with only an ~ 5-fold increase in bacterial number observed over the 16 h infection period. The ability of the Δ *bioB* mutant to replicate, albeit at a reduced rate relative to the WT, suggests that *S. Tm* has access to at least some biotin to support bacterial growth in the intracellular environment. This theory was substantiated by the decreased survival observed for the Δ *bioB* Δ *yigM* double mutant (~ 0.65 -fold change), indicating that bacterial viability is lost in the biotin auxotrophic mutant when the transport pathway is simultaneously disrupted. The data presented above suggests that biosynthetic pathway makes a much more significant contribution to *S. Tm* replication than biotin transport following infection of epithelial cells. While YigM mediates the transport of biotin to support low levels of growth in the absence of the biotin biosynthetic pathway, its ability to support WT levels of growth is restricted by the limited availability of biotin in the cytosol or SCVs of infected cells.

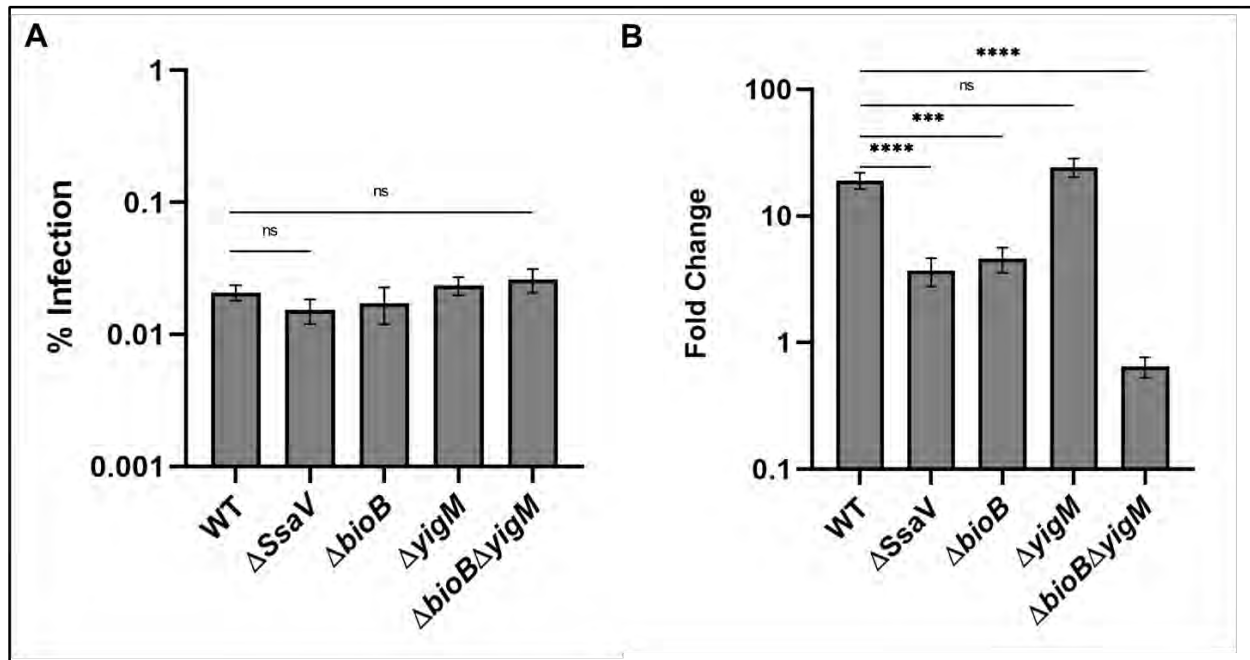


Figure 3.21: *S. Tm* biotin *de novo* biosynthesis mutants are attenuated in HeLa cells. *S. Tm* WT and mutant strains were grown to stationary phase in LB media and used to infect HeLa cells at an MOI of 100. **A)** The number of intracellular bacteria was enumerated at 2 h post-infection and the % infection was calculated by determining the number of intracellular bacteria present at 2 h relative to that present in the inoculum. **B)** The number of intracellular bacteria was enumerated at 2 and 16 h post-infection. The fold change is defined as the ratio of intracellular bacterial present at 16 h to 2 h post-infection (\pm SEM). One-way ANOVA with Sidak's post-tests were used for statistical analysis, ns, $p > 0.05$; ***, $p < 0.001$; ****, $p < 0.0001$.

3.4.2 Intracellular replication of *S. Tm* in murine RAW264.7 macrophages

In addition to epithelial cells, *S. Tm* can also infect phagocytic cells such as macrophages during systemic infections. We, therefore, assessed the intracellular proliferation of the WT and mutant strains in the murine macrophage-like cell line, RAW264.7. For these studies, the macrophages were infected with bacteria grown to late stationary phase to inhibit the expression of the invasion-associated SPI-1-TTSS, which may cause invasion-associated macrophage cytotoxicity (Chen *et al.*, 1996; Monack *et al.*, 1996). As shown in **Figure 3.22 A**, the phagocytic uptake of the strains by the RAW264.7 macrophages was comparable for the *S. Tm* WT (0.014 %) and single mutant strains, with 0.009 % and 0.008 % of the initial $\Delta bioB$ and $\Delta yigM$ inoculum internalised at 2 h p.i., respectively. Consistent with the results observed in HeLa cells, the intracellular proliferation of the $\Delta SsaV$ mutant was significantly reduced relative to the WT strain at 16 h p.i. (~ 3- and 300-

fold increases, respectively) (Figure 3.22 B). The $\Delta bioB$ mutant also displayed a significant growth defect relative to the WT strain and was present at ~ 60 -fold-lower levels. The $\Delta yigM$ mutant, by contrast, replicated at a similar level to the WT (~ 240 -fold), suggesting that biotin transport by YigM is not required when a functional biotin biosynthesis pathway is present.

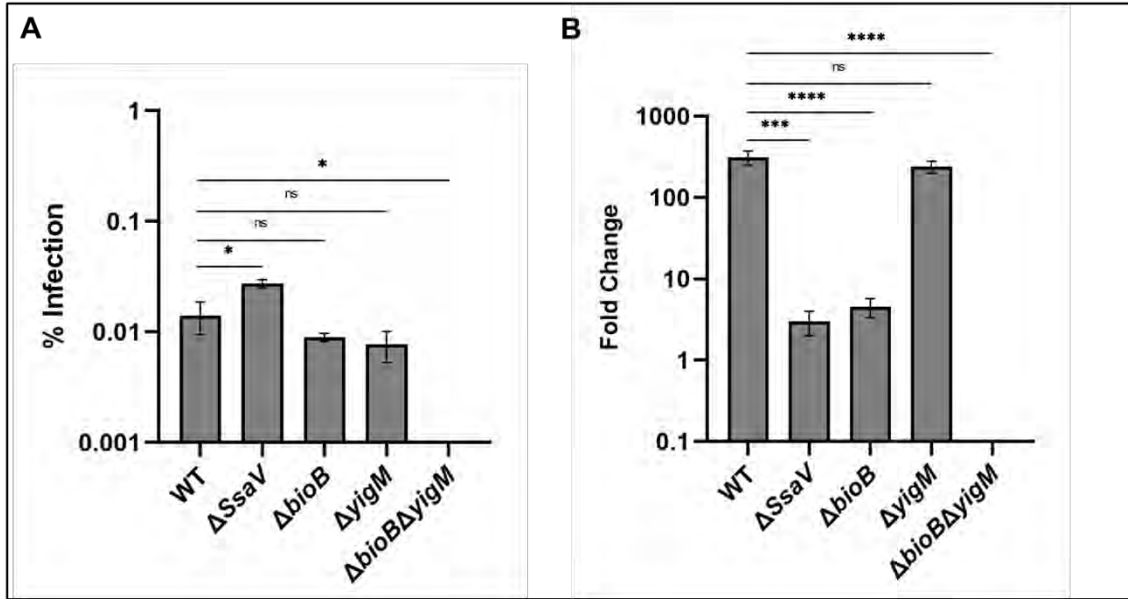


Figure 3.22: *S. Tm* biotin *de novo* biosynthesis mutants are attenuated in RAW264.7 cells. *S. Tm* WT and mutant strains were grown to stationary phase in LB media and used to infect RAW264.7 cells at an MOI of 10. **A)** The number of intracellular bacteria was enumerated at 2 h post-infection and the % infection was calculated by determining the number of intracellular bacteria present at 2 h relative to that present in the inoculum. **B)** The number of intracellular bacteria was enumerated at 2 and 16 h post-infection. The fold change is defined as the ratio of intracellular bacterial present at 16 h to 2 h post-infection (\pm SEM). One-way ANOVA with Sidak's post-tests were used for statistical analysis, ns, $p > 0.05$; ***, $p < 0.001$; ****, $p < 0.0001$.

In contrast to our observations in HeLa cells, the $\Delta bioB \Delta yigM$ double mutant was not recoverable from infected macrophages at either the 2 or 16 h time points p.i. (Figure 3.22 A and B, respectively). The reason for this may be due to the decreased phagocytic uptake of the strain since no bacteria were recoverable at 2 h p.i. The double mutant may, alternatively, display a reduced ability to survive within the more restrictive intracellular environment of RAW264.7 macrophages, which possesses a greater array of antibacterial effector mechanisms than HeLa cells and is also

more nutritionally limited (Röder and Hensel, 2020). The severe attenuation observed for the biotin auxotroph nevertheless suggests that the biotin concentration in the SCV is limited during infection of RAW264.7 macrophages, reducing the capacity of YigM-mediated biotin transport to rescue the growth defect of the strain.

3.5 Chemical inhibition of biotin biosynthesis reduces *S. Tm* proliferation in mammalian cells

The data presented above suggest that the biotin biosynthesis pathway is essential for *S. Tm*'s ability to maintain WT levels of growth following infection of both epithelial cells and macrophages. To establish whether chemical inhibition of the biotin biosynthesis pathway can inhibit the growth of *S. Tm* in the intracellular environment, we measured the proliferation of the WT, $\Delta bioB$, and $\Delta yigM$ strains following infection of RAW 264.7 macrophages in the absence and presence of the BioA inhibitor MAC-13722. For these studies, MAC-13722 was included in the cell culture medium at a concentration of 320 $\mu\text{g/ml}$, which did not possess any cytotoxicity against the host cells during infection (data not shown). As shown in **Figure 3.23**, the chemical inhibition of the biotin biosynthetic pathway with MAC-13722 resulted in a decrease in the intracellular proliferation of the WT strain (~ 40 -fold) over the assay period. This decrease was, however, not as pronounced as that caused by genetic inactivation of biotin biosynthesis in the $\Delta bioB$ mutant (**Figure 3.23**). While MAC-13722 had no effect on the growth of the $\Delta bioB$ mutant, it caused a significant reduction in the intracellular proliferation of the transport deficient $\Delta yigM$ mutant (~ 60 -fold). These observations indicate that MAC-13722 is capable of inhibiting the *S. Tm* BioA enzyme and biotin biosynthesis while the bacterium is present within the SCV of infected cells. Our results demonstrating that biotin biosynthesis is required for the optimal growth of *S. Tm* following infection of macrophages and epithelial cells, coupled with the pathway's susceptibility to chemical inhibition, suggests that the enzymes of the biotin biosynthetic pathway may represent a good antibacterial target. This is particularly true given the inability of the bacterium to salvage sufficient biotin from infected host cells to fully rescue the growth defect displayed following either genetic or chemical inhibition of the biosynthetic pathway (**Figures 3.21 to 3.23**).

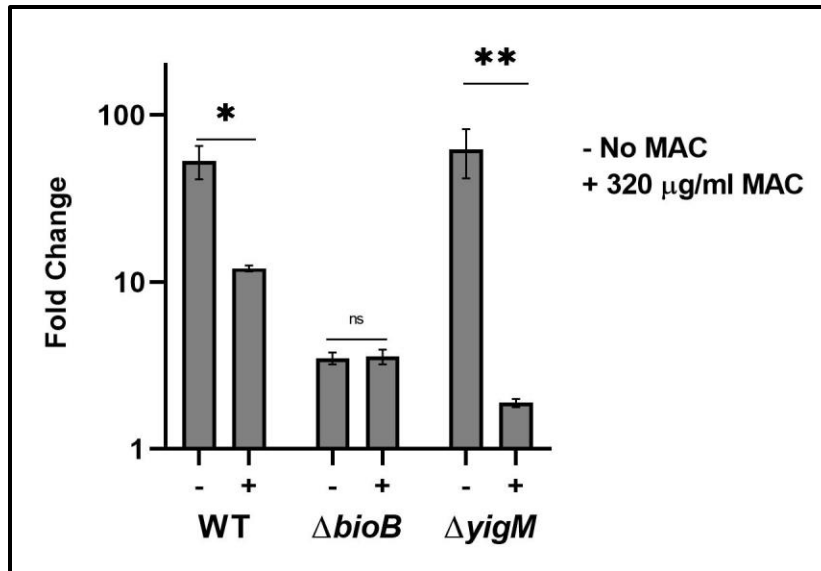


Figure 3.23: Inhibitory effect of MAC-13772 on *S. Tm* WT and mutant strains in RAW264.7 cells. *S. Tm* WT and mutant strains were grown to stationary phase in LB media and used to infect RAW264.7 cells at an MOI of 10. The number of intracellular bacteria in untreated cells was enumerated at 2 h post-infection. The remaining cells were incubated in the presence (+) or absence (-) of MAC-13277 (320 μg/ml) for an additional 14 h before the enumeration of intracellular bacteria. The fold change is defined as the ratio of intracellular bacterial present at 16 h to 2 h post-infection (±SEM). One-way ANOVA with Sidak's post-tests were used for statistical analysis, ns, $p > 0.05$; ***, $p < 0.001$; ****, $p < 0.0001$.

Chapter 4: Discussion

S. Tm is a facultative intracellular pathogen capable of causing both localised and systemic infection in humans and animals. The bacterium encounters a range of nutritional conditions during infection and must adjust its metabolism based on the availability of nutrients in each of the environments it occupies (Dandekar *et al.*, 2015). *S. Tm* possesses numerous metabolic pathways that are redundant and therefore dispensable for the growth of the organism during infection (Barat *et al.*, 2012; Becker *et al.*, 2006; Steeb *et al.*, 2013). Other pathways are, by contrast, essential for bacterial proliferation in the host and their identification and characterisation may enable the discovery of potentially useful drug targets (Hartman *et al.*, 2014; Jelsbak *et al.*, 2014; Wrande *et al.*, 2016). This study aimed to obtain a better understanding of one such pathway, biotin biosynthesis, which has been shown to be important for the growth and survival of *S. Tm in vitro* (Kröger *et al.*, 2013; Shi *et al.*, 2009b) and during the infection of host cells *ex vivo* and *in vivo* (Denkel *et al.*, 2013; Shi *et al.*, 2006; Sheikh *et al.*, 2011).

In line with previous observations, inactivation of the biotin biosynthesis pathway resulted in the production of a mutant ($\Delta bioB$) that was capable of growth in the presence, but not absence, of biotin (**Figure 3.13**). The ability of the $\Delta bioB$ mutant to grow at wild type levels in the presence of biotin concentrations < 100 nM showed that the biotin transport pathway can compensate for the loss of the biosynthetic pathway during the growth of *S. Tm in vitro*. While the YigM protein has been shown to serve as the high-affinity biotin transporter in *E. coli* and several other bacterial species (Carfrae *et al.*, 2020; Finkenwirth *et al.*, 2013; Ringlstetter, 2010; Xiao *et al.*, 2019) its biological function had not been experimentally validated in *S. Tm* to date. The results obtained during the course of this work (**Section 3.2.5**, **3.2.6** and **Section 3.2.9**) indicated that the primary function of YigM in *S. Typhimurium* is that of a high-affinity biotin transporter. This conclusion was based on several independent, but complementary, experiments. Firstly, we showed that the ability of the *S. Typhimurium* $\Delta bioB$ auxotrophic mutant to grow in the presence of trace amounts of biotin (< 100 nM) was dependent on the presence of a functional YigM protein. When the expression of YigM was eliminated in the $\Delta bioB$ background through either (i) genetic inactivation in the $\Delta bioB \Delta yigM$ double mutant (**Section 3.2.5** and **3.2.6**) or (ii) gene silencing in the absence of arabinose in the $\Delta bioB P_{BAD}::yigM$ mutant (**Section 3.2.9**), the viability of the mutant strain was lost. The growth of the mutant could be rescued by the plasmid-borne expression

of *yigM* in the $\Delta bioB \Delta yigM$ double mutant, or by inducing *yigM* expression with arabinose in the $\Delta bioB P_{BAD}::yigM$ conditional mutant, indicating that the growth defects of these strains were not due to any off-target effects. Interestingly, while mutants lacking both biotin and transport pathways were defective for growth at biotin concentrations ranging between 0 and 100 nM, their growth could be rescued by the inclusion of high concentrations of biotin ($\sim 1 \mu\text{M}$) in the growth medium (see **Figure. 3.18**). This concentration of biotin was included in the growth medium during the initial isolation of the $\Delta bioB \Delta yigM$ and $\Delta bioB P_{BAD}::yigM$ strains to avoid any detrimental effects arising from the simultaneous inactivation of biotin biosynthesis and transport. This approach was based on the studies of Finkenwirth *et al.* (2013, 2014), which showed that an *E. coli* $\Delta bioH \Delta yigM$ double mutant could grow at high concentrations of biotin (Finkenwirth *et al.*, 2013, 2014). Carfrae *et al.* (2020) recently reported that the growth of an *E. coli* biotin auxotroph could be restored to 50 % of that of the WT strain when the growth medium was supplemented with 0.8 to 1.6 nM biotin. This level was, however, increased to ~ 150 nM when YigM (BioP) was also inactivated. This observation suggests that while YigM may be essential for bacterial growth in the presence of trace amounts of biotin (< 100 nM), its function can be replaced by an alternative transport system when biotin is supplied in excess. The identity of this alternative transport system is currently unknown, but it is thought to be mediated by non-specific transmembrane proteins, such as aquaporins, in *E. coli* (Azhar *et al.*, 2015). The physiological levels of biotin in human plasma are estimated at ~ 1 nM, while murine plasma concentrations are ~ 40 nM (Carfrae *et al.*, 2020). The biotin concentration in the ileum and colon, by contrast, has been estimated to range between 30–45 nM and 450–700 nM, respectively (Yang *et al.*, 2015). These observations suggest that YigM activity may be dispensable for biotin uptake in the intestinal tract, where the biotin concentrations are high enough to allow for biotin uptake via facilitated diffusion by aquaporins or other non-specific transport systems. The *S. Tm* YigM protein may, however, play an important role in transporting biotin during systemic infections, where the lower biotin concentrations in plasma and/or within host cells are likely to make uptake by a high-affinity transporter essential.

Previous studies have shown that the biotin biosynthetic pathway is up-regulated following infection of RAW264.7 macrophages (Kröger *et al.*, 2013; Shi *et al.*, 2009b; Shi *et al.*, 2006; Srikumar *et al.*, 2015). The growth of *S. Tm* biotin auxotrophic strains has also been shown to be

attenuated following infection of RAW264.7 macrophages (Denkel *et al.*, 2013; Shi *et al.*, 2009b). The results obtained here confirmed these observations since the $\Delta bioB$ biosynthetic mutant displayed decreased intracellular growth relative to the WT strain (**Figure 3.23 B**). Biotin is present within both epithelial cells and macrophages and *S. Tm* can access the vitamin when present in either the SCV or host-cell cytosol (Röder *et al.*, 2020). The cell culture medium used during this study (DMEM) does not contain an endogenous source of biotin. The vitamin is, however, supplied by foetal calf serum (FCS) and is estimated to be present in the cell culture medium at a final concentration of ~ 19 nM. The ability of the $\Delta bioB$ mutant to replicate in RAW264.7 cells, albeit at a reduced level to the WT, indicates that *S. Tm* has access to sufficient quantities of biotin to support limited proliferation while residing within the SCV (**Section 3.4.2**). Since the biotin concentration in the DMEM cell culture medium was above the physiological range found in humans (~ 1 nM) during systemic infection, we did not examine the effect of additional biotin supplementation on bacterial growth. Denkel *et al.* (2013), however, reported that a $\Delta bioB$ auxotrophic mutant was attenuated following infection of RAW264.7 macrophages in RPMI medium, which has an endogenous biotin concentration of ~ 819 nM. This suggests that the levels of biotin within host cells may be too low to sustain maximal levels of *S. Tm* growth in the SCV of infected cells, even when the vitamin is supplied in the growth medium at supraphysiological levels. The ability of the $\Delta bioB$ strain to utilise available biotin is, however, dependent on YigM since the mutant strain lacking both BioB and YigM was not recoverable following macrophage infections (**Figure 3.23 B**). The inability to recover the double mutant following infection of macrophages was not due to differences in the size of the bacterial inoculum or viability of the strain immediately prior to infection (data not shown). We did not examine whether the double mutant possesses features such as altered cell envelope composition that may reduce its capacity to be phagocytosed by macrophages. To remove this as a potential source of variability in future studies, the WT and mutant strains could be opsonized with mouse serum prior to infection to ensure that equivalent numbers of bacteria are taken up by the macrophages (Beuzón *et al.*, 2002). The severe growth defect of the double mutant seen *in vitro* (**Figures 3.12 to 3.14**), coupled with its exposure to antimicrobial effector mechanisms in macrophages, may however result in the effective clearance of the strain following its phagocytic uptake. Taken together, our results demonstrate that *S. Tm* meets its biotin requirements following the infection of macrophages primarily via the biosynthetic pathway. The YigM-mediated biotin transport

pathway is furthermore dispensable for growth in cultured macrophages and is only partially capable of rescuing the growth of *S. Tm* in the absence of an intact biosynthesis pathway. This observation suggest that *S. Tm* may be unable to access sufficient levels of biotin to support WT levels of growth while residing in the SCV of infected RAW264.7 cells.

Our results in HeLa cells were similar to that observed following infection of RAW264.7 macrophages. The biotin biosynthetic pathway was essential for maintaining WT levels of growth following the invasion of epithelial cells (**Figure 3.22 B**). Inactivation of the biotin transport pathway also had no discernible effects on the growth of the strain while the biotin biosynthetic pathway remained active. The lack of attenuation observed for the biotin auxotroph in this study, however, differs from those of Hautefort *et al.*, (2003) and Husna *et al.*, (2019) who reported that biotin biosynthesis was dispensable for bacterial growth following the infection of HeLa cells. The reason for these different findings is currently unclear but may be attributable to differences in the bacterial strains and experimental methodologies used. The current study used *S. Tm* 14028s as the WT strain, while the studies of Hautefort *et al.*, (2003) and Husna *et al.*, (2019) used *S. Tm* SL1344. While these strains do not possess any differences in the coding sequences of their biotin biosynthetic or transport genes, *S. Tm* SL1344 harbours a prophage that encodes the SPI1-TTSS effector protein, SopE (Röder and Hensel, 2020). The expression of this effector has been shown to destabilise the SCV membrane, resulting in the increased release of bacteria from the SCV into the nutrient-rich host cell cytosol (Röder and Hensel, 2020). *S. Tm* 14028s, by contrast, does not encode SopE and bacteria are consequently retained in the SCV to a greater extent than SL1344. Following bacterial release from the SCV, the cytosolic population of *S. Tm* replicates more rapidly than bacteria residing in the SCV (Knodler *et al.*, 2013; Knodler, 2014). Cytosolic *S. Tm* also express the SPI1-TTSS and flagellar genes, as opposed to the SPI2-TTSS associated with survival in the SCV (Malik-Kale *et al.*, 2012). The transcriptomic study of Hautefort *et al.*, (2003) showed that the expression of the SPI1-TTSS and flagellar genes were induced following their infection of HeLa cells, confirming that a large proportion of the bacterial population was present in the cytosol of infected host cells. The biotin levels in the cytosol of epithelial cells have recently been shown to be greater than those encountered in the SCV (Röder *et al.*, 2020). The cytosolic population of *S. Tm* SL1344 may consequently have access to larger quantities of biotin than bacteria residing in the SCV, thereby masking the biotin auxotrophy of the strain. The study of Malik-Kale *et al.*, (2012) also demonstrated that the elevated replication of *S. Tm* in the cytosol of

infected epithelial cells can often obscure the growth defects of mutants replicating in the nutrient-limited SCV. This phenomenon was, furthermore, only apparent when bacterial replication was assayed at early (8 h) as opposed to late time points (16 h) post-infection. The authors attributed this to the effective elimination of the cytosolic bacterial population by gentamicin treatment at the later, but not earlier time point. During the current study, bacterial replication by *S. Tm* 14028s was assayed at 16 h post-infection. The studies of Hautefort *et al.*, (2003) and Husna *et al.*, (2019), by contrast, assayed bacterial replication at 6 and 10 h post-infection, respectively. The lack of attenuation observed for the biotin biosynthetic mutants in HeLa cells in previous studies may therefore be due to a combination of the predominantly cytosolic replication of *S. Tm* SL1344, combined with the earlier time points used to assay bacterial replication. The differential growth rates of the $\Delta bioB$ mutant in different cellular compartments could be evaluated in future studies by using drugs that selectively kill either vacuolar or cytosolic bacteria, or reporter strains that enable the differentiation of phagosomal and cytosolic bacterial populations. The results obtained in this study with *S. Tm* 14028s, however, support the notion that the *de novo* biosynthesis of biotin is essential for sustaining WT levels of growth in the SCVs of both epithelial cells and macrophages.

The transcriptional data shown in **Figure 3.1** indicates that the expression of the *bio* operon and *yigM* is induced following phagocytic uptake of *S. Tm* by RAW 264.7 macrophages. The data from our *in vitro* studies showed that although the $\Delta bioB$ auxotroph grew to similar levels as the WT at biotin concentrations >10 nM, its growth rate was reduced at concentrations below ~ 5 nM (see **Figure 3.10**, 1 nM vs. 10 nM and data not shown). Despite its increased intracellular expression levels, biotin transport by YigM is therefore unlikely to be able to restore bacterial growth to WT levels when the concentration of biotin is below this level in the absence of biotin biosynthesis. This observation suggests that inhibiting the biotin biosynthesis pathway may be a viable strategy for treating *Salmonella* infections in humans, where the plasma concentrations are ~1 nM. Our results shown in **Figure 3.19** revealed that the intracellular growth of WT *S. Tm* could be reduced following chemical inhibition of biotin biosynthesis with the known BioA inhibitor, MAC-13722. While chemical inhibition did not reduce bacterial growth to the same extent as genetic inactivation, the inhibition of biotin biosynthesis by MAC-13722 is known to be incomplete (Carfrae *et al.*, 2020). The identification and development of more effective biotin

biosynthetic inhibitors may therefore lead to more profound reductions in bacterial growth. The observations obtained in this study are consistent with additional findings by Carfrae *et al.*, (2020). These authors showed that biotin biosynthesis is dispensable for the growth of several bacterial pathogens, including *A. baumannii*, *K. pneumoniae*, *P. aeruginosa* and *S. Tm* during growth in mouse plasma, which has a biotin concentration of ~ 40 nM. Biotin auxotrophs of these species were also not attenuated during the mouse model of infection, indicating that the strains have access to sufficient levels of biotin during systemic infections of the murine host. The growth of the biotin auxotrophs were, however, reduced when cultivated in human plasma, confirming that the levels of biotin in humans are too low to support WT levels of bacterial growth. When the levels of biotin in mice were artificially reduced to mimic human biotin levels before infection, the growth of the *A. baumannii*, *K. pneumoniae*, and *P. aeruginosa* biotin auxotrophs were significantly attenuated (> 90 % reduction in bacterial numbers relative to the WT strains). These findings suggest that while biotin transport may rescue the growth of bacteria at the biotin concentrations encountered during systemic infections of mice, the levels present in humans are insufficient to compensate for the lack of the biosynthetic pathway. This observation may also explain the lack of attenuation observed for *S. Tm* biotin biosynthetic mutants during genome-wide essentiality screens performed in mice (Chaudhuri *et al.*, 2009). Due to the difficulties associated with reducing the biotin levels in mice during a systemic infection with *S. Tm* (~ 72 h), Carfrae *et al.*, (2020) did not examine the growth of *S. Tm* using this experimental system. The results obtained in this study, however, suggest that the growth of *S. Tm* is likely to be compromised at the biotin concentrations encountered in human plasma. The enzymes of the biotin biosynthetic pathway may consequently serve as good targets for the development of drugs to treat *Salmonella* infections, as has been recently for other medically important bacterial pathogens such as those listed above (Carfrae *et al.*, 2020).

4.1 Summary

The *de novo* biotin biosynthesis pathway is an attractive target for novel antimicrobial drug development since the vitamin cannot be synthesised by humans or other mammals. Until recently this pathway was overlooked as a drug target in *Salmonella* as the bacterium was thought to be capable of overcoming the growth defect caused by the inhibition of the biosynthetic pathway by transporting biotin from the extracellular environment. Previous studies also yielded contradictory

results regarding the essentiality of the biosynthetic pathway for the growth of *Salmonella* following infection of different cell lines, or in the murine model of infection. Here, we sought to establish the relative importance of biotin biosynthesis and transport pathways for the intracellular growth and survival of *Salmonella* by performing a side-by-side comparison of the proliferation of biotin biosynthesis- and transport-deficient strains in two infection-relevant cell lines. Our analysis revealed that while biotin biosynthesis is essential for maintaining WT levels of growth, biotin transport is dispensable for the intracellular proliferation of *Salmonella* in both macrophages and epithelial cell lines. While the requirement for biotin biosynthesis for the growth of *S. Tm* in epithelial cells contradicts the results of previous studies, we believe that this is likely due to differences in the experimental methodologies employed. This will, however, need to be corroborated in future studies that compare the growth and intracellular localisation of the different *S. Tm* strains at various times following infection. We cannot also exclude the possibility that the biotin concentration used in the cell culture medium during this study (estimated at ~19 nM) was too low to ameliorate the growth defects of the biotin auxotroph following infection of host cells. This could for instance be caused by batch-to-batch variation in the biotin levels present in FCS, resulting in the biotin levels being lower than that predicted by commercial vendors. This limitation can be overcome in future studies by examining the effects of supplementing the cell culture medium used during infection with defined concentrations of biotin. These potential limitations notwithstanding, our results confirmed that YigM serves as a high-affinity biotin transporter in *S. Tm*. Our results also suggest that chemical inhibition of biotin biosynthesis may represent an effective means of inhibiting the growth of *S. Tm* during infection. Whether the biotin concentrations in humans are sufficiently low to prevent biotin salvage by the pathogen will, however, have to be confirmed in future work. The biotin biosynthesis and transport mutants generated during this study may also serve as useful tools to probe the ability of *S. Tm* to gain access to nutrients in different cellular compartments, such as the cytosol, SCV or *Salmonella*-induced filaments and/or tubules during infection. Overall, this study has provided a basis for future work that will contribute to a greater understanding of the potential of biotin biosynthesis to serve as a drug target, as well as of the basic physiology and metabolism of *S. Tm* in the intracellular environment.

5. Reference List

- Abrahams, G. L., Müller, P., & Hensel, M. (2006). Functional Dissection of SseF, a Type III Effector Protein Involved in Positioning the Salmonella-Containing Vacuole: SseF and SCV positioning. *Traffic*, 7(8), 950–965. <https://doi.org/10.1111/j.1600-0854.2006.00454.x>
- Acheson, D., & Hohmann, E. L. (2001). Nontyphoidal Salmonellosis. *Clinical Infectious Diseases*, 32(2), 263–269.
- Arabyan, N., Park, D., Foutouhi, S., Weis, A. M., Huang, B. C., Williams, C. C., Desai, P., Shah, J., Jeannotte, R., Kong, N., Lebrilla, C. B., & Weimer, B. C. (2016). Salmonella Degrades the Host Glycocalyx Leading to Altered Infection and Glycan Remodeling. *Scientific Reports*, 6(1), 29525. <https://doi.org/10.1038/srep29525>
- Ausubel, F.M., Brent, R., Kingston, R.E., Moore, D.D., Seidman, J.G., Smith, J.A. & Struhl, K. (2012), Current Protocols in Molecular Biology. John Wiley & Sons, New York.
- Azhar, A., Booker, G. W., & Polyak, S. W. (2015). *Mechanisms of Biotin Transport*. 4(4), 9.
- Baba, T., Ara, T., Hasegawa, M., Takai, Y., Okumura, Y., Baba, M., Datsenko, K. A., Tomita, M., Wanner, B. L., & Mori, H. (2006). Construction of *Escherichia coli* K-12 in-frame, single-gene knockout mutants: The Keio collection. *Molecular Systems Biology*, 2(1). <https://doi.org/10.1038/msb4100050>
- Barat, S., Willer, Y., Rizos, K., Claudi, B., Mazé, A., Schemmer, A. K., Kirchhoff, D., Schmidt, A., Burton, N., & Bumann, D. (2012). Immunity to Intracellular Salmonella Depends on Surface-associated Antigens. *PLoS Pathogens*, 8(10), e1002966. <https://doi.org/10.1371/journal.ppat.1002966>
- Becker, D., Selbach, M., Rollenhagen, C., Ballmaier, M., Meyer, T. F., Mann, M., & Bumann, D. (2006). Robust Salmonella metabolism limits possibilities for new antimicrobials. *Nature*, 440(7082), 303–307. <https://doi.org/10.1038/nature04616>
- Berry, E. D., & Wells, J. E. (2018). Reducing foodborne pathogen persistence and transmission in animal production environments: Challenges and opportunities. *Preharvest Food Safety*, 177–203.
- Best, A., & Abu Kwaik, Y. (2019). Nutrition and Bipartite Metabolism of Intracellular Pathogens. *Trends in Microbiology*, 27(6), 550–561. <https://doi.org/10.1016/j.tim.2018.12.012>
- Beuzón, C. R., Salcedo, S. P., & Holden, D. W. (2002). Growth and killing of a Salmonella enterica serovar Typhimurium sifA mutant strain in the cytosol of different host cell lines. *Microbiology*, 148(9), 2705–2715. <https://doi.org/10.1099/00221287-148-9-2705>

- Bowden, S. D., Rowley, G., Hinton, J. C. D., & Thompson, A. (2009). Glucose and Glycolysis Are Required for the Successful Infection of Macrophages and Mice by *Salmonella enterica* Serovar Typhimurium. *Infection and Immunity*, *77*(7), 3117–3126. <https://doi.org/10.1128/IAI.00093-09>
- Boyd, E. F., Wang, F. S., Whittam, T. S., & Selander, R. K. (1996). Molecular genetic relationships of the salmonellae. *Applied and Environmental Microbiology*, *62*(3), 804–808. <https://doi.org/10.1128/AEM.62.3.804-808.1996>
- Brenner, F. W., Villar, R. G., Angulo, F. J., Tauxe, R., & Swaminathan, B. (2000). Salmonella Nomenclature. *Journal of Clinical Microbiology*, *38*(7), 2465–2467. <https://doi.org/10.1128/JCM.38.7.2465-2467.2000>
- Carey, M. E., Jain, R., Yousuf, M., Maes, M., Dyson, Z. A., Thu, T. N. H., Nguyen Thi Nguyen, T., Ho Ngoc Dan, T., Nhu Pham Nguyen, Q., Mahindroo, J., Thanh Pham, D., Sandha, K. S., Baker, S., & Taneja, N. (2021). Spontaneous Emergence of Azithromycin Resistance in Independent Lineages of *Salmonella* Typhi in Northern India. *Clinical Infectious Diseases*, *72*(5), e120–e127. <https://doi.org/10.1093/cid/ciaa1773>
- Carfrae, L. A., MacNair, C. R., Brown, C. M., Tsai, C. N., Weber, B. S., Zlitni, S., Rao, V. N., Chun, J., Junop, M. S., Coombes, B. K., & Brown, E. D. (2020). Mimicking the human environment in mice reveals that inhibiting biotin biosynthesis is effective against antibiotic-resistant pathogens. *Nature Microbiology*, *5*(1), 93–101. <https://doi.org/10.1038/s41564-019-0595-2>
- Chakravorty, D., Hansen-Wester, I., & Hensel, M. (2002). Salmonella Pathogenicity Island 2 Mediates Protection of Intracellular Salmonella from Reactive Nitrogen Intermediates. *Journal of Experimental Medicine*, *195*(9), 1155–1166. <https://doi.org/10.1084/jem.20011547>
- Chaudhuri, R. R., Peters, S. E., Pleasance, S. J., Northen, H., Willers, C., Paterson, G. K., Cone, D. B., Allen, A. G., Owen, P. J., Shalom, G., Stekel, D. J., Charles, I. G., & Maskell, D. J. (2009). Comprehensive Identification of *Salmonella enterica* Serovar Typhimurium Genes Required for Infection of BALB/c Mice. *PLoS Pathogens*, *5*(7), e1000529. <https://doi.org/10.1371/journal.ppat.1000529>
- Chen, L. M., Kaniga, K., & Galán, J. E. (1996). *Salmonella* spp. Are cytotoxic for cultured macrophages. *Molecular Microbiology*, *21*(5), 1101–1115. <https://doi.org/10.1046/j.1365-2958.1996.471410.x>
- Côté, J.-P., French, S., Gehrke, S. S., MacNair, C. R., Mangat, C. S., Bharat, A., & Brown, E. D. (2016). The Genome-Wide Interaction Network of Nutrient Stress Genes in *Escherichia coli*. *MBio*, *7*(6), e01714-16, /mbio/7/6/e01714-16.atom. <https://doi.org/10.1128/mBio.01714-16>
- Cronan, J. E. (2014). Biotin and Lipoic Acid: Synthesis, Attachment, and Regulation. *EcoSal Plus*, *3*(1). <https://doi.org/10.1128/ecosalplus.3.6.3.5>

- Cronan, J. E. (2018). Advances in synthesis of biotin and assembly of lipoic acid. *Current Opinion in Chemical Biology*, 47, 60–66. <https://doi.org/10.1016/j.cbpa.2018.08.004>
- Crowley, S. M., Knodler, L. A., & Vallance, B. A. (2016). Salmonella and the Inflammasome: Battle for Intracellular Dominance. In *Inflammasome Signaling and Bacterial Infections* (Vol. 397). Springer.
- Crump, J. A., Sjölund-Karlsson, M., Gordon, M. A., & Parry, C. M. (2015). Epidemiology, Clinical Presentation, Laboratory Diagnosis, Antimicrobial Resistance, and Antimicrobial Management of Invasive Salmonella Infections. *Clinical Microbiology Reviews*, 28(4), 901–937. <https://doi.org/10.1128/CMR.00002-15>
- Crump, J. A., & Wain, J. (2017). Salmonella. In *International Encyclopedia of Public Health* (2nd ed., pp. 425–433). Elsevier.
- Daberkow, R. L., White, B. R., Cederberg, R. A., Griffin, J. B., & Zemleni, J. (2003). Monocarboxylate Transporter 1 Mediates Biotin Uptake in Human Peripheral Blood Mononuclear Cells. *The Journal of Nutrition*, 133(9), 2703–2706. <https://doi.org/10.1093/jn/133.9.2703>
- Dandekar, T., Fieselmann, A., Fischer, E., Popp, J., Hensel, M., & Noster, J. (2015). Salmonella—how a metabolic generalist adopts an intracellular lifestyle during infection. *Frontiers in Cellular and Infection Microbiology*, 4. <https://doi.org/10.3389/fcimb.2014.00191>
- Das, P., Lahiri, A., Lahiri, A., Sen, M., Iyer, N., Kapoor, N., Balaji, K. N., & Chakravorty, D. (2010). Cationic Amino Acid Transporters and Salmonella Typhimurium ArgT Collectively Regulate Arginine Availability towards Intracellular Salmonella Growth. *PLoS ONE*, 5(12), e15466. <https://doi.org/10.1371/journal.pone.0015466>
- Datsenko, K. A., & Wanner, B. L. (2000). One-step inactivation of chromosomal genes in *Escherichia coli* K-12 using PCR products. *Proceedings of the National Academy of Sciences*, 97(12), 6640–6645. <https://doi.org/10.1073/pnas.120163297>
- Deiwick, J., & Hensel, M. (1999). *Regulation of virulence genes by environmental signals in Salmonella typhimurium*. 5.
- Deiwick, J., Nikolaus, T., Erdogan, S., & Hensel, M. (1999). Environmental regulation of Salmonella pathogenicity island 2 gene expression. *Molecular Microbiology*, 31(6), 1759–1773. <https://doi.org/10.1046/j.1365-2958.1999.01312.x>
- Denkel, L. a, Rhen, M., & Bange, F.-C. (2013). Biotin sulfoxide reductase contributes to oxidative stress tolerance and virulence in *Salmonella enterica* serovar Typhimurium. *Microbiology (Reading, England)*, 159(2013), 1447–1458. <https://doi.org/10.1099/mic.0.067256-0>

- Dougan, & Baker, S. (2014). *Salmonella enterica* Serovar Typhi and the Pathogenesis of Typhoid Fever. *Annual Review of Microbiology*, 68(1), 317–336. <https://doi.org/10.1146/annurev-micro-091313-103739>
- Drecktrah, D., Knodler, L. A., Ireland, R., & Steele-Mortimer, O. (2006). The Mechanism of Salmonella Entry Determines the Vacuolar Environment and Intracellular Gene Expression: The Mechanism of Salmonella Internalization Determines Virulence Gene Expression. *Traffic*, 7(1), 39–51. <https://doi.org/10.1111/j.1600-0854.2005.00360.x>
- El Zahed, S. S., & Brown, E. D. (2018). Chemical-Chemical Combinations Map Uncharted Interactions in Escherichia coli under Nutrient Stress. *IScience*, 2, 168–181. <https://doi.org/10.1016/j.isci.2018.03.018>
- Elhadad, D., Desai, P., Rahav, G., McClelland, M., & Gal-Mor, O. (2015). Flagellin Is Required for Host Cell Invasion and Normal Salmonella Pathogenicity Island 1 Expression by Salmonella enterica Serovar Paratyphi A. *Infection and Immunity*, 83(9), 3355–3368. <https://doi.org/10.1128/IAI.00468-15>
- Ellermeier, J. R., & Slauch, J. M. (2007). Adaptation to the host environment: Regulation of the SPI1 type III secretion system in Salmonella enterica serovar Typhimurium. *Current Opinion in Microbiology*, 10(1), 24–29. <https://doi.org/10.1016/j.mib.2006.12.002>
- Ellis, M. J., Tsai, C. N., Johnson, J. W., French, S., Elhenawy, W., Porwollik, S., Andrews-Polymenis, H., McClelland, M., Magolan, J., Coombes, B. K., & Brown, E. D. (2019). A macrophage-based screen identifies antibacterial compounds selective for intracellular Salmonella Typhimurium. *Nature Communications*, 10(1), 197. <https://doi.org/10.1038/s41467-018-08190-x>
- Eng, S.-K., Pusparajah, P., Ab Mutalib, N.-S., Ser, H.-L., Chan, K.-G., & Lee, L.-H. (2015). Salmonella: A review on pathogenesis, epidemiology and antibiotic resistance. *Frontiers in Life Science*, 8(3), 284–293. <https://doi.org/10.1080/21553769.2015.1051243>
- Eriksson, S., Lucchini, S., Thompson, A., Rhen, M., & Hinton, J. C. D. (2003). Unravelling the biology of macrophage infection by gene expression profiling of intracellular Salmonella enterica. *Molecular Microbiology*, 47(1), 103–118. <https://doi.org/10.1046/j.1365-2958.2003.03313.x>
- Faber, F., Thiennimitr, P., Spiga, L., Byndloss, M. X., Litvak, Y., Lawhon, S., Andrews-Polymenis, H. L., Winter, S. E., & Bäumlér, A. J. (2017). Respiration of Microbiota-Derived 1,2-propanediol Drives Salmonella Expansion during Colitis. *PLOS Pathogens*, 13(1), e1006129. <https://doi.org/10.1371/journal.ppat.1006129>
- Fabrega, A., & Vila, J. (2013). Salmonella enterica Serovar Typhimurium Skills To Succeed in the Host: Virulence and Regulation. *Clinical Microbiology Reviews*, 26(2), 308–341. <https://doi.org/10.1128/CMR.00066-12>
- Farrar, J., Hotez, P. J., Junghanss, T., Kang, G., Lalloo, D., & White, N. J. (2013). *Manson 's Tropical Diseases Twenty—Third Edition*.

- Feasey, N., & Gordon, M. (2013). Typhoid, paratyphoid and non-typhoid Salmonella. In *Principles of Medicine in Africa* (4th ed., pp. 308–315). Cambridge University Press.
- Fields, P. I., Swanson, R. V., Haidaris, C. G., & Heffron, F. (1986). Mutants of Salmonella typhimurium that cannot survive within the macrophage are avirulent. *Proceedings of the National Academy of Sciences*, 83(14), 5189–5193. <https://doi.org/10.1073/pnas.83.14.5189>
- Finkenwirth, F., & Eitinger, T. (2019). ECF-type ABC transporters for uptake of vitamins and transition metal ions into prokaryotic cells. *Research in Microbiology*, 170(8), 358–365. <https://doi.org/10.1016/j.resmic.2019.06.007>
- Finkenwirth, F., Kirsch, F., & Eitinger, T. (2013a). Solitary bio Y proteins mediate biotin transport into recombinant Escherichia coli. *Journal of Bacteriology*, 195(18), 4105–4111. <https://doi.org/10.1128/JB.00350-13>
- Finkenwirth, F., Kirsch, F., & Eitinger, T. (2013b). Solitary bio Y proteins mediate biotin transport into recombinant Escherichia coli. *Journal of Bacteriology*, 195(18), 4105–4111. <https://doi.org/10.1128/JB.00350-13>
- Finkenwirth, F., Kirsch, F., & Eitinger, T. (2014). A versatile Escherichia coli strain for identification of biotin transporters and for biotin quantification. *Bioengineered*, 5(2), 129–132. <https://doi.org/10.4161/bioe.26887>
- Fookes, M., Schroeder, G. N., Langridge, G. C., Blondel, C. J., Mammina, C., Connor, T. R., Seth-Smith, H., Vernikos, G. S., Robinson, K. S., Sanders, M., Petty, N. K., Kingsley, R. A., Bäuml, A. J., Nuccio, S.-P., Contreras, I., Santiviago, C. A., Maskell, D., Barrow, P., Humphrey, T., ... Thomson, N. R. (2011). Salmonella bongori Provides Insights into the Evolution of the Salmonellae. *PLoS Pathogens*, 7(8), e1002191. <https://doi.org/10.1371/journal.ppat.1002191>
- Galán, J. E. (1996). Molecular genetic bases of Salmonella entry into host cells. *Molecular Microbiology*, 20(2), 263–271.
- Galán, J. E. (2001). Salmonella Interactions with Host Cells: Type III Secretion at Work. *Annual Review of Cell and Developmental Biology*, 17(1), 53–86. <https://doi.org/10.1146/annurev.cellbio.17.1.53>
- Galán, J. E., & Collmer, A. (1999). Type III Secretion Machines: Bacterial Devices for Protein Delivery into Host Cells. *Science*, 284(5418), 1322–1328. <https://doi.org/10.1126/science.284.5418.1322>
- Gal-Mor, O., Boyle, E. C., & Grassl, G. A. (2014a). Same species, different diseases: How and why typhoidal and non-typhoidal Salmonella enterica serovars differ. *Frontiers in Microbiology*, 5(AUG), 1–10. <https://doi.org/10.3389/fmicb.2014.00391>

- Gal-Mor, O., Boyle, E. C., & Grassl, G. A. (2014b). Same species, different diseases: How and why typhoidal and non-typhoidal *Salmonella enterica* serovars differ. *Frontiers in Microbiology*, *5*. <https://doi.org/10.3389/fmicb.2014.00391>
- Garcia-Gutierrez, E., Chidlaw, A. C., Le Gall, G., Bowden, S. D., Tedin, K., Kelly, D. J., & Thompson, A. (2016). A Comparison of the ATP Generating Pathways Used by *S. Typhimurium* to Fuel Replication within Human and Murine Macrophage and Epithelial Cell Lines. *PLOS ONE*, *11*(3), e0150687. <https://doi.org/10.1371/journal.pone.0150687>
- Garrity, G. (Ed.). (2007). *Bergey's Manual of Systematic Bacteriology: Volume 2: The Proteobacteria, Part B: The Gammaproteobacteria* (Vol. 2). Springer Science and Business Media.
- Gilchrist, J. J., & MacLennan, C. A. (2019). Invasive Nontyphoidal *Salmonella* Disease in Africa. *EcoSal Plus*, *8*(2). <https://doi.org/10.1128/ecosalplus.ESP-0007-2018>
- Gillis, C. C., Hughes, E. R., Spiga, L., Winter, M. G., Zhu, W., Furtado de Carvalho, T., Chanin, R. B., Behrendt, C. L., Hooper, L. V., Santos, R. L., & Winter, S. E. (2018). Dysbiosis-Associated Change in Host Metabolism Generates Lactate to Support *Salmonella* Growth. *Cell Host & Microbe*, *23*(1), 54-64.e6. <https://doi.org/10.1016/j.chom.2017.11.006>
- Gonzalez-Escobedo, G., Marshall, J. M., & Gunn, J. S. (2011). Chronic and acute infection of the gall bladder by *Salmonella* Typhi: Understanding the carrier state. *Nature Reviews Microbiology*, *9*(1), 9–14. <https://doi.org/10.1038/nrmicro2490>
- Gordon. (2011). Invasive nontyphoidal *Salmonella* disease: Epidemiology, pathogenesis and diagnosis. *Current Opinion in Infectious Diseases*, *24*(5), 484–489. <https://doi.org/10.1097/QCO.0b013e32834a9980>
- Gordon, M. A., Graham, S. M., Walsh, A. L., Wilson, L., Phiri, A., Molyneux, E., Zijlstra, E. E., Heyderman, R. S., Hart, C. A., & Molyneux, M. E. (2008). Epidemics of Invasive *Salmonella enterica* Serovar Enteritidis and *S. enterica* Serovar Typhimurium Infection Associated with Multidrug Resistance among Adults and Children in Malawi. *Clinical Infectious Diseases*, *46*(7), 963–969. <https://doi.org/10.1086/529146>
- Grimont, P. A., & Weill, F. X. (2007). Antigenic formulae of the *Salmonella* serovars. *WHO Collaborating Centre for Reference and Research on Salmonella*, *9*, 1–166.
- Gueguen, E., & Cascales, E. (2013). Promoter swapping unveils the role of the *Citrobacter rodentium* CTS1 type VI secretion system in interbacterial competition. *Applied and Environmental Microbiology*, *79*(1), 32–38. <https://doi.org/10.1128/AEM.02504-12>
- Haraga, A., Ohlson, M. B., & Miller, S. I. (2008). *Salmonellae* interplay with host cells. *Nature Reviews Microbiology*, *6*(1), 53–66. <https://doi.org/10.1038/nrmicro1788>

- Hartman, H. B., Fell, D. A., Rossell, S., Jensen, P. R., Woodward, M. J., Thorndahl, L., Jelsbak, L., Olsen, J. E., Raghunathan, A., Daefler, S., & Poolman, M. G. (2014). Identification of potential drug targets in *Salmonella enterica* sv. Typhimurium using metabolic modelling and experimental validation. *Microbiology*, *160*(6), 1252–1266. <https://doi.org/10.1099/mic.0.076091-0>
- Haselbeck, A. H., Panzner, U., Im, J., Baker, S., Meyer, C. G., & Marks, F. (2017). Current perspectives on invasive nontyphoidal *Salmonella* disease: *Current Opinion in Infectious Diseases*, *30*(5), 498–503. <https://doi.org/10.1097/QCO.0000000000000398>
- Hautefort, I., Proença, M. J., & Hinton, J. C. D. (2003). Single-Copy Green Fluorescent Protein Gene Fusions Allow Accurate Measurement of *Salmonella* Gene Expression In Vitro and during Infection of Mammalian Cells. *Applied and Environmental Microbiology*, *69*(12), 7480–7491. <https://doi.org/10.1128/AEM.69.12.7480-7491.2003>
- Hautefort, I., Thompson, A., Eriksson-Ygberg, S., Parker, M. L., Lucchini, S., Danino, V., Bongaerts, R. J. M., Ahmad, N., Rhen, M., & Hinton, J. C. D. (2008). During infection of epithelial cells *Salmonella enterica* serovar Typhimurium undergoes a time-dependent transcriptional adaptation that results in simultaneous expression of three type 3 secretion systems. *Cellular Microbiology*, *10*(4), 958–984. <https://doi.org/10.1111/j.1462-5822.2007.01099.x>
- Hautefort, I., Thompson, A., Parker, M. L., Lucchini, S., Danino, V., Bongaerts, R. J. M., Ahmad, N., Rhen, M., & Hinton, J. C. D. (2008). *During infection of epithelial cells Salmonella enterica serovar Typhimurium undergoes a time-dependent transcriptional adaptation that results in simultaneous expression of three type 3 secretion systems.* *10*(December 2007), 958–984. <https://doi.org/10.1111/j.1462-5822.2007.01099.x>
- Hebbeln, P., Rodionov, D. A., Alfandega, A., & Eitinger, T. (2007). Biotin uptake in prokaryotes by solute transporters with an optional ATP-binding cassette-containing module. *Proceedings of the National Academy of Sciences*, *104*(8), 2909–2914. <https://doi.org/10.1073/pnas.0609905104>
- Hennigar, S. R., & McClung, J. P. (2016). Nutritional Immunity: Starving Pathogens of Trace Minerals. *American Journal of Lifestyle Medicine*, *10*(3), 170–173. <https://doi.org/10.1177/1559827616629117>
- Hensel, M. (2000). *Salmonella* Pathogenicity Island 2. *Molecular Microbiology*, *36*(5), 1015–1023. <https://doi.org/10.1046/j.1365-2958.2000.01935.x>
- Hensel, M., Shea, J., Gleeson, C., Jones, M., Dalton, E., & Holden, D. (1995). Simultaneous identification of bacterial virulence genes by negative selection. *Science*, *269*(5222), 400–403. <https://doi.org/10.1126/science.7618105>
- Herrero-Fresno, A., & Olsen, J. E. (2018). *Salmonella* Typhimurium metabolism affects virulence in the host – A mini-review. *Food Microbiology*, *71*, 98–110. <https://doi.org/10.1016/j.fm.2017.04.016>

- Holtkötter, P., & Hensel, M. (2016). Metabolism of Intracellular *Salmonella enterica*. In G. Uden, E. Thines, & A. Schöffler (Eds.), *Host—Pathogen Interaction* (pp. 37–56). Wiley-VCH Verlag GmbH & Co. KGaA. <https://doi.org/10.1002/9783527682386.ch3>
- Hölzer, S. U., & Hensel, M. (2012). Divergent Roles of Salmonella Pathogenicity Island 2 and Metabolic Traits during Interaction of *S. enterica* Serovar Typhimurium with Host Cells. *PLoS ONE*, 7(3), e33220. <https://doi.org/10.1371/journal.pone.0033220>
- Hume, P. J., Singh, V., Davidson, A. C., & Koronakis, V. (2017). Swiss Army Pathogen: The Salmonella Entry Toolkit. *Frontiers in Cellular and Infection Microbiology*, 7, 348. <https://doi.org/10.3389/fcimb.2017.00348>
- Husna, A. U., Wang, N., Wilksch, J. J., Newton, H. J., Hocking, D. M., Hay, I. D., Cobbold, S. A., Davies, M. R., McConville, M. J., Lithgow, T., & Strugnell, R. A. (2019). The multifunctional enzyme S-adenosylhomocysteine/methylthioadenosine nucleosidase is a key metabolic enzyme in the virulence of *Salmonella enterica* var Typhimurium. *Biochemical Journal*, 476(22), 3435–3453. <https://doi.org/10.1042/BCJ20190297>
- Ibarra, J. A., Knodler, L. A., Sturdevant, D. E., Virtaneva, K., Carmody, A. B., Fischer, E. R., Porcella, S. F., & Steele-Mortimer, O. (2010). Induction of Salmonella pathogenicity island 1 under different growth conditions can affect Salmonella–host cell interactions in vitro. *Microbiology*, 14. <https://doi.org/10.1099/mic.0.032896-0>
- Ibarra, J. A., & Steele-Mortimer, O. (2009). *Salmonella*—The ultimate insider. *Salmonella* virulence factors that modulate intracellular survival. *Cellular Microbiology*, 11(11), 1579–1586. <https://doi.org/10.1111/j.1462-5822.2009.01368.x>
- Inoue, H., Nojima, H., & Okayama, H. (1990). High efficiency transformation of *Escherichia coli* with plasmids. *Gene*, 96(1), 23–28. [https://doi.org/10.1016/0378-1119\(90\)90336-P](https://doi.org/10.1016/0378-1119(90)90336-P)
- Issenhuth-Jeanjean, S., Roggentin, P., Mikoleit, M., Guibourdenche, M., de Pinna, E., Nair, S., Fields, P. I., & Weill, F.-X. (2014). Supplement 2008–2010 (no. 48) to the White–Kauffmann–Le Minor scheme. *Research in Microbiology*, 165(7), 526–530. <https://doi.org/10.1016/j.resmic.2014.07.004>
- Jaehme, M., & Slotboom, D. J. (2015). Diversity of membrane transport proteins for vitamins in bacteria and archaea. *Biochimica et Biophysica Acta - General Subjects*, 1850(3), 565–576. <https://doi.org/10.1016/j.bbagen.2014.05.006>
- Jelsbak, L., Hartman, H., Schroll, C., Rosenkrantz, J. T., Lemire, S., Wallrodt, I., Thomsen, L. E., Poolman, M., Kilstrup, M., Jensen, P. R., & Olsen, J. E. (2014). Identification of Metabolic Pathways Essential for Fitness of *Salmonella* Typhimurium In Vivo. *PLoS ONE*, 9(7), e101869. <https://doi.org/10.1371/journal.pone.0101869>
- Jennings, E., Thurston, T. L. M., & Holden, D. W. (2017). Salmonella SPI-2 Type III Secretion System Effectors: Molecular Mechanisms And Physiological Consequences. *Cell Host & Microbe*, 22(2), 217–231. <https://doi.org/10.1016/j.chom.2017.07.009>

- Jepson, M. A., & Clark, M. A. (2001). The role of M cells in Salmonella infection. *Microbes and Infection*, 3(14–15), 1183–1190. [https://doi.org/10.1016/S1286-4579\(01\)01478-2](https://doi.org/10.1016/S1286-4579(01)01478-2)
- Kaniga, K., Tucker, S., Trollinger, D., & Galán, J. E. (1995). Homologs of the Shigella IpaB and IpaC invasins are required for Salmonella typhimurium entry into cultured epithelial cells. *Journal of Bacteriology*, 177(14), 3965–3971. <https://doi.org/10.1128/JB.177.14.3965-3971.1995>
- Kehl, A., Noster, J., & Hensel, M. (2020). Eat in or Take out? Metabolism of Intracellular Salmonella enterica. *Trends in Microbiology*, 28(8), 644–654. <https://doi.org/10.1016/j.tim.2020.03.005>
- Keithlin, J., Sargeant, J. M., Thomas, M. K., & Fazil, A. (2015). Systematic review and meta-analysis of the proportion of non-typhoidal *Salmonella* cases that develop chronic sequelae. *Epidemiology and Infection*, 143(7), 1333–1351. <https://doi.org/10.1017/S0950268814002829>
- Knodler, L. A. (2015). Salmonella enterica: Living a double life in epithelial cells. *Current Opinion in Microbiology*, 23, 23–31. <https://doi.org/10.1016/j.mib.2014.10.010>
- Knodler, L. A., Nair, V., & Steele-Mortimer, O. (2014). Quantitative Assessment of Cytosolic Salmonella in Epithelial Cells. *PLoS ONE*, 9(1), e84681. <https://doi.org/10.1371/journal.pone.0084681>
- Knowles, J. R. (1989). *The Mechanism of Biotin-Dependent Enzymes*. 27.
- Knuff, K., & Finlay, B. B. (2017). What the SIF Is Happening—The Role of Intracellular Salmonella-Induced Filaments. *Frontiers in Cellular and Infection Microbiology*, 7, 335. <https://doi.org/10.3389/fcimb.2017.00335>
- Knuff-Janzen, K., Tupin, A., Yurist-Doutsch, S., Rowland, J. L., & Finlay, B. B. (2020). Multiple Salmonella-pathogenicity island 2 effectors are required to facilitate bacterial establishment of its intracellular niche and virulence. *PLOS ONE*, 15(6), e0235020. <https://doi.org/10.1371/journal.pone.0235020>
- Krieger, V., Liebl, D., Zhang, Y., Rajashekar, R., Chlanda, P., Giesker, K., Chikkaballi, D., & Hensel, M. (2014). Reorganization of the Endosomal System in Salmonella-Infected Cells: The Ultrastructure of Salmonella-Induced Tubular Compartments. *PLoS Pathogens*, 10(9), e1004374. <https://doi.org/10.1371/journal.ppat.1004374>
- Kröger, C., Colgan, A., Srikumar, S., Händler, K., Sivasankaran, S. K., Hammarlöf, D. L., Canals, R., Grissom, J. E., Conway, T., Hokamp, K., & Hinton, J. C. D. (2013). An Infection-Relevant Transcriptomic Compendium for Salmonella enterica Serovar Typhimurium. *Cell Host & Microbe*, 14(6), 683–695. <https://doi.org/10.1016/j.chom.2013.11.010>

- Kuhle, V., Abrahams, G. L., & Hensel, M. (2006). Intracellular *Salmonella enterica* Redirect Exocytic Transport Processes in a *Salmonella* Pathogenicity Island 2-Dependent Manner: *Salmonella* Redirect Exocytosis. *Traffic*, *7*(6), 716–730. <https://doi.org/10.1111/j.1600-0854.2006.00422.x>
- LaRock, D. L., Chaudhary, A., & Miller, S. I. (2015). Salmonellae interactions with host processes. *Nature Reviews Microbiology*, *13*(4), 191–205. <https://doi.org/10.1038/nrmicro3420>
- Lathrop, S. K., Binder, K. A., Starr, T., Cooper, K. G., Chong, A., Carmody, A. B., & Steele-Mortimer, O. (2015). Replication of *Salmonella enterica* Serovar Typhimurium in Human Monocyte-Derived Macrophages. *Infection and Immunity*, *83*(7), 2661–2671. <https://doi.org/10.1128/IAI.00033-15>
- Lê-Bury, G., Deschamps, C., Kizilyaprak, C., Blanchard, W., Daraspe, J., Dumas, A., Gordon, M. A., Hinton, J. C. D., Humbel, B. M., & Niedergang, F. (2020). Increased intracellular survival of *Salmonella* Typhimurium ST313 in HIV-1-infected primary human macrophages is not associated with *Salmonella* hijacking the HIV compartment. *Biology of the Cell*, *112*(3), 92–101. <https://doi.org/10.1111/boc.201900055>
- Lê-Bury, G., & Niedergang, F. (2018). Defective Phagocytic Properties of HIV-Infected Macrophages: How Might They Be Implicated in the Development of Invasive *Salmonella* Typhimurium? *Frontiers in Immunology*, *9*, 531. <https://doi.org/10.3389/fimmu.2018.00531>
- Lin, S., & Cronan, J. E. (2011a). Closing in on complete pathways of biotin biosynthesis. *Mol. BioSyst. Mol. BioSyst*, *7*(7), 1811–1821. <https://doi.org/10.1039/c1mb05022b>
- Lin, S., & Cronan, J. E. (2011b). Closing in on complete pathways of biotin biosynthesis. *Mol. BioSyst. Mol. BioSyst*, *7*(7), 1811–1821. <https://doi.org/10.1039/c1mb05022b>
- Lin, S., Hanson, R. E., & Cronan, J. E. (2010). Biotin synthesis begins by hijacking the fatty acid synthetic pathway. *Nature Chemical Biology*, *6*(9), 682–688. <https://doi.org/10.1038/nchembio.420>
- Liss, V., & Hensel, M. (2015). Take the tube: Remodelling of the endosomal system by intracellular *S almonella enterica*: Intracellular *Salmonella*. *Cellular Microbiology*, *17*(5), 639–647. <https://doi.org/10.1111/cmi.12441>
- Liss, V., Swart, A. L., Kehl, A., Hermanns, N., Zhang, Y., Chikkaballi, D., Böhles, N., Deiwick, J., & Hensel, M. (2017). *Salmonella enterica* Remodels the Host Cell Endosomal System for Efficient Intravacuolar Nutrition. *Cell Host & Microbe*, *21*(3), 390–402. <https://doi.org/10.1016/j.chom.2017.02.005>
- Liu, Y., Zhang, Q., Hu, M., Yu, K., Fu, J., Zhou, F., & Liu, X. (2015). Proteomic Analyses of Intracellular *Salmonella enterica* Serovar Typhimurium Reveal Extensive Bacterial Adaptations to Infected Host Epithelial Cells. *Infection and Immunity*, *83*(7), 2897–2906. <https://doi.org/10.1128/IAI.02882-14>

- Lundberg, B. E., Wolf, R. E., Dinauer, M. C., Xu, Y., & Fang, F. C. (1999). Glucose 6-Phosphate Dehydrogenase Is Required for *Salmonella typhimurium* Virulence and Resistance to Reactive Oxygen and Nitrogen Intermediates. *Infection and Immunity*, 67(1), 436–438. <https://doi.org/10.1128/IAI.67.1.436-438.1999>
- Malik-Kale, P., Winfree, S., & Steele-Mortimer, O. (2012). The Bimodal Lifestyle of Intracellular *Salmonella* in Epithelial Cells: Replication in the Cytosol Obscures Defects in Vacuolar Replication. *PLoS ONE*, 7(6), e38732. <https://doi.org/10.1371/journal.pone.0038732>
- Manandhar, M., & Cronan, J. E. (2017). Pimelic acid, the first precursor of the *Bacillus subtilis* biotin synthesis pathway, exists as the free acid and is assembled by fatty acid synthesis: *Bacillus subtilis* biotin synthesis. *Molecular Microbiology*, 104(4), 595–607. <https://doi.org/10.1111/mmi.13648>
- Manesh, A., Meltzer, E., Jin, C., Britto, C., Deodhar, D., Radha, S., Schwartz, E., & Rupali, P. (2021). Typhoid and paratyphoid fever: A clinical seminar. *Journal of Travel Medicine*, taab012. <https://doi.org/10.1093/jtm/taab012>
- Marchello, C. S., Carr, S. D., & Crump, J. A. (2020). A Systematic Review on Antimicrobial Resistance among *Salmonella Typhi* Worldwide. *The American Journal of Tropical Medicine and Hygiene*, 103(6), 2518–2527. <https://doi.org/10.4269/ajtmh.20-0258>
- McGhie, E. J., Brawn, L. C., Hume, P. J., Humphreys, D., & Koronakis, V. (2009). *Salmonella* takes control: Effector-driven manipulation of the host. *Current Opinion in Microbiology*, 12, 8.
- McMahon, R. J. (2002). BIOTIN IN METABOLISM AND MOLECULAR BIOLOGY. *Annual Review of Nutrition*, 22(1), 221–239. <https://doi.org/10.1146/annurev.nutr.22.121101.112819>
- Milligan, R., Paul, M., Richardson, M., & Neuberger, A. (2018). Vaccines for preventing typhoid fever. *Cochrane Database of Systematic Reviews*. <https://doi.org/10.1002/14651858.CD001261.pub4>
- Monack, D. M., Raupach, B., Hromockyj, A. E., & Falkow, S. (1996). *Salmonella typhimurium* invasion induces apoptosis in infected macrophages. *Proceedings of the National Academy of Sciences*, 93(18), 9833–9838. <https://doi.org/10.1073/pnas.93.18.9833>
- Murphy, H. M., Thomas, M. K., Schmidt, P. J., Medeiros, D. T., McFADYEN, S., & Pintar, K. D. M. (2016). Estimating the burden of acute gastrointestinal illness due to *Giardia*, *Cryptosporidium*, *Campylobacter*, *E. coli* O157 and norovirus associated with private wells and small water systems in Canada. *Epidemiology and Infection*, 144(7), 1355–1370. <https://doi.org/10.1017/S0950268815002071>

- Ng, K. M., Ferreyra, J. A., Higginbottom, S. K., Lynch, J. B., Kashyap, P. C., Gopinath, S., Naidu, N., Choudhury, B., Weimer, B. C., Monack, D. M., & Sonnenburg, J. L. (2013). Microbiota-liberated host sugars facilitate post-antibiotic expansion of enteric pathogens. *Nature*, *502*(7469), 96–99. <https://doi.org/10.1038/nature12503>
- Noster, J., Chao, T.-C., Sander, N., Schulte, M., Reuter, T., Hansmeier, N., & Hensel, M. (2019). Proteomics of intracellular *Salmonella enterica* reveals roles of *Salmonella* pathogenicity island 2 in metabolism and antioxidant defense. *PLOS Pathogens*, *15*(4), e1007741. <https://doi.org/10.1371/journal.ppat.1007741>
- Noster, J., Persicke, M., Chao, T.-C., Krone, L., Heppner, B., Hensel, M., & Hansmeier, N. (2019). Impact of ROS-Induced Damage of TCA Cycle Enzymes on Metabolism and Virulence of *Salmonella enterica* serovar Typhimurium. *Frontiers in Microbiology*, *10*, 762. <https://doi.org/10.3389/fmicb.2019.00762>
- Nuccio, S.-P., & Bäumlner, A. J. (2014). Comparative Analysis of *Salmonella* Genomes Identifies a Metabolic Network for Escalating Growth in the Inflamed Gut. *MBio*, *5*(2), e00929-14. <https://doi.org/10.1128/mBio.00929-14>
- Park, S.-Y., Pontes, M. H., & Groisman, E. A. (2015). Flagella-independent surface motility in *Salmonella enterica* serovar Typhimurium. *Proceedings of the National Academy of Sciences*, *112*(6), 1850–1855. <https://doi.org/10.1073/pnas.1422938112>
- Park, Y. M., Lee, H. J., Jeong, J.-H., Kook, J.-K., Choy, H. E., Hahn, T.-W., & Bang, I. S. (2015). Branched-chain amino acid supplementation promotes aerobic growth of *Salmonella* Typhimurium under nitrosative stress conditions. *Archives of Microbiology*, *197*(10), 1117–1127. <https://doi.org/10.1007/s00203-015-1151-y>
- Park, Y. M., Park, H. J., Joung, Y. H., & Bang, I. S. (2011). Nitrosative stress causes amino acid auxotrophy in hmp mutant *Salmonella* Typhimurium: *Salmonella* amino acid auxotrophy by NO. *Microbiology and Immunology*, *55*(10), 743–747. <https://doi.org/10.1111/j.1348-0421.2011.00367.x>
- Perez-Sepulveda, B. M., & Hinton, J. C. D. (2018). Functional Transcriptomics for Bacterial Gene Detectives. In Storz & Papenfort (Eds.), *Regulating with RNA in Bacteria and Archaea* (pp. 549–561). American Society of Microbiology. <https://doi.org/10.1128/microbiolspec.RWR-0033-2018>
- Polyak, S. W., & Chapman-Smith, A. (2013). Biotin. In *Encyclopaedia of Biological Chemistry* (2nd ed.). Academic Press.
- Popoff, M. Y., & Le Minor, L. E. (2015). *Salmonella*. *Bergey's Manual of Systematics of Archaea and Bacteria*.
- Popp, J., Noster, J., Busch, K., Kehl, A., zur Hellen, G., & Hensel, M. (2015). Role of Host Cell-Derived Amino Acids in Nutrition of Intracellular *Salmonella enterica*. *Infection and Immunity*, *83*(12), 4466–4475. <https://doi.org/10.1128/IAI.00624-15>

- Prasad, P. D., Wang, H., Kekuda, R., Fujita, T., Fei, Y.-J., Devoe, L. D., Leibach, F. H., & Ganapathy, V. (1998). Cloning and Functional Expression of a cDNA Encoding a Mammalian Sodium-dependent Vitamin Transporter Mediating the Uptake of Pantothenate, Biotin, and Lipoate. *Journal of Biological Chemistry*, 273(13), 7501–7506. <https://doi.org/10.1074/jbc.273.13.7501>
- Pulford, C. V., Perez-Sepulveda, B. M., Canals, R., Bevington, J. A., Bengtsson, R. J., Wenner, N., Rodwell, E. V., Kumwenda, B., Zhu, X., Bennett, R. J., Stenhouse, G. E., Malaka De Silva, P., Webster, H. J., Bengoechea, J. A., Dumigan, A., Tran-Dien, A., Prakash, R., Banda, H. C., Alufandika, L., ... Hinton, J. C. D. (2021). Stepwise evolution of Salmonella Typhimurium ST313 causing bloodstream infection in Africa. *Nature Microbiology*, 6(3), 327–338. <https://doi.org/10.1038/s41564-020-00836-1>
- Reeves, M. W., Evins, G. M., Heiba, A. A., Plikaytis, B. D., & Farmer, J. J. (1989). Clonal nature of Salmonella typhi and its genetic relatedness to other salmonellae as shown by multilocus enzyme electrophoresis, and proposal of Salmonella bongori comb. Nov. *Journal of Clinical Microbiology*, 27(2), 313–320.
- Rescigno, M., Urbano, M., Valzasina, B., Francolini, M., Rotta, G., Bonasio, R., Granucci, F., Kraehenbuhl, J.-P., & Ricciardi-Castagnoli, P. (2001). Dendritic cells express tight junction proteins and penetrate gut epithelial monolayers to sample bacteria. *Nature Immunology*, 2(4), 361–367. <https://doi.org/10.1038/86373>
- Ringlstetter, S. L. (2010a). *Identification of the biotin transporter in Escherichia coli , biotinylation of histones in Saccharomyces cerevisiae and analysis of biotin sensing in Saccharomyces cerevisiae*. 1–152.
- Ringlstetter, S. L. (2010b). *Identification of the biotin transporter in Escherichia coli, biotinylation of histones in Saccharomyces cerevisiae and analysis of biotin sensing in Saccharomyces cerevisiae* [PHD]. University of Regensburg.
- Rivera-Chávez, F., & Bäuml, A. J. (2015). The Pyromaniac Inside You: *Salmonella* Metabolism in the Host Gut. *Annual Review of Microbiology*, 69(1), 31–48. <https://doi.org/10.1146/annurev-micro-091014-104108>
- Rivera-Chávez, F., Zhang, L. F., Faber, F., Lopez, C. A., Byndloss, M. X., Olsan, E. E., Xu, G., Velazquez, E. M., Lebrilla, C. B., Winter, S. E., & Bäuml, A. J. (2016). Depletion of Butyrate-Producing Clostridia from the Gut Microbiota Drives an Aerobic Luminal Expansion of Salmonella. *Cell Host & Microbe*, 19(4), 443–454. <https://doi.org/10.1016/j.chom.2016.03.004>
- Röder, J., Felgner, P., & Hensel, M. (2020). *Comprehensive single cell analyses of the nutritional environment of intracellular Salmonella enterica* [Preprint]. *Microbiology*. <https://doi.org/10.1101/2020.11.01.364018>

- Röder, J., & Hensel, M. (2020a). Presence of SopE and mode of infection result in increased *Salmonella* -containing vacuole damage and cytosolic release during host cell infection by *SALMONELLA ENTERICA*. *Cellular Microbiology*, 22(5). <https://doi.org/10.1111/cmi.13155>
- Röder, J., & Hensel, M. (2020b). Presence of SopE and mode of infection result in increased *Salmonella* -containing vacuole damage and cytosolic release during host cell infection by *SALMONELLA ENTERICA*. *Cellular Microbiology*, 22(5). <https://doi.org/10.1111/cmi.13155>
- Rodionov, D. A., Mironov, A. A., & Gelfand, M. S. (2002). Conservation of the Biotin Regulon and the BirA Regulatory Signal in Eubacteria and Archaea. *Genome Research*, 12(10), 1507–1516. <https://doi.org/10.1101/gr.314502>
- Rong Fu Wang, & Kushner, S. R. (1991). Construction of versatile low-copy-number vectors for cloning, sequencing and gene expression in *Escherichia coli*. *Gene*, 100, 195–199. [https://doi.org/10.1016/0378-1119\(91\)90366-J](https://doi.org/10.1016/0378-1119(91)90366-J)
- Russell, D. W., & Sambrook, J. (2001). *Molecular Cloning: A laboratory Manual* (Vol. 1). Cold Spring Harbor Laboratory.
- Sajib, M. S. I., Tanmoy, A. M., Hooda, Y., Rahman, H., Andrews, J. R., Garrett, D. O., Endtz, H. P., Saha, S. K., & Saha, S. (2021). Tracking the Emergence of Azithromycin Resistance in Multiple Genotypes of Typhoidal *Salmonella*. *MBio*, 12(1), e03481-20, /mbio/12/1/mBio.03481-20.atom. <https://doi.org/10.1128/mBio.03481-20>
- Salaemae, W., Booker, G. W., & Polyak, S. W. (2016a). The Role of Biotin in Bacterial Physiology and Virulence: A Novel Antibiotic Target for *Mycobacterium tuberculosis*. *Microbiology Spectrum*, 4(2), 1–20. <https://doi.org/10.1128/microbiolspec.VMBF-0008-2015>
- Salaemae, W., Booker, G. W., & Polyak, S. W. (2016b). The Role of Biotin in Bacterial Physiology and Virulence: A Novel Antibiotic Target for *Mycobacterium tuberculosis*. *Microbiology Spectrum*, 4(2). <https://doi.org/10.1128/microbiolspec.VMBF-0008-2015>
- Salcedo, S. P., & Holden, D. (2003). SseG, a virulence protein that targets *Salmonella* to the Golgi network. *The EMBO Journal*, 22(19), 5003–5014. <https://doi.org/10.1093/emboj/cdg517>
- Sánchez-Vargas, F. M., Abu-El-Haija, M. A., & Gómez-Duarte, O. G. (2011). *Salmonella* infections: An update on epidemiology, management, and prevention. *Travel Medicine and Infectious Disease*, 9(6), 263–277. <https://doi.org/10.1016/j.tmaid.2011.11.001>
- Santos, R. L., & Bäumlner, A. J. (2004). Cell tropism of *Salmonella enterica*. *International Journal of Medical Microbiology*, 294(4), 225–233. <https://doi.org/10.1016/j.ijmm.2004.06.029>

- Satiaputra, J., Shearwin, K. E., Booker, G. W., & Polyak, S. W. (2016). Mechanisms of biotin-regulated gene expression in microbes. *Synthetic and Systems Biotechnology*, 1(1), 17–24. <https://doi.org/10.1016/j.synbio.2016.01.005>
- Severi, E., Hosie, A. H. F., Hawkhead, J. A., & Thomas, G. H. (2010). Characterization of a novel sialic acid transporter of the sodium solute symporter (SSS) family and in vivo comparison with known bacterial sialic acid transporters: An SSS transporter for sialic acid from Salmonella. *FEMS Microbiology Letters*, 304(1), 47–54. <https://doi.org/10.1111/j.1574-6968.2009.01881.x>
- Shea, J. E., Hensel, M., Gleeson, C., & Holden, D. W. (1996). Identification of a virulence locus encoding a second type III secretion system in Salmonella typhimurium. *Proceedings of the National Academy of Sciences*, 93(6), 2593–2597. <https://doi.org/10.1073/pnas.93.6.2593>
- Sheba. (2017). https://eng.sheba.co.il/Infectious_Diseases_Research_Lab
- Sheikh, A., Charles, R. C., Sharmeen, N., Rollins, S. M., Harris, J. B., Bhuiyan, Md. S., Arifuzzaman, M., Khanam, F., Bukka, A., Kalsy, A., Porwollik, S., Leung, D. T., Brooks, W. A., LaRocque, R. C., Hohmann, E. L., Cravioto, A., Logvinenko, T., Calderwood, S. B., McClelland, M., ... Ryan, E. T. (2011). In Vivo Expression of Salmonella enterica Serotype Typhi Genes in the Blood of Patients with Typhoid Fever in Bangladesh. *PLoS Neglected Tropical Diseases*, 5(12), e1419. <https://doi.org/10.1371/journal.pntd.0001419>
- Shi, L., Adkins, J. N., Coleman, J. R., Schepmoes, A. A., Dohnkova, A., Mottaz, H. M., Norbeck, A. D., Purvine, S. O., Manes, N. P., Smallwood, H. S., Wang, H., Forbes, J., Gros, P., Uzzau, S., Rodland, K. D., Heffron, F., Smith, R. D., & Squier, T. C. (2006). Proteomic Analysis of Salmonella enterica Serovar Typhimurium Isolated from RAW 264.7 Macrophages. *Journal of Biological Chemistry*, 281(39), 29131–29140. <https://doi.org/10.1074/jbc.M604640200>
- Shi, L., Ansong, C., Smallwood, H., Rommereim, L., E, J., Brewer, H. M., Norbeck, A. D., Taylor, R. C., Gustin, J. K., Heffron, F., Smith, R. D., Adkins, J. N., & Northwest, P. (2009). Proteome of Salmonella Enterica Serotype Typhimurium Grown in a Low Mg²⁺/pH Medium. *Proteomics*, 38105(509), 388–397. <https://doi.org/10.4172/jpb.1000099>. Proteome
- Shi, L., Chowdhury, S. M., Smallwood, H. S., Yoon, H., Mottaz-Brewer, H. M., Norbeck, A. D., McDermott, J. E., Clauss, T. R. W., Heffron, F., Smith, R. D., & Adkins, J. N. (2009). Proteomic Investigation of the Time Course Responses of RAW 264.7 Macrophages to Infection with Salmonella enterica. *Infection and Immunity*, 77(8), 3227–3233. <https://doi.org/10.1128/IAI.00063-09>
- Sirithanakorn, C., & Cronan, J. E. (2021). Biotin, a universal and essential cofactor: Synthesis, ligation and regulation. *FEMS Microbiology Reviews*, fuab003. <https://doi.org/10.1093/femsre/fuab003>

- Sprenger, M., Kasper, L., Hensel, M., & Hube, B. (2018). Metabolic adaptation of intracellular bacteria and fungi to macrophages. *International Journal of Medical Microbiology*, 308(1), 215–227. <https://doi.org/10.1016/j.ijmm.2017.11.001>
- Srikumar, S., Kröger, C., Hébrard, M., Colgan, A., Owen, S. V., Sivasankaran, S. K., Cameron, A. D. S., Hokamp, K., & Hinton, J. C. D. (2015). RNA-seq Brings New Insights to the Intra-Macrophage Transcriptome of Salmonella Typhimurium. *PLOS Pathogens*, 11(11), e1005262. <https://doi.org/10.1371/journal.ppat.1005262>
- Stanaway, J. D., Parisi, A., Sarkar, K., Blacker, B. F., Reiner, R. C., Hay, S. I., Nixon, M. R., Dolecek, C., James, S. L., Mokdad, A. H., Abebe, G., Ahmadian, E., Alahdab, F., Alemnew, B. T. T., Alipour, V., Allah Bakeshei, F., Animut, M. D., Ansari, F., Arabloo, J., ... Crump, J. A. (2019). The global burden of non-typhoidal salmonella invasive disease: A systematic analysis for the Global Burden of Disease Study 2017. *The Lancet Infectious Diseases*, 19(12), 1312–1324. [https://doi.org/10.1016/S1473-3099\(19\)30418-9](https://doi.org/10.1016/S1473-3099(19)30418-9)
- Stanaway, J. D., Reiner, R. C., Blacker, B. F., Goldberg, E. M., Khalil, I. A., Troeger, C. E., Andrews, J. R., Bhutta, Z. A., Crump, J. A., Im, J., Marks, F., Mintz, E., Park, S. E., Zaidi, A. K. M., Abebe, Z., Abejie, A. N., Adedeji, I. A., Ali, B. A., Amare, A. T., ... Hay, S. I. (2019). The global burden of typhoid and paratyphoid fevers: A systematic analysis for the Global Burden of Disease Study 2017. *The Lancet Infectious Diseases*, 19(4), 369–381. [https://doi.org/10.1016/S1473-3099\(18\)30685-6](https://doi.org/10.1016/S1473-3099(18)30685-6)
- Steeb, B., Claudi, B., Burton, N. A., Tienz, P., Schmidt, A., Farhan, H., Maze, A., & Bumann, D. (2013). Parallel Exploitation of Diverse Host Nutrients Enhances Salmonella Virulence. *PLOS Pathogens*, 9(4), 16.
- St-Pierre, F., Cui, L., Priest, D. G., Endy, D., Dodd, I. B., & Shearwin, K. E. (2013). One-Step Cloning and Chromosomal Integration of DNA. *ACS Synthetic Biology*, 2(9), 537–541. <https://doi.org/10.1021/sb400021j>
- Streit, W. R., & Entcheva, P. (2003). Biotin in microbes, the genes involved in its biosynthesis, its biochemical role and perspectives for biotechnological production. *Applied Microbiology and Biotechnology*, 61(1), 21–31. <https://doi.org/10.1007/s00253-002-1186-2>
- Tailford, L. E., Crost, E. H., Kavanaugh, D., & Juge, N. (2015). Mucin glycan foraging in the human gut microbiome. *Frontiers in Genetics*, 6. <https://doi.org/10.3389/fgene.2015.00081>
- Tam, M. A., Rydström, A., Sundquist, M., & Wick, M. J. (2008). Early cellular responses to *Salmonella* infection: Dendritic cells, monocytes, and more. *Immunological Reviews*, 225(1), 140–162. <https://doi.org/10.1111/j.1600-065X.2008.00679.x>
- Tchawa Yimga, M., Leatham, M. P., Allen, J. H., Laux, D. C., Conway, T., & Cohen, P. S. (2006). Role of Gluconeogenesis and the Tricarboxylic Acid Cycle in the Virulence of *Salmonella enterica* Serovar Typhimurium in BALB/c Mice. *Infection and Immunity*, 74(2), 1130–1140. <https://doi.org/10.1128/IAI.74.2.1130-1140.2006>

- Tennant, S. M., MacLennan, C. A., Simon, R., Martin, L. B., & Khan, M. I. (2016). Nontyphoidal salmonella disease: Current status of vaccine research and development. *Vaccine*, *34*(26), 2907–2910. <https://doi.org/10.1016/j.vaccine.2016.03.072>
- Thiennimitr, P., Winter, S. E., & Bäumlner, A. J. (2012). Salmonella, the host and its microbiota. *Current Opinion in Microbiology*, *15*(1), 108–114. <https://doi.org/10.1016/j.mib.2011.10.002>
- Thiennimitr, P., Winter, S. E., Winter, M. G., Xavier, M. N., Tolstikov, V., Huseby, D. L., Sterzenbach, T., Tsohis, R. M., Roth, J. R., & Baumler, A. J. (2011). Intestinal inflammation allows Salmonella to use ethanolamine to compete with the microbiota. *Proceedings of the National Academy of Sciences*, *108*(42), 17480–17485. <https://doi.org/10.1073/pnas.1107857108>
- Thierauf, A., Perez, G., & Maloy, S. (2009). Generalized Transduction. In M. R. J. Clokie & A. M. Kropinski (Eds.), *Bacteriophages* (Vol. 501). Human Press. <https://doi.org/10.1007/978-1-60327-164-6>
- Thomas, C., & Tampé, R. (2020). Structural and Mechanistic Principles of ABC Transporters. *Annual Review of Biochemistry*, *89*(1), 605–636. <https://doi.org/10.1146/annurev-biochem-011520-105201>
- Thompson, A., Fulde, M., & Tedin, K. (2018). The metabolic pathways utilized by *Salmonella* Typhimurium during infection of host cells: Metabolic pathways utilized by *Salmonella* Typhimurium. *Environmental Microbiology Reports*, *10*(2), 140–154. <https://doi.org/10.1111/1758-2229.12628>
- Tindall, B. J., Grimont, P. A. D., Garrity, G. M., & Euzéby, J. P. (2005). Nomenclature and taxonomy of the genus Salmonella. *International Journal of Systematic and Evolutionary Microbiology*, *55*(1), 521–524. <https://doi.org/10.1099/ijs.0.63580-0>
- Tong, L. (2013). Structure and function of biotin-dependent carboxylases. *Cellular and Molecular Life Sciences*, *70*(5), 863–891. <https://doi.org/10.1007/s00018-012-1096-0>
- Uche, I. V., MacLennan, C. A., & Saul, A. (2017). A Systematic Review of the Incidence, Risk Factors and Case Fatality Rates of Invasive Nontyphoidal Salmonella (iNTS) Disease in Africa (1966 to 2014). *PLOS Neglected Tropical Diseases*, *11*(1), e0005118. <https://doi.org/10.1371/journal.pntd.0005118>
- Waldrop, G. L., Holden, H. M., & Maurice, M. St. (2012). The enzymes of biotin dependent CO₂ metabolism: What structures reveal about their reaction mechanisms: Biotin Dependent Enzymes. *Protein Science*, *21*(11), 1597–1619. <https://doi.org/10.1002/pro.2156>
- Wikswow, M. E., Kambhampati, A., Shioda, K., Walsh, K. A., Bowen, A., & Hall, A. J. (2015). Outbreaks of Acute Gastroenteritis Transmitted by Person-to-Person Contact, Environmental Contamination, and Unknown Modes of Transmission—United States, 2009–2013. *MMWR*, *64*(12), 17.

- Woodman, M. E. (2008). Direct PCR of intact bacteria (colony PCR). *Current Protocols in Microbiology*, 9(1), A-3D.
- World Health Organization. (2019). Typhoid vaccines: WHO position paper, March 2018. *Recommendations Vaccine*, 37, 214–216.
- Wrande, M., Del Bel Belluz, L., Guidi, R., Pateras, I. S., Levi, L., Mihaljevic, B., Rouf, S. F., Candela, M., Turrone, S., Nastasi, C., Consolandi, C., Peano, C., Tebaldi, T., Viero, G., Gorgoulis, V. G., Krejsgaard, T., Rhen, M., & Frisan, T. (2016). The Typhoid Toxin Promotes Host Survival and the Establishment of a Persistent Asymptomatic Infection. *PLOS Pathogens*, 12(4), e1005528. <https://doi.org/10.1371/journal.ppat.1005528>
- Xiao, F., Wang, H., Shi, Z., Huang, Q., Huang, L., Lian, J., Cai, J., & Xu, Z. (2020). Multi-level metabolic engineering of *Pseudomonas putillensis* ATCC31014 for efficient production of biotin. *Metabolic Engineering*, 61, 406–415. <https://doi.org/10.1016/j.ymben.2019.05.005>
- Xiao, X., Saha, P., Yeoh, B. S., Chen, Q., Katkere, B., Kirimanjeswara, G. S., & Vijay-Kumar, M. (2019). The bacterial siderophore enterobactin confers survival advantage to *Salmonella* in macrophages. *Gut Microbes*, 10(3), 412–423. <https://doi.org/10.1080/19490976.2018.1546519>
- Yang, B., Feng, L., Wang, F., & Wang, L. (2015). Enterohemorrhagic *Escherichia coli* senses low biotin status in the large intestine for colonization and infection. *Nature Communications*, 6(1), 6592. <https://doi.org/10.1038/ncomms7592>
- Zempleni, J. (2005). UPTAKE, LOCALIZATION, AND NONCARBOXYLASE ROLES OF BIOTIN. *Annual Review of Nutrition*, 25(1), 175–196. <https://doi.org/10.1146/annurev.nutr.25.121304.131724>
- Zempleni, J., Wijeratne, S. S. K., & Hassan, Y. I. (2009). Biotin. *BioFactors*, 35(1), 36–46. <https://doi.org/10.1002/biof.8>
- Zlitni, S., Ferruccio, L. F., & Brown, E. D. (2013a). Metabolic suppression identifies new antibacterial inhibitors under nutrient limitation. *Nature Chemical Biology*, 9(12), 796–804. <https://doi.org/10.1038/nchembio.1361>
- Zlitni, S., Ferruccio, L. F., & Brown, E. D. (2013b). Metabolic suppression identifies new antibacterial inhibitors under nutrient limitation. *Nature Chemical Biology*, 9(12), 796–804. <https://doi.org/10.1038/nchembio.1361>

Appendix A: Chemicals and Reagents

Table A1: List of chemicals and reagents used in this study

Product name	Company	Reference number
2X Phusion Flash PCR Master Mix	ThermoFisher Scientific	F-548
50X TAE Electrophoresis Buffer	ThermoFisher Scientific	B49
Agar Bacteriological	Merck	HG000BX1.500
Ammonium Chloride crystals	Merck	1122700
Ampicillin Sodium Salt	VWR Life Science	339
Anza 10 <i>DpnI</i>	ThermoFisher Scientific	IVGN010-6
Anza 11 <i>EcoRI</i>	ThermoFisher Scientific	IVGN0116
Anza 12 <i>XbaI</i>	ThermoFisher Scientific	IVGN0126
Anza 16 <i>HindIII</i>	ThermoFisher Scientific	IVGN0166
Anza 17 <i>KpnI</i>	ThermoFisher Scientific	IVGN0176
Anza 5 <i>BamHI</i>	ThermoFisher Scientific	IVGN0056
Anza 8 <i>XhoI</i>	ThermoFisher Scientific	IVGN0086
Anza Buffer	ThermoFisher Scientific	IVGM2008
Biotin	Sigma-Aldrich	B4501
Calcium Chloride dihydrate	Merck	1524920EM
Chloramphenicol	Sigma-Aldrich	C0378
Chloroform	Riedel-deHaën	D-3016
Citric Acid Monohydrate	Merck	SAAR1605020EM
CloneJET PCR Cloning kit	ThermoFisher Scientific	K1231
D-(+)- Glucose	Sigma-Aldrich	G7021
Difco Vitamin Assay Casamino Acids	Difco	228820
diSodium Hydrogen orthophosphate Anhydrous	Merck	SAAR5822870EM
DMEM (1X)	Gibco	21969-035
dNTP solution Mix	New England BioLabs	N0447S
DPBS (1X)	Gibco	14190-094
DreamTaq PCR Master Mix (2X)	ThermoFisher Scientific	K1071
EN300-256446 (C ₈ H ₉ N ₃ O ₃ S)	Enamine	4871-40-3
Ethidium Bromide, 10mg/ml	VWR Life Science	X328
Ethylene glycol-O,O'-bis(2-aminoethyl)-N,N,N',N'-tetraacetic acid	Alfa Aesar	A1608b
Evans Blue	Sigma-Aldrich	E2129
Fast AP Thermosensitive Alkaline phosphatase	Thermo Scientific	EF0651
FastDigest Buffer (1X)	ThermoFisher Scientific	K1991

Product name	Company	Reference number
FastDigest Value Pack	ThermoFisher Scientific	K1991
Fetal Bovine Serum Gamma Irradiated	Biowest	S181G-500
Fluorescein Sodium Salt	Sigma-Aldrich	46960-100G-F
GeneArt Seamless Cloning and Assembly Reaction Kit	ThermoFisher Scientific	A13288
GeneJET Gel extraction and DNA cleanup Micro Kit	ThermoFisher Scientific	K0831
GeneJet Genomic DNA Purification Kit	ThermoFisher Scientific	K0721
GeneRuler 1kb Plus DNA Ladder	ThermoFisher Scientific	SM1333
GeneRuler 50bp DNA Ladder	ThermoFisher Scientific	SM0373
Gentamicin Solution	Sigma-Aldrich	G1272
Glycerol	Merck	SAAR2676520LC
Kanamycin Sulfate	VWR Life Science	408
KAPA Taq Ready Mix PCR Kit	Sigma-Aldrich	KK1006
KAPA Taq Ready Mix with dye	Sigma-Aldrich	KK1024
KAPA Universal DNA Ladder	Sigma-Aldrich	KK6302
L-(+)- Arabinose	Sigma-Aldrich	A3256
Magnesium Sulphate Heptahydrate	Merck	SAAR4124000EM
Mix n Go! E.coli Transformation Kit	Zymo Research	T3001
Mueller-Hinton Agar	Merck	HG000C37.500
Pancreatic Digest of Casein	Merck	HG000BX4.250
Phusion High-Fidelity DNA polymerase	ThermoFisher Scientific	F-530S
Potassium dihydrogen orthophosphate	Merck	5043600EM
Potassium phosphate dibasic	Sigma-Aldrich	P2222
PureLink Genomic DNA Mini Kit	ThermoFisher Scientific	K1820-01
Resazurin Sodium Salt	Sigma-Aldrich	R7 017
Rnase A	ThermoFisher Scientific	8003088
Sodium Chloride	Sigma-Aldrich	S7653
T4 DNA Ligase	Promega	M180A
Thiamine hydrochloride	Sigma-Aldrich	T4625
TopVision Agarose Tablets	ThermoFisher Scientific	R2 801
Triton ×-100	Sigma-Aldrich	T8787
TriTrack Loading Dye (6X)	ThermoFisher Scientific	R1 161
TrypLE Express (1X)	Gibco	12605-010
Ultra Pure Distilled water	ThermoFisher Scientific	10977-035
Ultra Pure IPTG	ThermoFisher Scientific	15529-019
×-gal	ThermoFisher Scientific	R404
Yeast Extract Powder	Merck	HG000BX6.500

Appendix B: Molecular Weight Markers

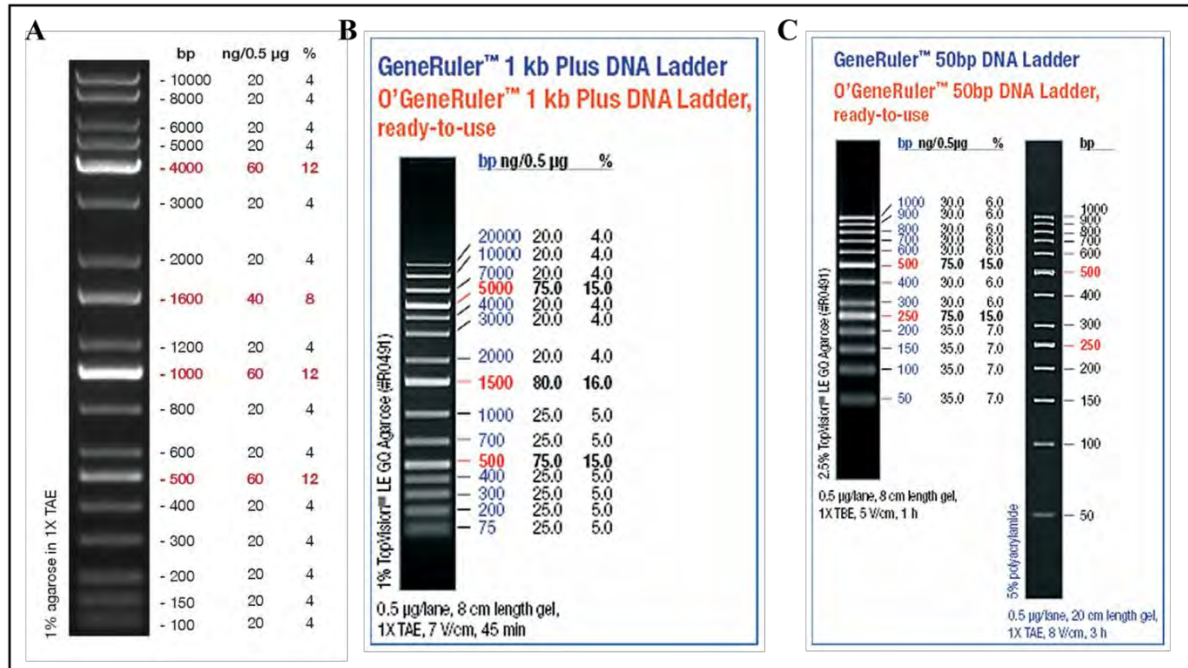


Figure B1: Molecular Weight Markers used in this study. A) KAPA Universal ladder. B) GeneRuler 1Kb Plus DNA Ladder. C) GeneRuler 50bp DNA Ladder.

Appendix C: Plasmid Construction

C1: Construction of BioB complement construct pBioB

In order to generate a plasmid capable of complementing the deletion of the *bioB* gene, the *bioB* gene along with its original promoter was amplified with primers designed to anneal on either side of the gene. An appropriate size *bioB* amplicon of ~ 1.6 kb can be seen in **Lane 3** of **Figure C1.1**. This *bioB* amplicon then underwent PCR purification and restriction enzyme digestion with *Bam*HI and *Hind*III, whose recognition sites were incorporated into the forward and reverse primers, respectively. The digested insert was then ligated into the low copy number plasmid pWSK29, which had been digested with the same enzymes. The ligated *bioB* insert and pWSK29 plasmid were then transformed into *E. coli* DH5 α competent cells and transformants selected for on LB/Amp agar plates. The presence of an insert of the correct size was confirmed by RE digestion of the recombinant plasmid DNA with *Bam*HI and *Hind*III (**Figure C1.2**). The sequence of the PCR amplified regions of the vector was subsequently confirmed by Sanger sequencing. Once confirmed, the complementation construct, pBioB, was electroporated into the *S. Typhimurium* $\Delta bioB$ Km^R marked strain as well as the *S. Typhimurium* $\Delta bioB$ $\Delta yigM$ marked strain for subsequent phenotypic analysis *in vitro* (**Section 3.2.6, Figure 3.13**). The plasmid map of the pBioB construct can be seen in **Figure C1.3**.

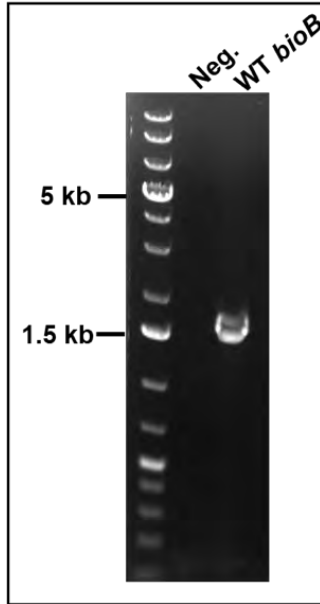


Figure C1.1: Generation of a construct for genetic complementation of the *bioB* gene. The insert for the generation of the complementation construct was generated by PCR amplification using *S. Typhimurium* genomic DNA and *bioB*-*Bam*HI-For and *bioB*-*Hind*III-Rev primers. The PCR reaction products were subjected to electrophoresis on a 0.8 % agarose gel at 80 V for ~ 50 min. **Lane 1:** MW marker. **Lane 2:** PCR product of no DNA template, negative control. **Lane 3:** PCR product from WT genomic DNA template.

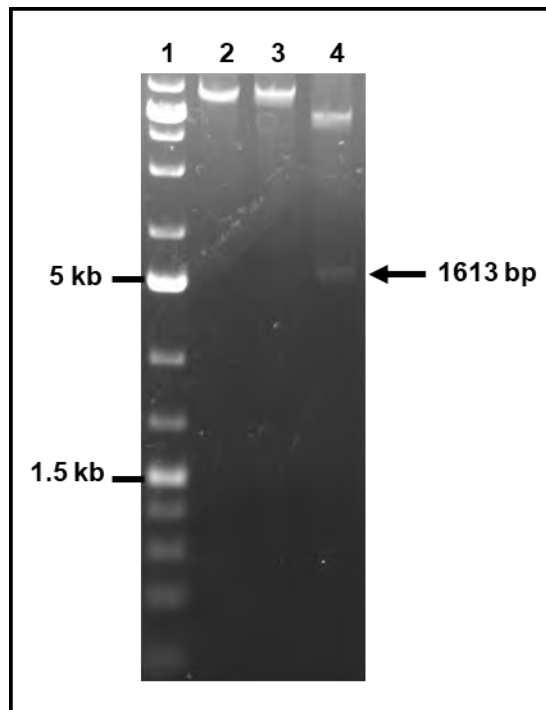


Figure C2.2: Restriction enzyme digests of recombinant pBioB plasmid. Plasmids were digested with *Bam*HI, *Hind*III, *Bam*HI/*Hind*III for 16 h at 37 °C and then electrophoresed on a 0.8 % agarose gel at 80 V for 50 min. **Lane 1:** MW marker, **Lane 2:** pBioB digested with *Bam*HI, **Lane 3:** pBioB digested with *Hind*III, **Lane 4:** pBioB digested with *Bam*HI, and *Hind*III.

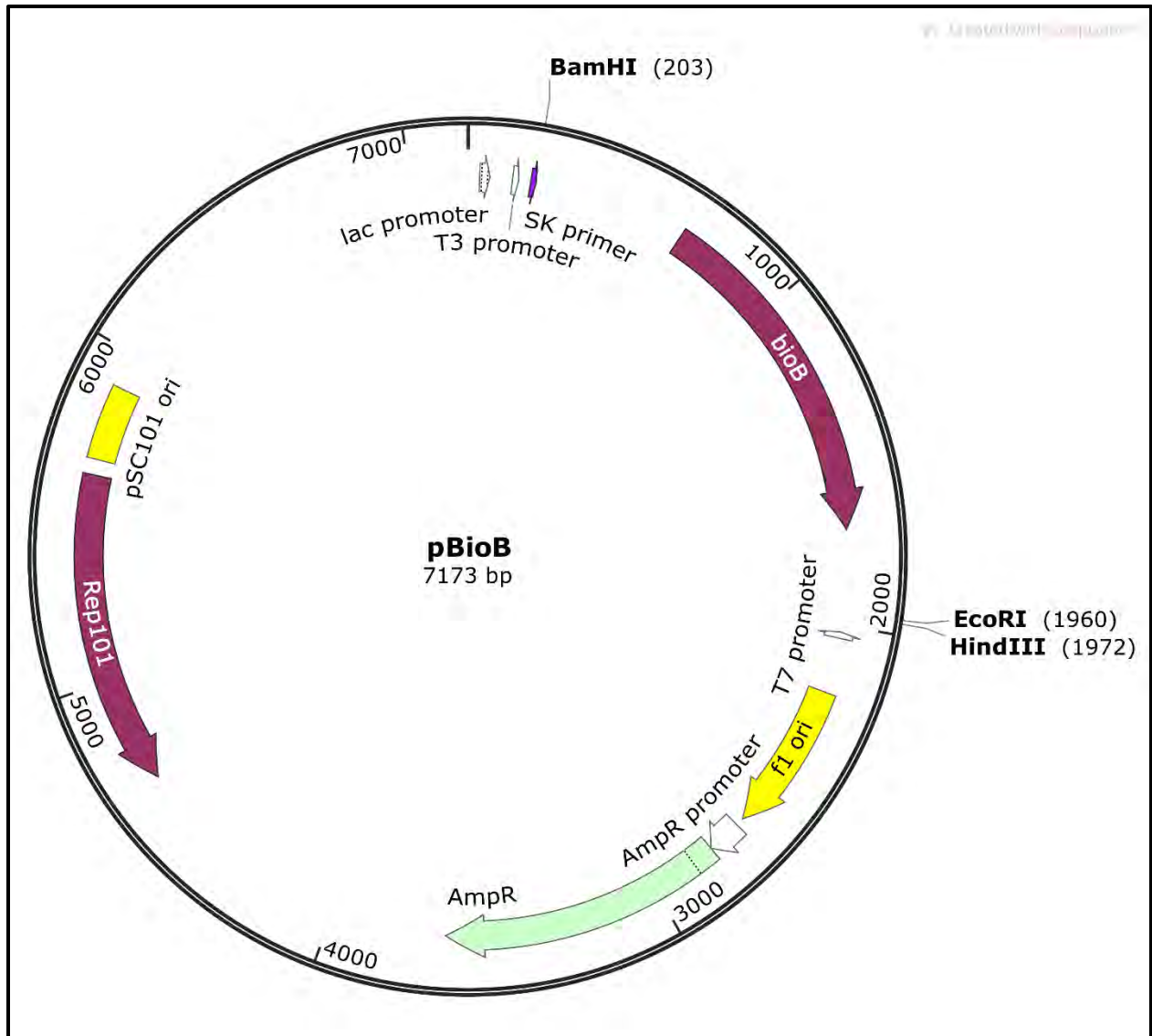


Figure C1.3: Complement construct pBioB map. Indicating direction of replication, the inserted gene of interest (*bioB*) and restriction enzyme sites (*Bam*HI and *Hind*III) as well as primers (*bioB*-*Bam*HI-For and *bioB*-*Hind*III-Rev) used for the construction of the construct.

C2: Construction of YigM complement construct: pYigM

In order to generate a plasmid capable of complementing the deletion of the *yigM* gene, the *yigM* gene along with its native promoter was amplified with primers designed to anneal on either side of the gene. An appropriate size *bioB* amplicon of ~ 1.5 kb can be seen in **Lane 3** of **Figure C2.1**. This *bioB* amplicon then underwent PCR purification and restriction enzyme digestion with *Bam*HI and *Eco*RI, whose recognition sites were incorporated into the forward and reverse primers, respectively. The digested insert was then ligated into the low copy number plasmid pWSK29, which had been digested with the same enzymes. The ligated *bioB* insert and pWSK29 plasmid were then transformed into *E. coli* DH5 α competent cells and transformants selected for on LB/Amp agar plates. The presence of an insert of the correct size was confirmed by RE digestion of the recombinant plasmid DNA with *Bam*HI, *Hind*III, and/or *Eco*RI (**Figure C2.2**). The sequence of the PCR amplified regions of the vector was subsequently confirmed by Sanger sequencing. Once confirmed, the complementation construct, pYigM, was electroporated into the *S. Typhimurium* Δ *yigM* single mutant as well as the *S. Typhimurium* Δ *bioB* Δ *yigM* double mutant for subsequent phenotypic analysis *in vitro* (**Section 3.2.6, Figure 3.13**). The plasmid map of the pYigM construct can be seen in **Figure C2.3**.

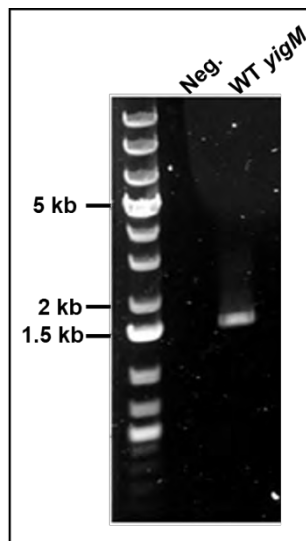


Figure C2.1: Generation of a construct for genetic complementation of the *yigM* gene. The insert for the generation of the complementation construct was generated by PCR amplification using *S. Typhimurium* genomic DNA and *yigM*-*Bam*HI-For and *yigM*-*Eco*RI-Rev primers. The PCR reaction products were subjected to electrophoresis on a 0.8 % agarose gel at 80 V for ~ 50 min. **Lane 1:** MW marker. **Lane 2:** PCR product from no DNA template, negative control. **Lane 3:** PCR product from WT genomic DNA template.

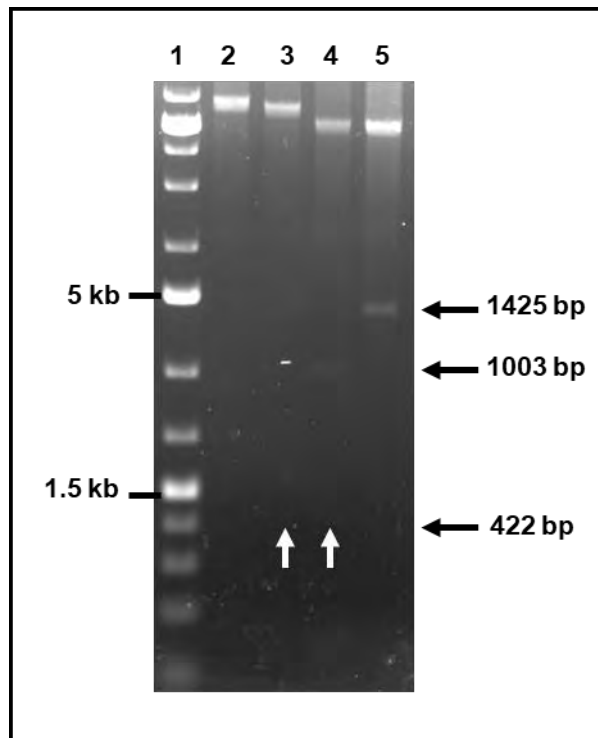


Figure C2.2: Restriction enzyme digests of recombinant pYigM plasmid. Plasmids were digested with *Bam*HI, *Hind*III, *Bam*HI/*Hind*III, or *Bam*HI/*Eco*RI for 16 h at 37 °C and then electrophoresed on a 0.8 % agarose gel at 80 V for 50 min. **Lane 1:** MW marker, **Lane 2:** pYigM digested with *Bam*HI, **Lane 3:** pYigM digested with *Hind*III, **Lane 4:** pYigM digested with *Bam*HI and *Hind*III **Lane 5:** pYigM digested with *Bam*HI/*Eco*RI

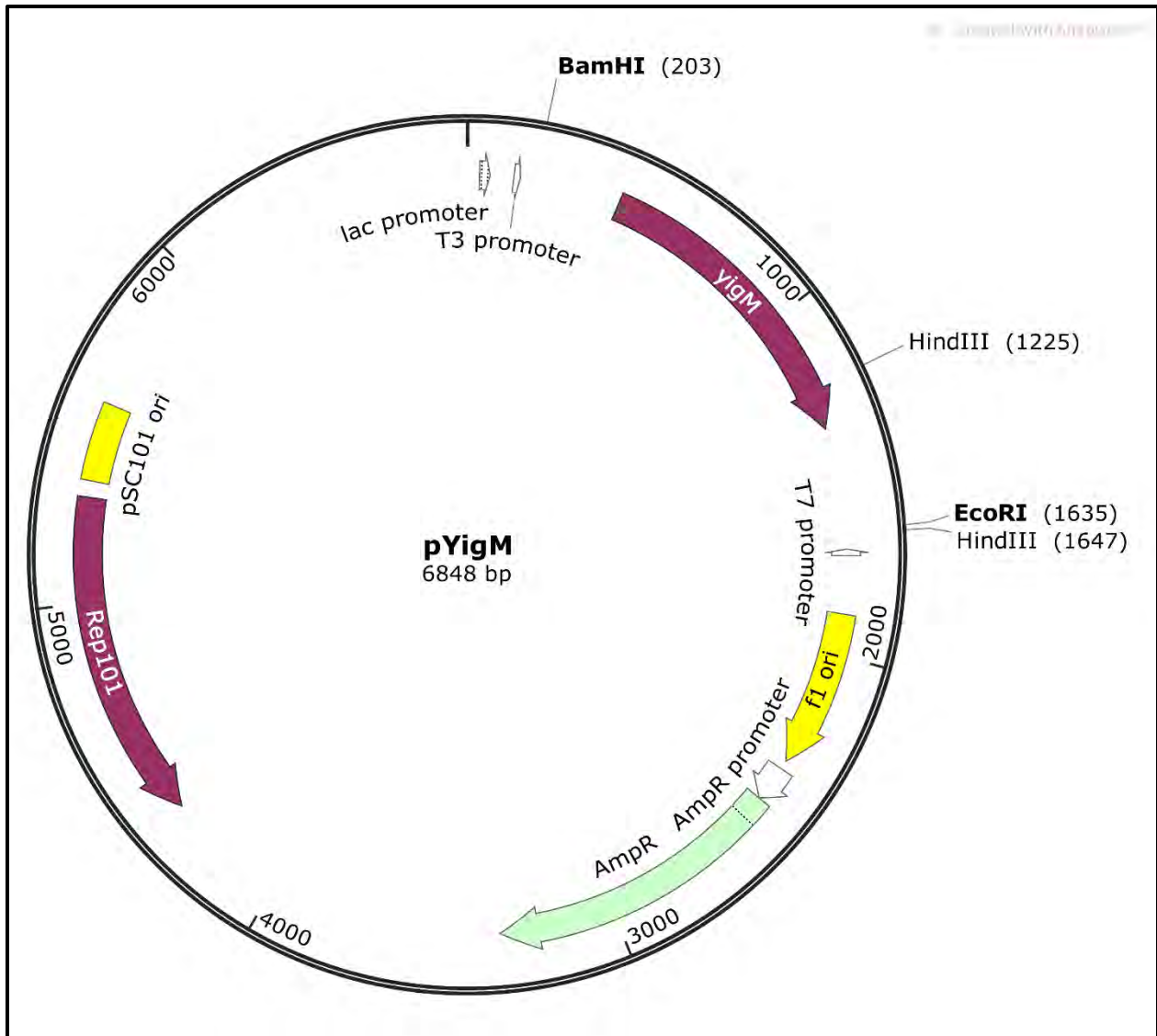


Figure C2.3: Complement construct pYigM map. Indicating direction of replication, the inserted gene of interest (*yigM*) and restriction enzyme sites (*Bam*HI and *Eco*RI) as well as primers (*yigM*-*Bam*HI-For and *yigM*-*Eco*RI-Rev) used for the construction of the construct.